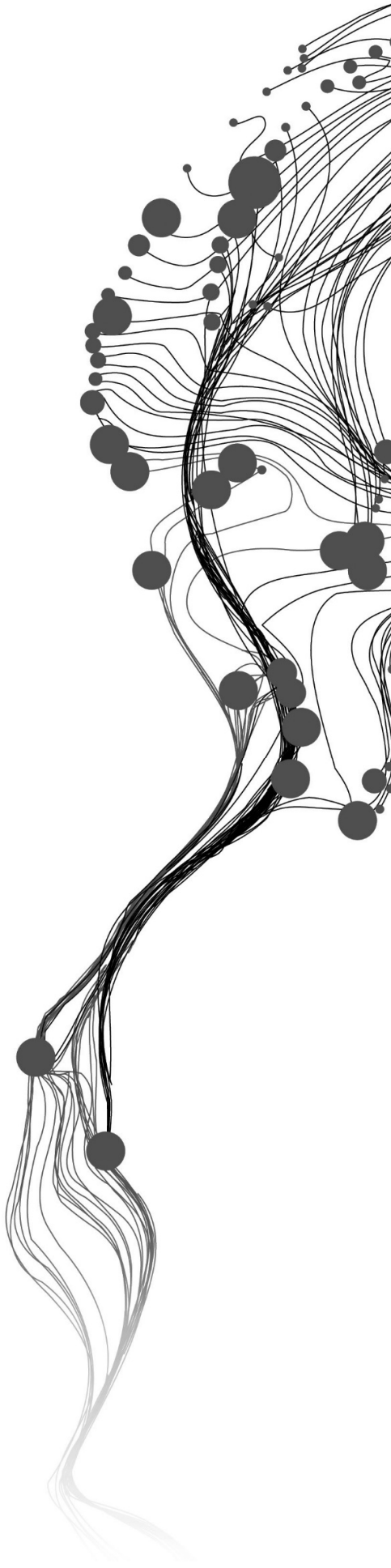# ANALYSIS OF URBAN SURFACE TEMPERATURE FOR GREEN SPACES PLANNING IN BANDUNG CITY, INDONESIA

INU KUSUMA WARDANA
S6019307
September, 2015

SUPERVISORS:
Ms. M. Kuffer, MSc
Ridwan Sutriadi, ST., MT., Dr.

ANALYSIS OF URBAN SURFACE TEMPERATURE FOR GREEN SPACES PLANNING IN BANDUNG CITY, INDONESIA

INU KUSUMA WARDANA
Enschede, The Netherlands, September, 2015

Thesis submitted to the Faculty of Geo-Information Science and Earth Observation of the University of Twente in partial fulfilment of the requirements for the degree of Master of Science in Geo-information Science and Earth Observation.
Specialization: Urban Planning and Management

SUPERVISORS:
Ms. M. Kuffer, MSc
Ridwan Sutriadi, ST., MT., Dr.

THESIS ASSESSMENT BOARD:
Dr. R.V. Sliuzas (Chair)
Drs. R.G. Nijmeijer (External Examiner, University of Twente)

ABSTRACT

Urban heat island refers to the higher temperature of urban areas compared to the surrounding rural areas. Previous studies on UHI often prove the existence of significant effects of land cover and vegetation density on urban surface temperature. However, they have not looked into the impact of the different arrangement of urban typologies. This study analysed land surface temperature extracted from thermal satellite imagery as a consideration for green spaces planning, with a case study on Bandung city, Indonesia. Satellite images from Landsat Thematic Mapper (TM) and Aster in 1994-2014 period were used for analysis. Pearson correlation was calculated between surface temperature and NDVI, Percentage of Landscape (PLAND) and Aggregation Index (AI). While, the temperature profiles for the different urban typologies were analysed. The findings indicate that the mean surface temperature has increased over the years. High density built-up areas in particular are most affected by high surface temperature. The composition and the configuration of vegetation cover have a strong influence to the surface temperature. However, the cooling effect of green area is also very much depend on the size and the type of green area, with a significant role of the high density trees. The provision of green space to decrease surface temperature need to consider the allocation of larger patches of tree covers adjacent to densely built-up areas.

Keywords: aggregation index; green spaces planning; land surface temperature; percentage of landscape; urban heat island; urban typologies

ACKNOWLEDGEMENTS

TABLE OF CONTENTS

LIST OF FIGURES

LIST OF TABLES

1. INTRODUCTION

1.1. Background and Justification

Along with rapid urbanization, the challenges of sustainable development are increasingly concentrated in the cities. In 1950, only 30% of the world's population was urban. Today, more people live in urban areas than in rural areas, with 54% of the world's population residing in urban areas (United Nations, 2014). Rapid urban growth can easily leads to urban sprawl and environmental degradation if necessary plans and policies are not implemented.

One of the environmental aspects that can be influenced by urban growth is the urban microclimate. It is well known that human activities and urban development can have a significant effect on the increase in air temperature in urban areas. Anthropogenic heat from industrial, transportation, and domestic activities adds warmth to the surroundings. Urban development often gives rise to dramatic changes in urban land use, where natural green spaces are removed and replaced by built-up areas. Green spaces, that have lower temperatures, are replaced by land uses that have higher thermal contents, such as industrial, commercial and residential areas. The domination of built-up surfaces causes higher temperature in urban areas compared to the surrounding rural areas. This phenomena is known as urban heat island (UHI) (Liu & Zhang, 2011).

The spatial characteristics of the UHI are contingent upon the configuration and topographic setting of the urban area, however, the spatial pattern of UHI isotherms are typically aligned with the urban-rural boundary (Voogt & Oke, 2003). Moreover, the increased temperatures associated with the UHI phenomenon are not uniform across the urban area as a whole, as intra-urban thermal patterns are generally influenced by urban surface features. Illustration of a typical UHI profile is shown in Figure 1.1.

Generally, areas with high UHI intensity are located in the city centre. Land cover in the city centre are usually dominated by pavement with high heat capacity and low solar reflectivity. Heat absorbed by buildings, roads, and other pavements is released back in the night so that air temperature in the city centre becomes higher than the surrounding area. Wind may not help to reduce the heat because it is blocked by buildings so it cannot move smoothly. Greenhouse gases that are produced from high intensity activities in the city centre restrain the release of solar radiation thus exacerbating local warming.
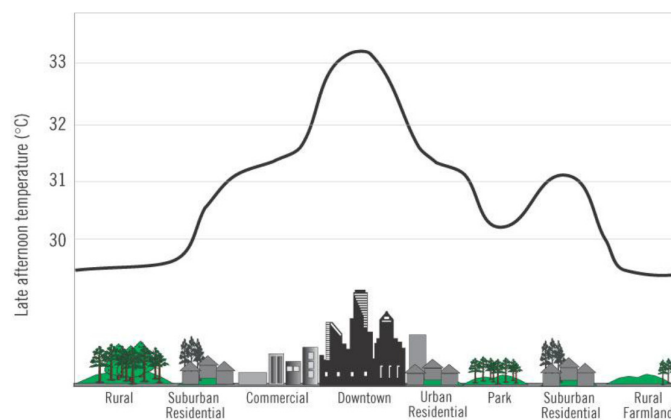
Figure 1.1 - Sketch of a Typical UHI Profile
Source: Arrau & Peña, 2011

UHI can have a severe impact on urban environments and human beings. UHI can affect the local climate, rainfall, wind patterns, and cloud. UHI effect may cause discomfort and affect human health. In an indirect manner, elevated temperatures in cities often result in the need for increased energy consumption due to a higher demand for air conditioning. This, in turn, often requires increased use of fossil-fuel powered plants, increasing emissions of greenhouse gases such as carbon dioxide (CO_2) into the atmosphere (Santana, 2007; U.S. Environmental Protection Agency, 2012).

Remote sensing is an excellent tool to assess UHI. Unlike temperature measurement at meteorological station that can only provide temperature data at one location, remote sensing can measure the temperature on a city scale. In addition, satellite imagery facilitates study on the relationship of UHI with other spatial variables, such as building and vegetation density. In particular, thermal infrared images from Landsat Thematic Mapper (TM) and Enhanced Thematic Mapper (ETM+) are widely used in UHI analysis (Anniballe et al., 2014).

1.2. Study Area

This study use Bandung municipality as case study. Bandung is the capital of West Java province and is the third largest city in Indonesia by population (2,455,517 inhabitants in 2012). Bandung city covers an area of 16,730 hectares, which is divided into 30 districts. The city is located at 6°50'38"-6°58'50" and 107°33'34"-107°43'50", approximately 140 kilometres south east of Jakarta as the capital of Indonesia. Administrative area of Bandung Municipality is shown in Figure 1.2.

Bandung lies in a basin surrounded by mountains. Topographically, Bandung has an average elevation of 791 metres above sea level with elevation ranged between 675 to 1,050 metres above sea level. The climate of Bandung is influenced by the surrounding mountains so the local climate is humid and cool. Based on the 1952-2011 data, the annual average temperature in Bandung is 22.4°C. For the same period, Bandung receives an average total rainfall of 1,293 millimetres per year during the rainy season within the period of October to March (Meteorology, Climatology, and Geophysics Agency of Indonesia, 2012).
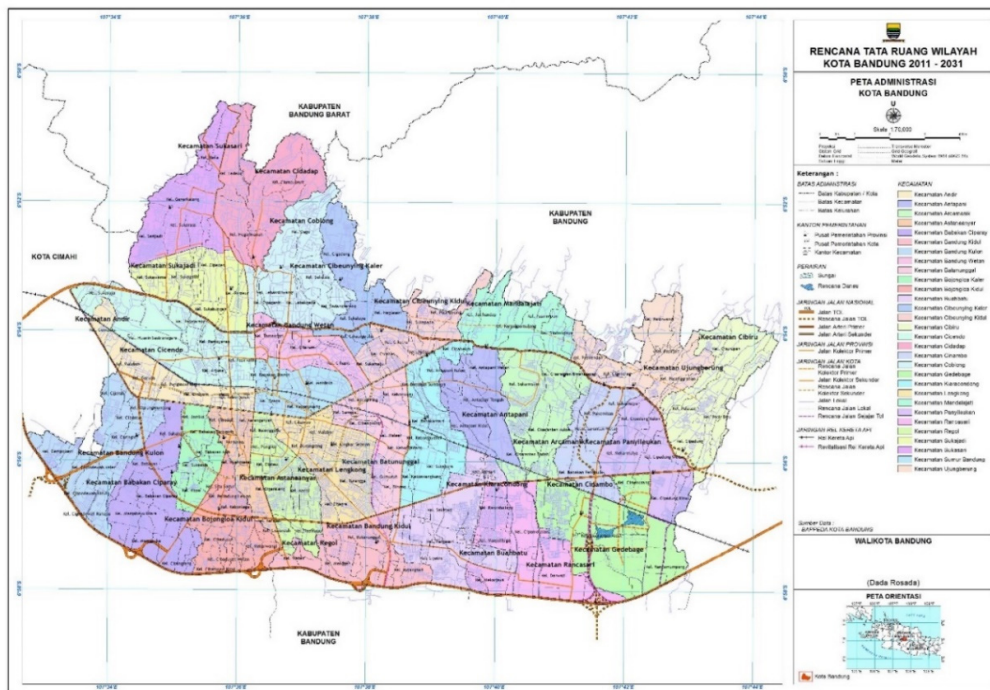
Figure 1.2 - Map of Bandung Municipality Administrative Area
Source: Government of Bandung Municipality, 2011

Over the past twenty years, rapid population growth in Bandung has led to expansion of built-up areas, and consequently an increase in air temperature. As a service, commercial, and civic centre, Bandung has been a magnet for migrants and has experienced rapid urban growth. During 1990 to 2012, population of Bandung city had grown by 36%, from 1,808,261 to 2,455,517 inhabitants, with an average growth rate of 1.44% per year. Along with the increasing population, there had been a sizeable land conversion from unbuilt land to built-up land. Based on the 1990 and 2008 data, there had been conversions of vacant land (-468 ha), rice field (-373 ha), and other uses (-357 ha) to services and commercial (663 ha), housing (498 ha), and industry (37 ha). This had resulted in an increasing proportion of built-up area from 63% in 1990 to 70% in 2008. Furthermore, the expansion of built-up area was also followed by an increase in air temperature. Based on the 1996-2012 data, the annual average temperature had shown an increase of 0.01°C per year with temperature ranging between 22.9-23.6°C. Moreover, the highest maximum temperature per ten years since 1980 to 2010 has increased by 0.95°C. Between 2001 and 2010, the highest temperature recorded was 35°C (Meteorology, Climatology, and Geophysics Agency of Indonesia, 2012). The proportion of land use and annual average temperature trend in Bandung city is shown in Figure 1.3.

Issues that may significantly influence urban thermal conditions in Bandung are the insufficient green covers and rapid expansion of built-up areas. Indonesia Spatial Planning Act No. 26/2007 (Government of Indonesia, 2007) states that green spaces should cover a minimum of 30% of the city area. However, based on the 2011 data, green spaces in Bandung only cover 11% of the city area. In case the expansion trend continues, green cover in Bandung will decline further. Caused by the rapid population growth, built-up areas have been sprawling towards the fringe areas of Bandung city. New residential areas continue to be established especially in the districts which are part of Bandung city region directly adjacent to the surrounding regencies. This expansion trend will undoubtedly exacerbate urban warming in Bandung.
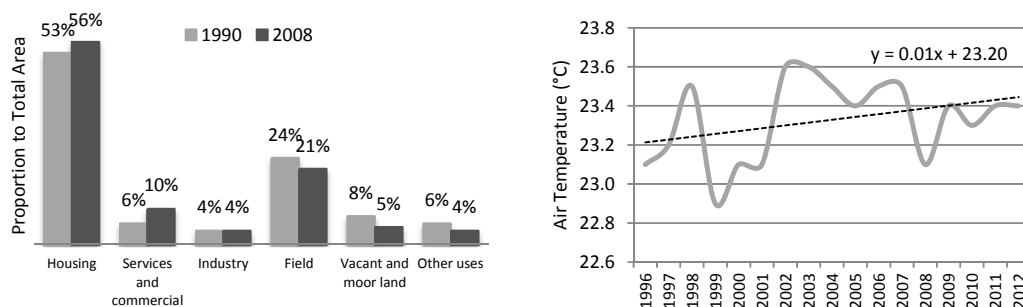
Figure 1.3 - Land Use (1990 and 2008) and Annual Average Temperature (1996-2012) in Bandung Municipality
Source: Government of Bandung Municipality, 2011; Meteorology, Climatology, and Geophysics Agency of Indonesia, 2012

1.3.   Research Problem

Vegetation density and land cover/land use characteristics are considered to have the most significant influence on UHI intensity (Arrau & Peña, 2011; Xian & Crane, 2006). Vegetated surfaces are capable of decreasing UHI intensity as they provide for cooler microclimates. The evapotranspiration of plants helps to improve air quality and reduce urban air temperatures. A study in Greater Manchester, UK, predicted that increasing 10% of urban green cover in high-density areas could decrease expected maximum surface temperature in the 2080s by 2.4°C to 2.5°C. Conversely, removing 10% of the green cover was estimated to increase temperature by 7°C to 8.2°C (Gill et al., 2007). In addition, a strong correlation is found between land cover/land use and intra-urban thermal patterns with industrial areas being the warmest and vegetated, riverine, and coastal areas being the coolest (Roth, Oke, & Emery, 1989). As different vegetation density and land cover characteristics can modify thermal conditions in cities, it becomes increasingly important to do research on UHI that can enhance to understand the influence of vegetation density and land cover on

surface temperature in order to provide useful information and advice for urban planning, and in particular for green space planning.

Previous studies on UHI often prove the existence of significant effects of land cover and vegetation density on urban surface temperature (Maimaitiyiming et al., 2014; Weng et al., 2004). However, studies that look into the temperature profile of the different urban typology and assessing the impact of green spaces planning on urban surface temperature have rarely been done. Generally, previous studies on surface temperature and UHI have been done to deepen the understanding of urban climate science, however they have not looked into the different arrangement of urban typology in their analysis. Furthermore, the benefit of the results of surface temperature and UHI studies in urban planning will be largely determined by the availability of information about the area or location that has higher temperature intensity or concentration compared to other areas, so that mitigation through green spaces planning can be implemented. Without this information, it will be difficult to perform a prioritization for mitigation, thus the applicability of such studies in urban planning will be weak.

1.4.   Research Objectives

This study aims to analyse urban surface temperature pattern extracted from thermal satellite imagery as a consideration for green spaces planning, with a case study on Bandung city, Indonesia. The research sub-objectives are as follows:

1. To analyse the trend of land cover in Bandung city.
2. To analyse the trend of land surface temperature in Bandung city.
3. To identify the relationship between land surface temperature and the composition and configuration of land cover in Bandung city.
4. To analyse the relation between green space planning and land surface temperature in Bandung city.

1.5.   Research Questions

For each research sub-objective, several research questions have been formulated. They can be seen as an operational guidance to realize the sub-objectives. Based on the discussion in the previous chapters, this study will address the following research questions:

- Sub-objective 1: To analyse the trend of land cover in Bandung city.
    - What are the changes in the area coverage of each land cover type?
    - What are the changes in the spatial pattern of land cover?
- Sub-objective 2: To analyse the trend of land surface temperature in Bandung city.
    - What are the changes in the spatial pattern of land surface temperature?
    - What are the changes in the land surface temperature for the overall study area?
    - What are the changes in the land surface temperature for each land cover type?
- Sub-objective 3: To identify the relationship between land surface temperature and the composition and configuration of land cover in Bandung city.
    - What is the relationship between the land surface temperature and the composition of land cover?
    - What is the relationship between the land surface temperature and the configuration of land cover?
- Sub-objective 4: To analyse the relation between green space planning and land surface temperature in Bandung city.
    - What are the land surface temperature profile from the city centre to the urban fringe areas of Bandung city?
    - What are the land surface temperature profile for the different urban land use and typology?

1.6. Conceptual Framework

The conceptual framework of this study is based on the results of previous studies on UHI and urban surface temperature that has been described in the Section 1.1. It has been known that land cover and vegetation density has a strong relationship on urban surface temperature. In addition to the composition, the configuration and the typology of urban land cover/land use will affect the urban surface temperature. Caused by the concentration of higher surface temperature in urban areas, attention is given to mitigation through urban green spaces planning. However, planning efforts cannot be made directly to reduce the surface temperature, but only can be done by implementing planning strategies that will result in changes in the distribution of land cover/land use in urban areas. The conceptual framework is shown in Figure 1.4.
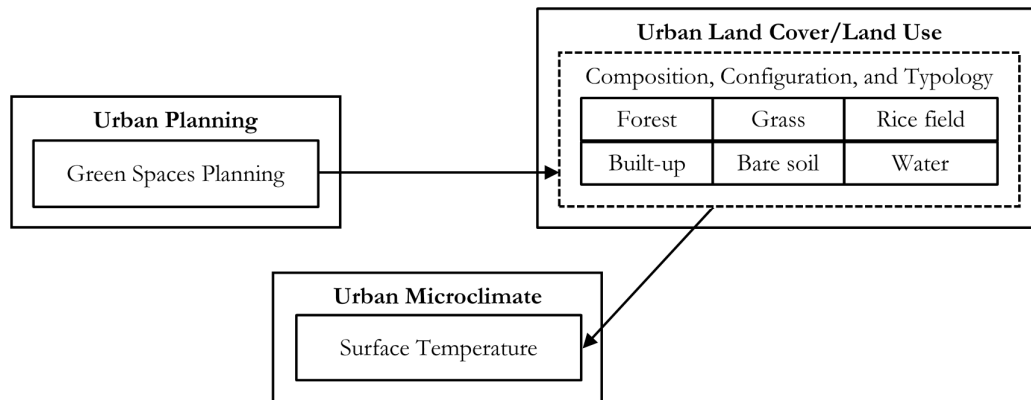
Figure 1.4 - Conceptual Framework

1.7. Structure of Thesis

This study will consists of six chapters with the following structure:

Chapter 1: Introduction
This chapter explains background of the study, study area, research problem, research objectives, and research questions and conceptual framework.

Chapter 2: Literature Review
This chapter reviews concepts related to urban heat island, as well as methods and results from previous researches on urban heat island.

Chapter 3: Methodology
This chapter describes data collection, data processing, and methods for land cover classification and land surface temperature extraction.

Chapter 4: Results and Discussion
This chapter presents the results and the discussion regarding the trend of land cover, the trend of land surface temperature, the relationship between land surface temperature and the composition and configuration of land cover, and the relation between urban typologies and the land surface temperature.

Chapter 5: Conclusion and Recommendations
This chapter presents conclusion and recommendations based on the findings of this study.

2. LITERATURE REVIEW

UHI can be divided into two categories: urban canopy layer (UCL), and urban boundary layer (UBL) (Oke, 1976). UCL is the layer where human activity occurs, which stretches from the ground to the building's roof and treetops. Meanwhile, UBL is the layer from the top of the tree and building to approximately 1.5 km into the atmosphere where the difference in urban landscape is considered no longer affects the atmosphere. Traditionally, UHI research was done by measuring air temperature at a particular location (in situ). In further developments, remote sensing technology has made it possible to study the UHI on a city or regional scale. Studies using satellite-derived radiant temperature have been termed as the land surface temperature (LST) heat islands (Streutker, 2003). LST heat islands is believed to correspond more closely with the UCL heat islands (Nichol, 1994).

Temperature data as the basis for the analysis have been obtained by the researchers with a variety of methods, including temperature measurements from meteorological stations, ground surveys at fixed locations, mobile surveys from ground vehicles, mobile surveys from airborne vehicles, and surface temperature extraction from satellite images. Researchers have also used combination of these methods. For example, Schwarz et al. (2012) combined air temperature data from meteorological stations, mobile surveys from ground and airborne vehicles, and surface temperature extraction from satellite images in analysing the relationship of surface and air temperature and its implications for quantifying UHI indicators in Leipzig, Germany.

Satellite remote sensing is an excellent tool for examining the UHI effects. Unlike in situ measurements, which provide sparsely distributed data, spaceborne sensors facilitate the monitoring of the urban heating with a global spatial coverage. Remotely sensed images that have been extensively used to analyse the UHI are derived from NOAA AVHRR (Roth et al., 1989; Streutker, 2003), Landsat TM and ETM+ (Chen et al., 2006; Li et al., 2009; Nichol, 1994; Santana, 2007; Weng et al., 2004; Xian & Crane, 2006), Aster (Liu & Zhang, 2011; Mallick et al., 2013; Nichol et al., 2009), and Modis (Anniballe et al., 2014; Quan et al., 2014; Tran et al., 2006).

In a series of application of remote sensing technology, urban thermal environment and UHI has been studied in a variety of themes. Some of the common themes are, among others, assessment on the intensity and spatial pattern of UHI (Anniballe et al., 2014; Li et al., 2009; Nichol et al., 2009; Quan et al., 2014; Tran et al., 2006), assessment on the relationship of UHI and land use/land cover (Chen et al., 2006; Jusuf et al., 2007), and assessment on the relationship of surface temperature and vegetation abundance (Maimaitiyiming et al., 2014; Weng et al., 2004).

The results from these studies have expanded the understanding of UHI and have provided insights for further study. Using two sets of NOAA AVHRR imagery within 12 years difference (1985-1999), Streutker (2003) measured the growth of UHI in Houston, USA. The results of the study revealed that the UHI intensity within the period grew by 0.8 K (35%). Roth et al. (1989) also used NOAA AVHRR to extract the surface temperature of three coastal cities in northern USA. The results of the study found that the UHI intensities are largest in the daytime and in the warm season, with thermal patterns are highly correlated with land use. Nichol (1994) used the results of surface temperature extraction from Landsat TM image to monitor the microclimate on several housing estates in Singapore. The results of the study showed a strong negative relationship between surface temperature and biomass (Leaf Area Index). Weng et al. (2004) used Landsat ETM+ to estimate the relationship of land surface temperature and vegetation abundance in Indianapolis, USA. Aside for Normalized Difference Vegetation Index (NDVI), the study also used vegetation fraction derived from a spectral mixture models as indicator of vegetation abundance. The results demonstrated that surface temperature possessed a strong negative correlation with NDVI and vegetation fraction for all land cover types.

A recent shift in the analysis of UHI is the use of local climate zone (Bechtel et al., 2015) that allow to establish a relationship between urban typologies and their impact on surface temperature. Local climate zones (LCZ) is beneficial for UHI studies because it can classify a wide range of surfaces that are common in urban areas. Some examples of common classes in LCZ are compact high-rise built-up, sparsely built-up, dense trees, scattered trees, etc.

2.1.   Overview of the UHI

Along with the increasing changes of natural surfaces, especially vegetation, into built-up and impervious surfaces in urban areas, differences in air temperature between urban areas and the surrounding rural areas are increasing. With the differences in the size and concentration of built-up surfaces, the differences in air temperature will tend to be greater with the increasing size of the cities (U.S. Environmental Protection Agency, 2012).

There are two types of UHI, namely Surface Urban Heat Island (SUHI) and Atmospheric Urban Heat Island (AUHI) (U.S. Environmental Protection Agency, 2012). SUHI occurs during both the day and the night, but the intensity reach its peak during the day when the sun is shining brightly. This is related to the intensity of solar radiation and thermal characteristics possessed by built-up surfaces that dominate urban areas that generally have a strong ability to absorb heat. Solar radiation may heat up the built-up surfaces such as roofs, walls and pavement to above the surrounding air temperature value. In contrast, at the same time, the moist natural surfaces in rural areas can have a surface temperature values that are similar to the surrounding air temperatures. On the average, SUHI intensity between urban areas and the surrounding rural areas can reach 5-10°C at night. Meanwhile, during the day, the difference can reach 10-15°C (U.S. Environmental Protection Agency, 2012).

The magnitude of SUHI is different for each ground cover, weather condition, and season. SUHI is strongly influenced by the intensity of solar radiation, therefore the largest intensity of SUHI generally occurs in the summer. SUHI intensity is also strongly influenced by the weather, where the intensity will reach its peak under the clear sky (not cloudy) and calm wind (U.S. Environmental Protection Agency, 2012). Thick cloud cover can block the radiation so that it can reduce the heating effect. In addition, strong wind may increases the atmospheric mixing, thereby reducing the temperature difference between urban areas with the surrounding rural areas. To identify and measure SUHI, scientists often apply remote sensing technology with the use of thermal images as indirect measurement tool and technique.
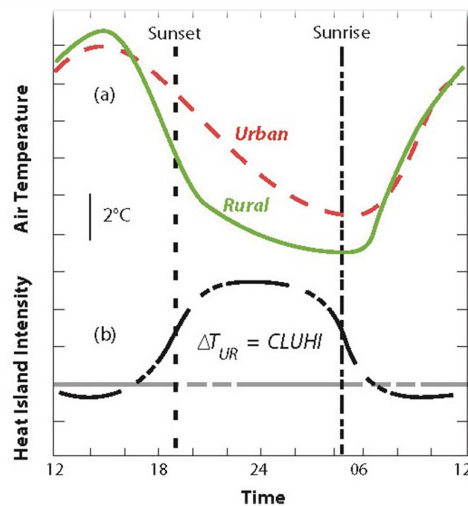
Figure 2.1 - Conceptual Drawing of the Diurnal Evolution of AUHI
Source: (U.S. Environmental Protection Agency, 2012)

Similar to SUHI, AUHI influenced by weather, seasons, and surface characteristics in urban areas. However, contrary to SUHI, AUHI generally reach its peak intensity at night where the heat absorbed by the built-up surfaces is released. The differences are also caused by the differences in cooling rates of natural surfaces that generally dominate rural areas. Illustration of AUHI intensity can be seen in Figure 2.1.

Compared to SUHI, variations in the intensity of AUHI are generally lower. It is more noticeable during the day where the air temperatures in urban areas may correspond with the air temperature in the surrounding rural areas. The difference in annual average air temperature between urban and rural areas may reach 1-3°C. Researchers generally measure AUHI by direct measurement at fixed and mobile stations.

Relationship between surface temperature and air temperature can be explained by the effect of the difference type of surface to air temperature, especially in the canopy layer that is more close to the surface. For example, vegetated surfaces that have a low surface temperature can contribute to lowering the surrounding air temperature through evapotranspiration. Because the air mixed in the atmosphere, the relationship between surface temperature with air temperature is always changing (not constant). The value of surface temperature and air temperature has closer similarity at night. However, during the day, the value of surface temperature and air temperature can be very different, with greater variations occur in surface temperature rather than air temperature (U.S. Environmental Protection Agency, 2012). Variations of surface and atmospheric temperatures can be seen in Figure 2.2.
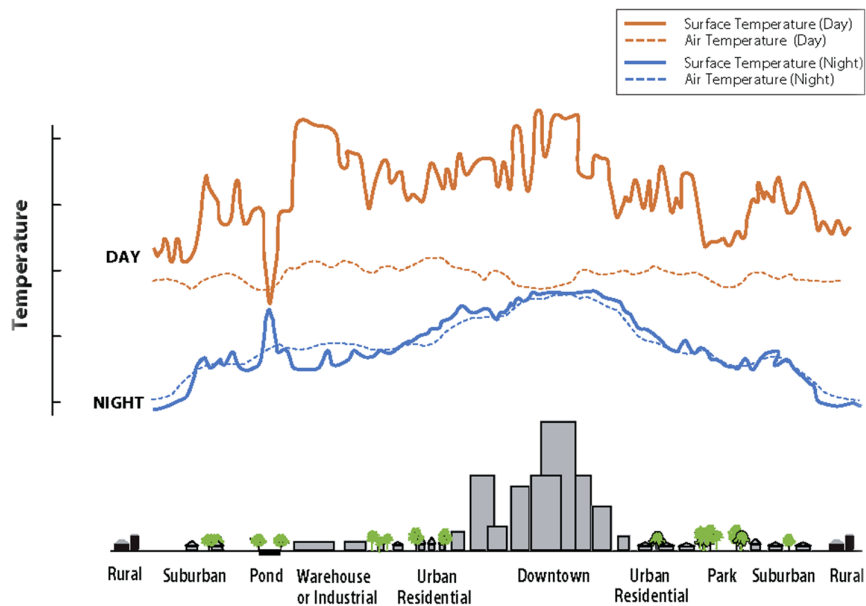
Figure 2.2 - Variations of Surface and Atmospheric Temperatures
Source: (U.S. Environmental Protection Agency, 2012)

2.2. Contributing Factors to UHI Formation

2.2.1. Reduced Vegetation in Urban Areas

Vegetation has evaporation and transpiration features by releasing water into the air which can reduce the surrounding air temperature. However, along with the growth of cities, moist natural vegetation that also gives shading for the urban areas is more and more replaced by dry impervious surfaces such as pavement and roof. Reduced vegetation means less moisture and shading to keep urban areas cool (U.S. Environmental Protection Agency, 2012).
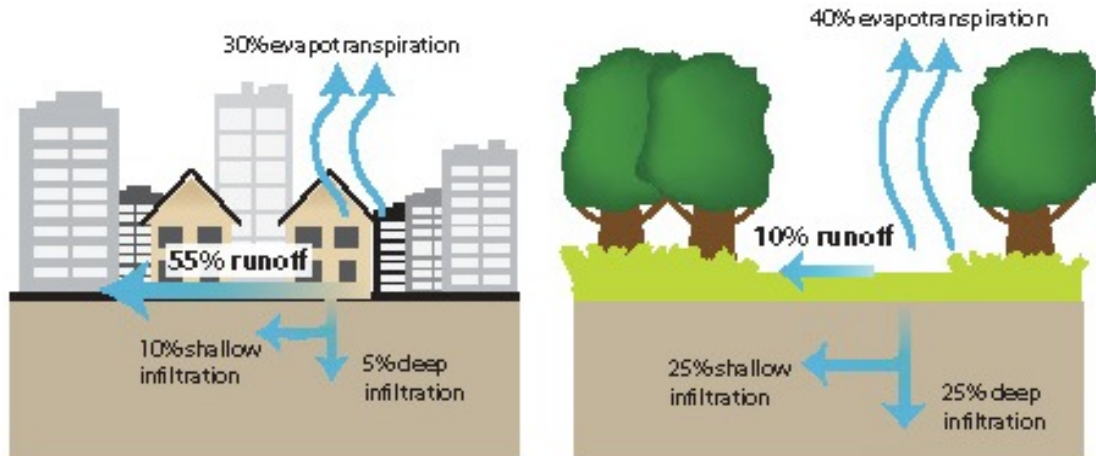
Figure 2.3 - Illustration of Reduced Evapotranspiration in an Urban Area
Source: (U.S. Environmental Protection Agency, 2012)

2.2.2. Properties of Urban Materials

Main properties of urban material that influence the formation of UHI is solar reflectance, thermal emissivity, and heat capacity (U.S. Environmental Protection Agency, 2012). Solar reflectance or albedo is the ability of material to reflect incoming solar energy. Since most of the incoming solar radiation into the earth is in the visible wavelength, albedo is generally associated with the colour of material, where material with a dark colour generally has a lower albedo than material with a light colour. Generally, materials that dominate urban areas such as roofs and pavements have a low albedo value. Therefore, urban areas reflect less and absorb more solar energy. Thermal emissivity is material's ability to dissipate heat. Material with high emittance will have a lower temperature because of its readiness to release heat. Metal is one of the examples of urban material that has a low thermal emissivity. Heat capacity is material's ability to store heat, e.g. a material commonly found in urban areas with high heat capacity is steel.

2.2.3. Urban Geometry

Urban geometry is the size, space and layout of the buildings located in urban areas. Urban geometry can affect the wind flow, solar energy absorption and heat emission from the surface into the atmosphere (U.S. Environmental Protection Agency, 2012). In a city centre that is crowded with buildings, urban surface or structure often obstructed by neighbouring buildings. In metropolitan cities, a phenomenon that can be encountered is the formation of an urban canyon, which is a relatively narrow space or road oppressed by tall buildings. At night, urban canyon may block cooling effects where buildings may block the heat emitted by the surfaces into the atmosphere. During the day, urban canyon can have positive and negative impacts. On the one hand, tall buildings provide shading that reduces surface and air temperature. On the other hand, when the sunlight reaches the surface in the urban canyon, the sun's energy is reflected and absorbed by the building walls and thus increases the temperature (U.S. Environmental Protection Agency, 2012).

The effect of urban geometry often described by the researchers through the Sky View Factor (SVF), which is area of the sky that could be seen from a point on the ground surface. Open spaces with only a little obstructions would have a large SVF value (close to 1), while the urban canyon with small visible area would have a small SVF value (close to 0) (U.S. Environmental Protection Agency, 2012).

2.2.4. Anthropogenic Heat

Anthropogenic heat is the heat generated from human activities, such as household, industrial and transportation activities. Anthropogenic heat mainly contributes to the AUHI (U.S. Environmental Protection Agency, 2012).

2.2.5. Weather

There are two main factors of weather that influence the formation of UHI, the wind and the cloud cover (U.S. Environmental Protection Agency, 2012). Generally, high UHI intensity formed under condition of clear sky and calm wind because this condition can maximizes the amount of solar energy that can reach the Earth's surface and reduces the heat that can be convected in the atmosphere. Conversely, strong wind and thick cloud cover can reduce the intensity of UHI.

2.2.6. Geographic Location

Geographic location and topography of the city and its surrounding regions can also affect the formation of UHI (U.S. Environmental Protection Agency, 2012). For example, closeness to the large water bodies can reduces temperature and may generates wind that can convect the heat away from the city. Nearby mountain can hinder wind to reach a city or create wind patterns that can pass the wind through the city.

3.   METHODOLOGY

3.1.   Data

The data used in this study only consists of secondary data (Table 3.1). Aside from satellite images obtained from the Unites States Geological Survey (USGS), other spatial and non-spatial data was obtained through institutional survey to several government agencies of Bandung municipality. The spatial data consists of administration boundary, land use, road network, and river network of Bandung city. The spatial data was acquired from the Development Planning Agency of Bandung Municipality (Bappeda). The spatial data are in vector format, and are part of the dataset of the Spatial Plan of Bandung Municipality 2011-2031. The non-spatial data consists of daily air temperature data from Meteorology, Climatology and Geophysics Agency of Indonesia (BMKG) and published government document such as the Spatial Plan and the Green Spaces Masterplan of Bandung Municipality 2011-2031.

Data	Format	Year	Data Sources	Data Collection
Landsat TM images	Raster	1994, 1997, 2000	USGS	Download
Terra Aster images	Raster	2003, 2005, 2008, 2011, 2014	USGS	Order
Administration boundary	Vector	2011	Bappeda	Institutional survey
Land use	Vector	2011	Bappeda	Institutional survey
Road network	Vector	2011	Bappeda	Institutional survey
River network	Vector	2011	Bappeda	Institutional survey
Spatial plan	Document	2011-2031	Bappeda	Institutional survey
Green spaces masterplan	Document	2011-2031	Bappeda	Institutional survey
Air temperature (daily data)	Table	1994-2014	BMKG	Institutional survey

Table 3.1 - Data Used in This Study

The main data that were used to assess surface temperature and land cover are satellite images from Landsat 5 Thematic Mapper (TM) and Terra Aster. The selection of images from these sensors is based on consideration that the medium spatial resolution of the images (30-90 metres) is sufficient to be used for examining surface temperature and land cover in the study area, which in this case is the whole administrative area of Bandung municipality. The spectral characteristics of each sensor are given in the Appendix 2.

Based on a previous research (Roth et al., 1989), UHI intensities are higher during the daytime than night-time. Therefore, images that were used are limited to the ones that were captured during the daytime. UHI intensities are also at their greatest during the dry season (Roth et al., 1989), thus image selection was limited to the ones that were captured during the dry season (May-October). Other parameter used in the image selection was the cloud cover, which was limited to ≤ 10% to ensure the effectiveness of the images for information extraction. Finally, the selection of one representative image for each year from alternative images was done based on the lowest cloud cover criteria.

The availability of Landsat TM and Terra Aster images in USGS website also becomes a decisive factor in limiting the period of this study, which cover over 20 years from 1994 to 2014. Ideally, a representative image should be available each year to build a time series. However, because the available images for each year do not always meet the criteria described above, representative images are not available continuously every year. This is one of the encountered limitations of this study. As a result, eight satellite images with 3 years interval (except for 2003-2005) were selected for this study. Information about the acquisition date and time, the satellite and sensor, and the percentage of cloud cover of each image is given in Table 3.2. While, the satellite images is shown in Appendix 3.

	Acquisition Date	Acquisition Time	Satellite and Sensor	Cloud Cover
1	22 September 1994	09.16	Landsat 5 TM	4%
2	26 June 1997	09.30	Landsat 5 TM	5%
3	20 July 2000	09.37	Landsat 5 TM	5%
4	12 June 2003	10.11	Terra Aster	1%
5	7 October 2005	10.10	Terra Aster	3%
6	25 June 2008	10.12	Terra Aster	5%
7	22 September 2011	10.10	Terra Aster	5%
8	5 September 2014	10.18	Terra Aster	1%

Table 3.2 - Satellite Images Used in This Study
Source: USGS, 2014

3.2. Data Processing

All satellite images used in this study, both TM and Aster, were geometrically corrected by the USGS. The images were also georeferenced to the WGS1984 datum and Universal Transverse Mercator (UTM) Zone 48N coordinate system. To match the vector dataset from The Government of Bandung Municipality, preprocessing was executed by reprojecting each image into UTM Zone 48S.

3.2.1. Conversion of Digital Number (DN) Values to Reflectance and Brightness Temperature

Since all the satellite images were captured under different cloud coverage condition, atmospheric corrections were applied by converting DN values into reflectance and brightness temperature. The steps in the extraction process of reflectance and brightness temperature were as follows:

- Conversion of DN values to at-sensor spectral radiance
  For TM images, the following equation was used to perform the conversion (Chander et al., 2009):

$$L_\lambda = \left(\frac{LMAX_\lambda - LMIN_\lambda}{Q_{calmax} - Q_{calmin}} \right)(Q_{cal} - Q_{calmin}) + LMIN_\lambda$$

or

$$L_\lambda = G_{rescale} \times Q_{cal} + B_{rescale}$$

where

$$G_{rescale} = \frac{LMAX_\lambda - LMIN_\lambda}{Q_{calmax} - Q_{calmin}}$$

$$B_{rescale} = LMIN_\lambda - \left(\frac{LMAX_\lambda - LMIN_\lambda}{Q_{calmax} - Q_{calmin}} \right) Q_{calmin}$$

where

L_λ	:	spectral radiance at the sensor's aperture [W/m² sr µm]
Q_{cal}	:	quantized calibrated pixel value [DN]
Q_{calmin}	:	minimum Q_{cal} corresponding to $LMIN_\lambda$ [DN]
Q_{calmax}	:	maximum Q_{cal} corresponding to $LMAX_\lambda$ [DN]
$LMIN_\lambda$	:	spectral at-sensor radiance that is scaled to Q_{calmin} [W/m² sr µm]
$LMAX_\lambda$	:	spectral at-sensor radiance that is scaled to Q_{calmax} [W/m² sr µm]
$G_{rescale}$	:	band-specific rescaling gain factor [(W/m² sr µm)/DN]
$B_{rescale}$	:	band-specific rescaling bias factor [W/m² sr µm]

While for Aster images, the conversion was performed by using the following equation (Ghulam, 2009):

$$L_{rad} = (DN - 1) \times UCC$$

where

L_{rad} : spectral radiance at the sensor's aperture [W/m^2 sr μm]

DN : digital number [DN]

UCC : unit conversion coefficient [W/m^2 sr μm]

- Conversion of at-sensor spectral radiance to Top of Atmosphere (TOA) reflectance

Both for TM and Aster images, the TOA reflectance was computed according to the following equation (Chander, Markham, & Helder, 2009; Ghulam, 2009):

$$\rho_\lambda = \frac{\pi \, L_\lambda \, d^2}{ESUN_\lambda \, cos\theta_s}$$

where

ρ_λ : planetary TOA reflectance [unitless]

π : mathematical constant (3.14159) [unitless]

d : earth–sun distance [astronomical units]

$ESUN_\lambda$: mean exoatmospheric solar irradiance [W/m^2 μm]

θ_s : solar zenith angle [degrees]; $\theta_s = 90^o$ – solar elevation angle

- Conversion of at-sensor spectral radiance to at-sensor brightness temperature

Based on the assumption of uniform emissivity of Earth's surface as a blackbody, the equation used to convert spectral radiance to brightness temperature was as follows (Chander et al., 2009; Ghulam, 2009):

$$T_B = \frac{K2}{\ln (K1 \, / \, L_\lambda + 1)}$$

where

T_B : effective at-sensor brightness temperature [K]

K1 : calibration constant 1 [W/m^2 sr μm]

K2 : calibration constant 2 [K]

The workflow of and the parameters used for the conversion of DN values to reflectance and brightness temperature is shown in Appendix 4.

3.2.2. Extraction of Land Surface Temperature

Brightness temperature needs to be adjusted based on the surface emissivity. The correction of emissivity will use Normalized Difference Vegetation Index (NDVI) Thresholds Method developed by Sobrino et al. (2004), which is assigning emissivity based on NDVI value. Pixels with NDVI values < 0.2 will be considered as built-up and bare soil, and will be given emissivity value of 0.97. Pixels with NDVI values > 0.5 will be considered as vegetation and will be given emissivity value of 0.99. For $0.2 \leq NDVI \geq 0.5$, the pixels are considered as mix of vegetation and bare soil. The emissivity for $0.2 \leq NDVI \geq 0.5$ is calculated by using the following equation:

$$\varepsilon = 0.004 \, P_v + 0.986$$

where

$$P_v = \left(\frac{NDVI - NDVI_{min}}{NDVI_{max} - NDVI_{min}}\right)^2$$

where

$$NDVI = \frac{\rho_{NIR} - \rho_{red}}{\rho_{NIR} + \rho_{red}}$$

where

ε   : emissivity
P_v : proportion of vegetation
$NDVI_{max}$: 0.5
$NDVI_{min}$: 0.2
ρ_{red} : reflectance values in the red channel
ρ_{NIR} : reflectance values in the near infra-red channel

The equation used for land surface temperature calculation is as follows (Artis & Carnahan, 1982):

$$T_S = \frac{T_B}{1 + (\lambda \times T_B / \rho) \ln \varepsilon}$$

where,

λ : wavelength of emitted radiance
ρ : hc / σ (1.438 x 10^{-2} mK)
h : Planck's constant (6.626 x 10^{-34} Js)
c : velocity of light (2.998 x 10^8 m/s)
σ : Boltzmann's constant (1.38 x 10-23 J/K)

The workflow of the extraction of land surface temperature is shown in Appendix 5.

3.3. Steps of the Analysis

3.3.1. Analysis on the Trend of Land Cover

The first step is a land cover classification employed to all images. The classification was performed using supervised classification method with maximum likelihood algorithm. The land cover was classified into four classes, which are water/shadow, bare soil, built-up, and vegetation. The selection of classes is based on the consideration that these classes are the main land cover types relevant for the study and identification of the training sets will be feasible. Post processing was performed by imposing that non built-up cover was never built-up in previous year, and by imposing road and river network from vector dataset as built-up and water/shadow cover respectively.

Four historical Google Earth images that were captured in the same year or in one year difference with Aster images were used as references for accuracy assessment since historical land cover maps of the study area were not available. 256 random points were generated and were overlaid on the historical Google Earth images, and served as sample points for accuracy assessment. The accuracy of the samples was then assessed for compliance with the reference points. The accuracy was measured by both the overall accuracy and Kappa statistics. Descriptive statistics analysis was conducted to clarify the area coverage (proportion) of each land cover type and its changes throughout the period.

3.3.2. Analysis on the Trend of Land Surface Temperature

Spatial pattern and descriptive statistics analysis of the surface temperature trend was conducted based on surface temperature maps. From 5 thermal channels of Aster (band 10-14), surface temperature was calculated for band 13 (10.25-10.95 μm) and band 14 (10.95-11.65 μm) because their wavelength are in the range of the wavelength of Landsat TM thermal channel (10.4-12.5 μm). However, only band 14 was used for the analysis since the temperature values extracted from band 13 show consistently higher values than band 14. Thus, the temperature values extracted from Aster band 14 are closer to the temperature values extracted from Landsat TM. Moreover, the central wavelength of Landsat TM thermal channel (11.4 μm) has a closer similarity with the central wavelength of Aster band 14 (11.3 μm) compared to Aster band 13 (10.6 μm). The comparison between mean temperature extracted from Landsat TM, Aster band 13 and 14 is shown in Figure 3.1. Spatial pattern analysis was performed to identify changes in hotspots and coldspots of surface temperature. Meanwhile, descriptive statistics analysis was carried out to clarify the temperature

values (mean temperature), intensities (range between maximum and minimum temperature), and changes, both for the overall study area and for each land cover class.
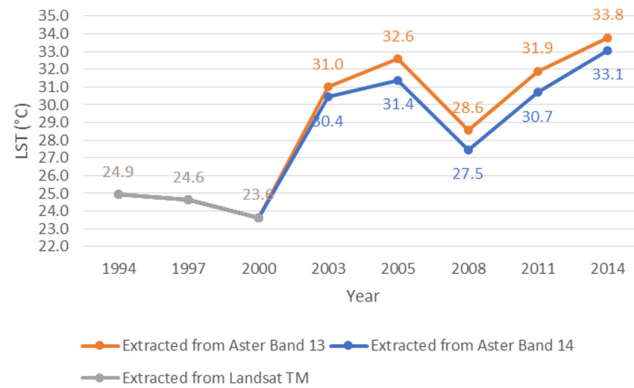
Figure 3.1 - Comparison between Mean Temperature Extracted from Landsat TM, Aster Band 13 and 14

3.3.3. Analysis on the Relationship between Land Surface Temperature and the Composition and Configuration of Land Cover

This analysis is limited to the years 2003-2014 because the accuracy assessment was not carried out for the land cover classification for 1994-2000 due to the absence of reference image. Thus, surface temperature and land cover maps which were the input for this analysis are entirely extracted from Aster images.

For identifying the relationship between land surface temperature and land cover, it is not only necessary to find out the effect of the composition of the land cover, but also the influence of the configuration (pattern) of the land cover. To represent the composition of land cover, the density of land cover was used as parameters while the aggregation of land cover was used as parameter to represent the configuration of land cover. The spatial metrics used for calculating the density of land cover was the Percentage of Landscape (PLAND), while the aggregation of land cover was calculated using the Aggregation Index (AI). PLAND and AI are Landscape Metrics. They were calculated for each type of land cover using Fragstat software. PLAND and AI were generated based on pixels that represent a land cover class in a binary raster map, so other land cover classes were previously assigned as background. PLAND and AI were performed using moving window method with a circular kernel for a certain radius from central pixel.

PLAND and AI values are expressed in percentage. PLAND value equal to 0% means that in an area with a certain radius, there is no pixel that represents a certain type of land cover. PLAND value equal to 100% means that all pixels in the area represent a certain type of land cover. Meanwhile, AI value equal to 0% means that every pixels in the area that represent a certain type of land cover are completely fragmented with no adjacent pixels. AI value equal to 100% means that every pixel in the area that represent a certain type of land cover are perfectly aggregated or clumped.

In addition, the Normalized Difference Vegetation Index (NDVI) was also used to represent vegetation density. NDVI is an indicator that is commonly used to represent vegetation density. Many researchers have studied the relationship of NDVI and land surface temperatures. Thus, it was expected that the results of the analysis on the relationship between land surface temperature and NDVI can be compared with the results of the analysis on the relationship between land surface temperature and vegetation density calculated using PLAND.

The correlation analysis was conducted between the land surface temperature and land cover density and between the land surface temperature and aggregation index of land cover to identify the presence of a linear relationship between the variables. Therefore, the analysis was performed using Pearson correlation and simple linear regression method to clarify the type, the direction, the strength, and the significance of the

relationship. In regression analysis, the dependent variable was land surface temperature, while the independent variables were land cover density and aggregation index.

The values for PLAND and AI varies depending on the selected search radius. Therefore, a sensitivity analysis was performed to identify the optimal radius that gives the highest correlation coefficient. The sensitivity analysis was done only for the correlation calculation between land surface temperature and PLAND. However, the identified optimal radius was then used to generate AI. Thus, it was expected that results of correlation calculation between land surface temperature and PLAND and between land surface temperature and AI could be compared. The sensitivity analysis was performed for radii with a difference of 15 m, in accordance with the spatial resolution of Aster image. Thus, the sensitivity analysis started from 15 m radius and stopped when a continuous declining trend was found for at least three radii in a row.

To identify whether the NDVI values of neighbouring pixels influence land surface temperature at the central pixel, correlation was calculated between land surface temperature and mean value of NDVI based on the result of a focal analysis. Focal analysis was done by calculating the mean value of NDVI in area with a certain radius from the central pixel, and the mean value was then assigned for the central pixel. This analysis was performed using moving window method with a circular kernel to produce consistent results with the PLAND analysis. Focal analysis was assigned for mean NDVI calculation because the value of NDVI is floating value. While, PLAND calculation was more appropriate for binary maps. Focal analysis was performed using Erdas software. The correlation between land surface temperature and mean NDVI showed variations for different search radius (kernel size). Therefore, a sensitivity analysis was also performed to identify the optimal radius that gives the highest correlation coefficient.

In the sensitivity analysis, the correlation was calculated using pixel by pixel correlation between land surface temperature and mean NDVI and PLAND for the different search radius. However, because the number of observation (pixels) was considerably large (approximately 10,000 - 750,000 pixels), the observation points on the scatterplot were very dense and the relationship pattern between land surface temperature and mean NDVI and PLAND was difficult to be observed. Therefore, for PLAND and AI, samples were selected by limiting observation only for the pixels that have the same land cover type with the observed land cover density or aggregation index. For example, samples of built-up density was selected by restricting observation only to built-up pixels. This was done only for PLAND and AI generated with identified optimal radius. Afterwards, correlation and regression analysis were performed between the mean temperature and the unique value of mean NDVI, PLAND, and AI.

3.3.4.   Analysis on the Relation between Green Spaces Planning and Land Surface Temperature

For this purpose, areas that represent different urban typologies were selected using ArcGIS Online Imagery, Google Earth, existing land use, and land use plan of the city. The observed urban typology consist of 20 areas to represent the different typology which are common in the study area. The typology also represents the different types of vegetation, water bodies and built-up cover. Typology representing vegetation cover is urban forest, parks, golf courses and sports fields, grass land, rice fields, farm fields (non-rice fields), and plantation. Typology representing water bodies is wet rice fields and river. While, typology representing built-up cover is industrial with more green spaces, industrial with less green spaces, commercial, offices, low density formal residential, medium density formal residential, high-density formal residential, high-density non-formal residential, road with street trees, road without street trees, and narrow road surrounded by high buildings (urban canyon). The surface temperature values were obtained by creating 30 random points for each typology, then the temperature value for each point were extracted using zonal statistics tool in ArcGIS. The relationship between surface temperature and urban typologies was analysed based on boxplot of temperature and visual analysis of the image. Moreover, transects and buffer zones around the city centre were used to analysis the spatial pattern of surface temperature from the city centre towards the urban fringe.

4.   RESULTS AND DISCUSSION

4.1.   The Trend of Land Cover

The overall accuracy of land cover classification has a range of 78%-84%, while Kappa statistics has a range of 0.69-0.77. Lower accuracy were found for bare soil cover. The accuracy assessment report for land cover classification of 2014 showed that many pixels of bare soil were wrongly classified as built-up (Appendix 6). From the accuracy totals and the error matrix of land cover classification assessment report for the year 2014, bare soil cover had the lowest producers accuracy (76%) compared to the other classes and most of the incorrectly classified pixels were built-up cover. The number of correctly classified bare soil cover was 32 pixels from 42 reference pixels. Meanwhile, six pixels are incorrectly classified as built-up, two pixels are incorrectly classified as vegetation, and two pixels are incorrectly classified as water/shadow cover.

In the study area, bare soil was found only in small areas. With 30 m and 15 m spatial resolution of Landsat TM and Aster respectively, a quite large and homogeneous area of bare soil was difficult to find. Bare soil was also found in various types. This included wet bare soil (for example, rice field in planting season), bare soil with a small portion of vegetation (for example, neglected land which overgrown with shrubs or bushes), and bare soil in the construction site. Thus, the reflectance of the different type of bare soil was affected by the other types of land cover and became very close to the reflectance of water, vegetation, or built-up cover. This caused difficulty in the selection of good and quite consistent training sets for bare soil in the land cover classification process.

Aster Image Acquisition Date	Google Earth Image Acquisition Date	Reference Totals	Classified Correct	Overall Accuracy	Kappa Statistics
12 June 2003	21 August 2003	256	214	84%	0.77
25 June 2008	26 May 2007	256	209	82%	0.75
22 September 2011	13 June 2010	256	199	78%	0.69
5 September 2014	15 September 2014	256	215	84%	0.77

Table 4.1 - Land Cover Classification Accuracy Assessment

Based on the result of image classification, land cover trends in Bandung city 1994-2014 are shown in Table 4.2, Table 4.3, and Figure 4.1. There are small differences of the total area of the city between the land cover classified from Landsat TM images (1994-2000) and Aster images (2003-2014). These differences are due to the difference in spatial resolution between the two images, where Landsat TM image has a spatial resolution of 30 m while Aster image has a spatial resolution of 15 m, the difference in the area coverage occurred for the edge pixels in the sub-setting (clipping) process which was based on the vector boundary of the city. The total area in land cover classified from Landsat TM image was 169.0 km², while the total area in land cover classified from Aster image was 168.2 km². Therefore, the explanation on the trend of land cover is carried out by referring to the proportion of land cover to the total area of the city or the percentage value. Water/shadow cover shows a stable trend but with a little fluctuation. For the overall period, area with water/shadow cover had a range of 4% to 9%. The largest decrease occurred in 2003 (2%), while the largest increase occurred in 2014 (4%). The water/shadow cover had an average of 0.1% increase per year.

Built-up and vegetation were dominant land covers in the study area. For the overall period, built-up showed an increasing trend. Area with built-up cover in 2014 increased dramatically compared to 1994, from 35% in 1994 to 60% in 2014, or increased by 25%. Built-up cover consistently increased every year except in 2000 where built-up cover slightly decreased by 0.5%. The 2000 image is one of the images that has thick cloud covers. Therefore, it is possible that the thick clouds covered some built-up areas in 2000. The increase of built-up cover had an average of 4% per year. The largest increase occurred in the last period of 2011-2014 when built-up cover increased by 15%.

In general, vegetation cover showed a little decreasing trend for the overall period. The decrease of vegetation cover had an average of 1% per year. Area with vegetation cover in 2014 decreased by 6% compared to 1994, from 36% in 1994 to 30% in 2014. However, anomalies occurred in 1997 and 2000 when the vegetation cover increased dramatically from 36% in 1994 to 58% in 1997, and then slightly decreased to 55% in 2000. The drastic increase of vegetation cover in this period needs to be related to the drastic decline of bare soil cover. Thus, inconsistencies were likely to occur in the process of land cover classification for the year 1997 and 2000, especially in the selection of training sets, so that mixed pixels of bare soil and a bit of vegetation cover were classified as vegetation. Unfortunately, this presumption could not be proven because the accuracy assessment for the land cover classification result for the period 1994-2000 could not be performed due to the absence of the reference image. This has become one of the limitations of this study.

For the overall period, bare soil cover showed a fluctuating pattern. However, anomalies or irregularities were particularly seen on the drastic decline in 1997, 2000 and 2014. In these years, proportion of bare soil cover to the total area of the city was 0.1%, 0.2% and 1.5% respectively. Meanwhile, for the other years, area with bare soil cover had a range of 20-25%. As previously mentioned, this raised presumption of inconsistencies in the process of land cover classification.

Although all satellite images have cloud cover that varies from 1-5% (see Table 3.2), but thick cloud covers and shadows from the clouds over some areas of the city were only found in the images of 2000, 2005, and 2008. In the images for those years, some areas also have a thin layer of cloud (haze). However, the identification of cloud cover was only performed for areas with a thick cloud cover. Thick clouds were masked out, while the shadows from the clouds were not masked and were generally classified as water/shadow cover. Area with cloud cover in 2000, 2005 and 2008 was 0.2%, 1.3% and 0.4% respectively. In every next step, the areas or the pixels that were identified as thick cloud cover were excluded from information extraction and analysis.

Land Cover	Area (km²)							
	1994	1997	2000	2003	2005	2008	2011	2014
Bare soil	37.8	0.2	0.4	37.5	35.2	41.7	31.9	2.6
Built-up	59.1	61.4	60.7	60.6	63.4	67.3	76.8	101.4
Vegetation	60.2	98.4	92.6	58.3	58.2	49.2	52.4	50.9
Water/Shadow	11.8	8.9	14.9	11.8	9.3	9.3	7.2	13.3
Cloud	-	-	0.4	-	2.2	0.7	-	-
Total	169.0	169.0	169.0	168.2	168.2	168.2	168.2	168.2

Table 4.2 - Land Cover Trend of Bandung City by Area 1994-2014

Land Cover	Proportion to Total Area (%)							
	1994	1997	2000	2003	2005	2008	2011	2014
Bare soil	22.4	0.1	0.2	22.3	20.9	24.8	19.0	1.5
Built-up	35.0	36.4	35.9	36.0	37.7	40.0	45.6	60.3
Vegetation	35.6	58.3	54.8	34.7	34.6	29.3	31.1	30.3
Water/Shadow	7.0	5.3	8.8	7.0	5.5	5.5	4.3	7.9
Cloud	-	-	0.2	-	1.3	0.4	-	-
Total	100.0	100.0	100.0	100.0	100.0	100.0	100.0	100.0

Table 4.3 - Land Cover Trend of Bandung City by Proportion to Total Area 1994-2014
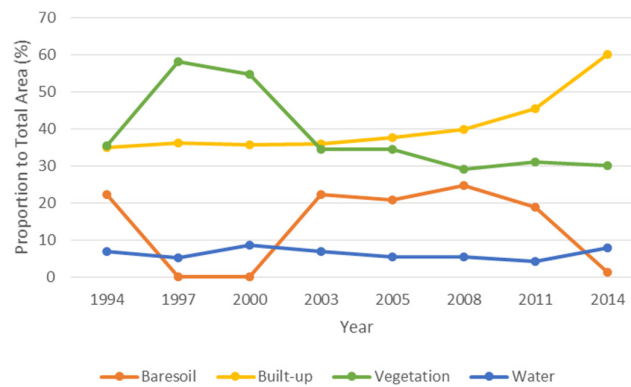
Figure 4.1 - Land Cover Trend of Bandung City by Proportion to Total Area 1994-2014

Land cover of Bandung city 1994-2014 is shown in Figure 4.2. In general, the concentration of built-up cover is located in the central part of the city. This concentration seems getting bigger every year and mainly expands to the eastern part of the city. The concentration of vegetation cover appears in the southeast, the northeast, and the northwest parts of the city. Bare soil cover does not have a concentration area or scattered in small areas in all parts of the city. Areas with water/shadow cover seem to change every year, but generally found in the southeast part of the city. Areas with water/shadow cover are generally wet rice fields. Thus, the changes are very likely influenced by the planting and the harvesting season.

Analysis of spatial pattern of land cover is performed based on spatial pattern that appears on the land cover density maps generated using PLAND method. The land cover density maps were generated using a moving window method with a circular kernel for a radius of 135 m. This radius is the result of sensitivity analysis which gives the highest correlation coefficient between land cover density and land surface temperature (see Section 4.3). The spatial pattern of land cover is analysed only for built-up and vegetation cover as the dominant land covers in the study area. However, bare soil and water/shadow density maps can be seen in Appendix 7 and 8.

Built-up density maps of Bandung city 1994-2014 are shown in Figure 4.3. The maps show that areas with high built-up density have been more concentrated in the central part of the city and the concentration has been getting bigger every year. Increased concentration has especially occurred in recent years which appeared on the difference between built-up density maps of 2011 and 2014. In addition, areas with high built-up density have mainly spread to the eastern part of the city. Thus, the growth of built-up areas have been more intensive and more compact in the central part of the city and has been more extensive to the eastern part of the city.

The opposite situation is found for the spatial pattern of vegetation. Based on vegetation density maps of Bandung city 1994-2014 (Figure 4.4) areas with high and medium vegetation density have been diminishing and are more difficult to find in the central part of the city. This could mean that vegetation patches in the central part of the city have been increasingly converted to built-up areas and have been more fragmented. Areas with high vegetation density are more concentrated in the urban fringe areas in the southeast, the northeast, and the northwest part of the city, which are the remainder of the agricultural areas. However, these areas also have been getting smaller every year, indicating the conversion of agricultural land into built-up area in the urban fringes. Irregularities appear on the vegetation density maps of 1997 and 2000. For these years, areas with high and medium vegetation density appear much larger compared to the other years. Based on the results of the land cover classification, vegetation cover in 1997 and 2000 does have a very large area compared to the other years.

Figure 4.2 - Land Cover of Bandung City 1994-2014

Built-up Density of Bandung City 1994

Built-up Density of Bandung City 1997

Built-up Density of Bandung City 2000

Built-up Density of Bandung City 2003

Built-up Density of Bandung City 2005

Built-up Density of Bandung City 2008

Built-up Density of Bandung City 2011

Built-up Density of Bandung City 2014
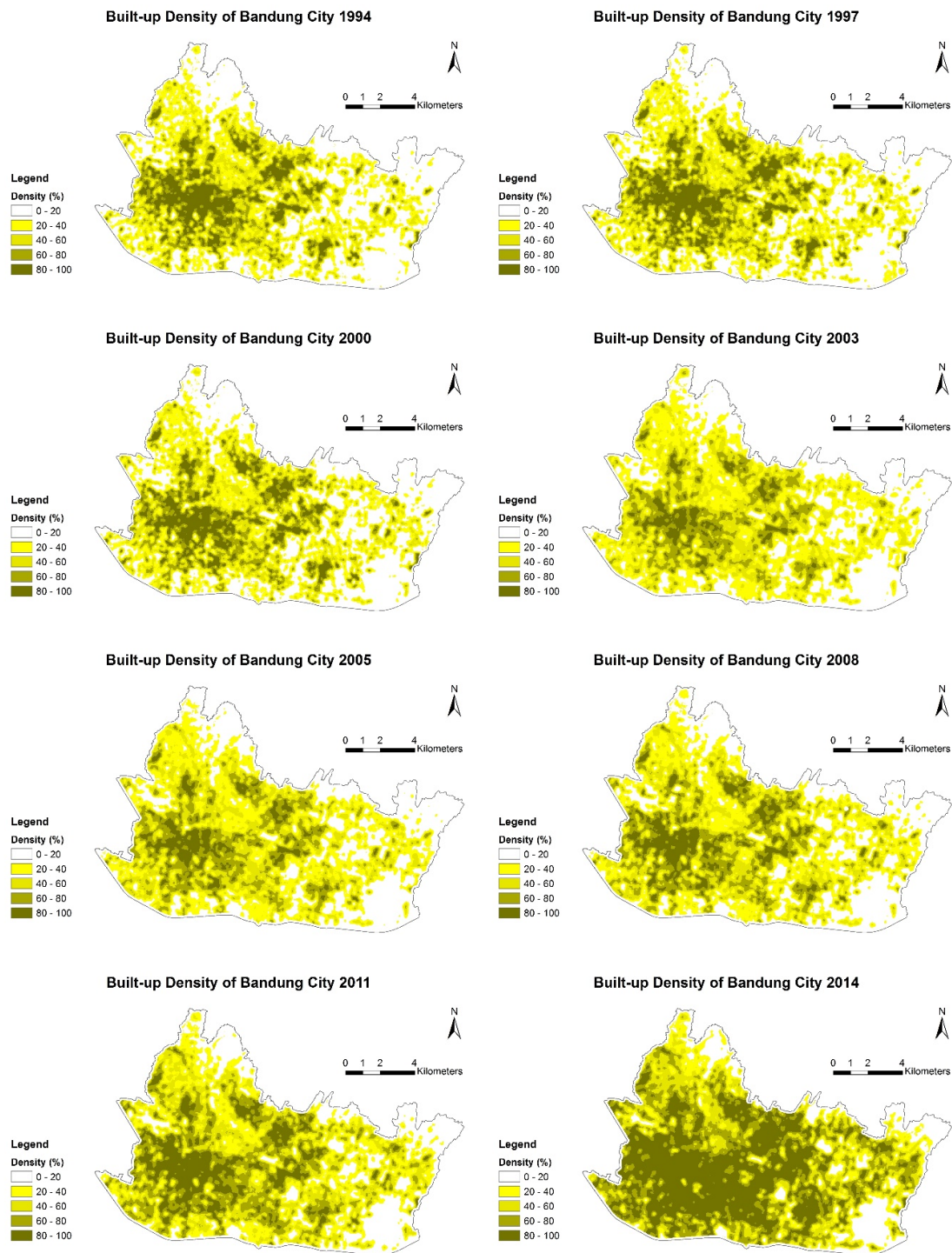
Figure 4.3 - Built-up Density of Bandung City 1994-2014
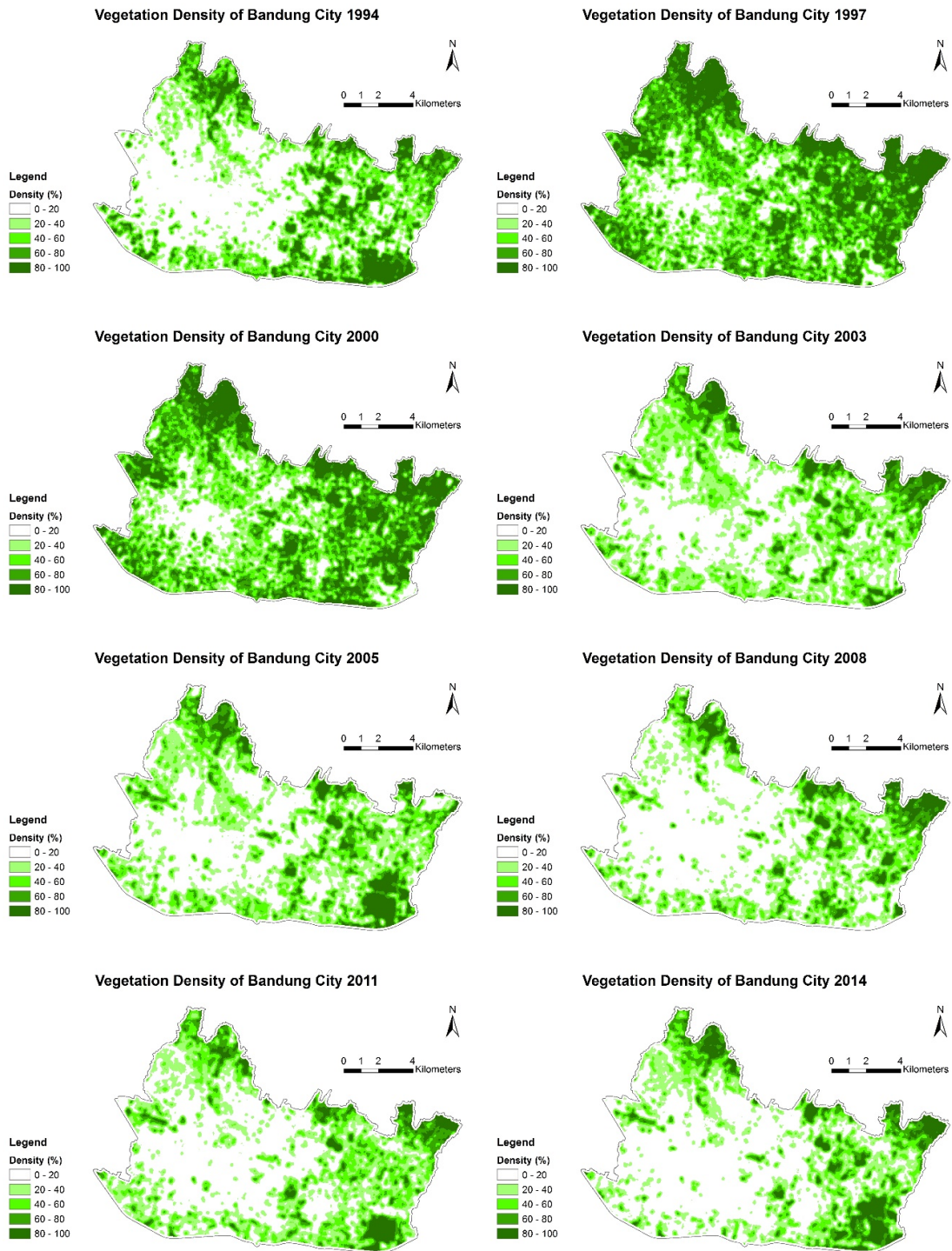
Figure 4.4 - Vegetation Density of Bandung City 1994-2014

4.2.   The Trend of Surface Temperature

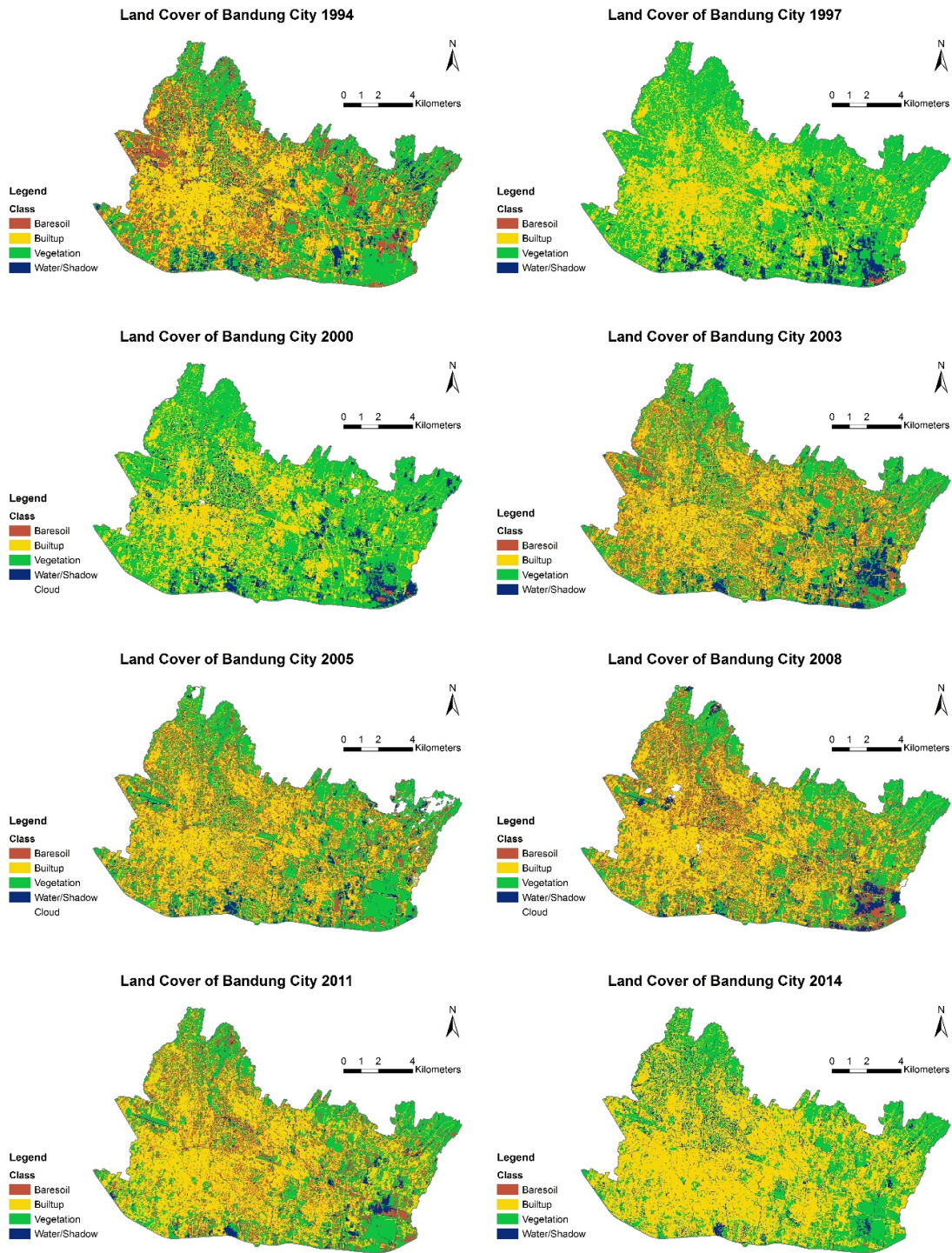Within this section, the land surface temperature statistics in Bandung city for 1994-2014 are analysed (Table 4.4). For the overall study period, minimum temperature had a range of 10-18°C, 30-43°C for the maximum temperature, and 24-33°C for the mean temperature. The lowest values for the minimum, the maximum, and the mean temperature occurred in 1997 and 2000, using Landsat TM images for the surface temperature extraction. The lowest minimum temperature occurred in 1997 (10°C), the lowest maximum temperature occurred in 1997 and 2000 (30°C), and the lowest mean temperature occurred in 2000 (24°C). Meanwhile, the highest values for the minimum, the maximum, and the mean temperature occurred in 2014 (18, 43 and 33°C respectively). In this most recent year Aster images were used, the mean temperature value in 2014 was even equal with the highest maximum temperature value in the 1994-2000 period (33°C), using Landsat TM images for the surface temperature extraction. In addition, for the overall study period, temperature intensity or the difference between the maximum and the minimum temperature had a range of 16-28°C. The lowest intensity occurred in 2000 (16°C), while the highest intensity occurred in 2005 and 2011 (28°C). The average difference between the maximum and the minimum temperature is 23°C.

In general, the mean temperature values show an increasing trend from year to year (Figure 4.5). Despite the slight decreases in 1997 and 2000 and more significant decreases in 2008, the overall mean temperature still shows an increasing trend. In fact, the mean temperature in 2014 has a very big difference when compared with 1994, which is 8°C.

In addition to the overall trend, there are also significant differences between the mean temperature values in the period 1994-2000, when the surface temperatures were extracted from Landsat TM images, and in the period 2003-2014, when the surface temperatures were extracted from Aster images. The mean temperature values in the period 2003-2014 are always much higher compared to the mean temperature values in the period 1994-2000. The mean temperature values in 1994-2000 had a range of 24-25°C, while the mean temperature values in 2003-2014 had a range of 27-33°C. It can be concluded that the land surface temperature extracted from Aster images tends to have a higher value than the land surface temperature extracted from Landsat TM images. This striking difference is also shown comparing the mean temperature value in 2000 (Landsat TM) and 2003 (Aster), where the mean temperature in 2003 is higher by 6°C compared to 2000. Although strongly influenced by variations in the intensity of solar radiation and other factors described in the Literature Review (Chapter 2), but the differences in the thermal bandwidth and spatial resolution of the Landsat TM and Aster sensor are influencing factor for this condition.

Year	Land Surface Temperature (°C)			
	Min.	Max.	Range	Mean
1994*	15.7	33.2	17.5	24.9
1997*	10.1	30.4	20.3	24.6
2000*	14.3	30.4	16.1	23.6
2003**	13.8	39.4	25.6	30.4
2005**	11.4	39.5	28.1	31.4
2008**	16.6	36.2	19.6	27.5
2011**	14.8	43.0	28.2	30.7
2014**	17.7	43.3	25.7	33.1

Table 4.4 - Land Surface Temperature 1994-2014
Note:
* Extracted from Landsat TM image
** Extracted from Aster image
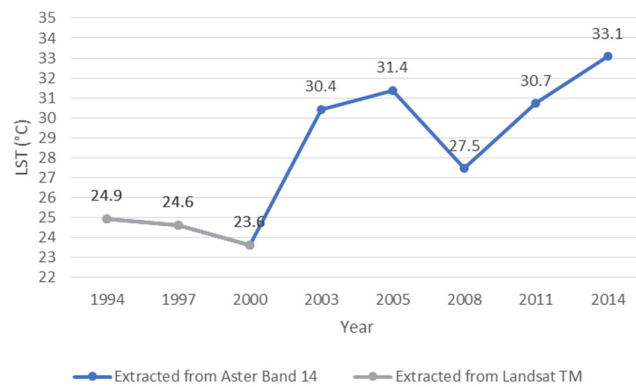
Figure 4.5 - Mean Surface Temperature 1994-2014

The spatial pattern of land surface temperature in Bandung city for 1994-2014 in 10 temperature ranges (classes) are shown in Figure 4.6. Quantile visualization method was used to assign the same number of data values to each class. Therefore, caution is needed in interpreting the spatial pattern of temperature as shown on the maps. For example, areas with the same colour on the maps in different years do not mean that they have the same temperature values/ranges. The spatial pattern of land surface temperature visualized in equal temperature classes can be seen in Appendix 9.

It can be observed that there is a general similarity in the spatial pattern of land surface temperature for the different years where the hotspots are mainly located in the central and the west parts of the city. The coldspots are mainly located in the northwest, the northeast, and the southeast parts of the city. However, in more details, the locations of hotspots (areas under the highest temperature range) show variations for each year while the locations of coldspots (areas under the lowest temperature range) are more stable. The coldspots that consistently become areas with lower temperatures are large areas dominated by vegetation cover (agricultural fields) in the northwest, the northeast, and the southeast parts of the city. Another cooler area is a smaller area in the south part of the city which is covered by water (wet rice field). Meanwhile, areas with higher temperatures are consistently high density built-up areas, however, the locations of the hotspots show variations for the different years. A very stable hotspot area is an area in the west part of the city which is a part of airport area. The differences in hotspot locations can be affected by various factors. One factor is differences in the weather, the speed and the direction of the wind at the time of image acquisition and variations in radiometric conditions (e.g. thin cloud cover of part of the image).

An anomaly or a quite different spatial pattern of temperature compared to the other years appears in the year 2000. In this year, an area in the central part of the city has a rather low temperature. This is different with the pattern for the other years where this area generally has high temperature. This anomaly is influenced by the presence of thin clouds in this area in the 2000 satellite image.

The spatial pattern of surface temperature as shown in Figure 4.6 will show a different pattern when visualized by using a different classification method for the different temperature classes. For example, visualization using a stretch of the minimum-maximum value method will provides more detailed information on the areas that have the highest and the lowest temperature values for each year. However, by using these methods, it will be more difficult to compare the general spatial patterns of temperature among different years. Visualization with quantile method is considered as the most appropriate method in this case because the differences in the variations of the minimum and the maximum temperature values among different years are quite high. For example, in 1994, the temperature values have a range of 10-30°C, while in 2014 the temperature values have a range of 18-43°C.
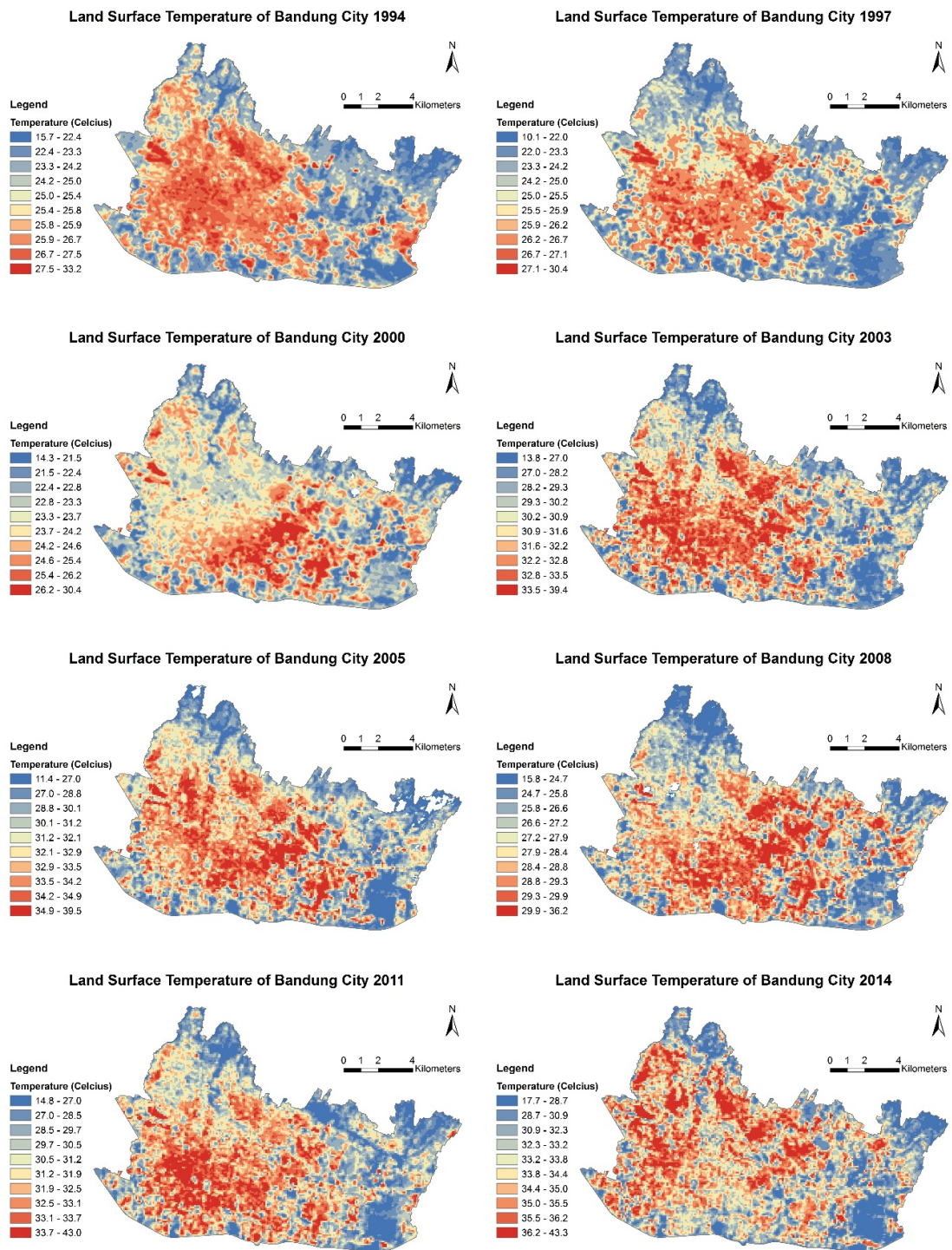
Figure 4.6 - Spatial Pattern of Land Surface Temperature in Bandung City 1994-2014
Note: White spots are areas of clouds that have been masked.

In Figure 4.7, the mean temperature trend is compared with the trends of built-up and vegetation cover. In general, it can be observed that the mean temperature trend shows a relationship with built-up and vegetation cover trend. Mean temperature and built-up cover show a positive relationship, while on the contrary, mean temperature and vegetation cover show a negative relationship. This means that an increase in the built-up cover will tend to increase the mean temperature. Conversely, an increase in the vegetation cover will tend to decrease the mean temperature.

The discussion in this section gives a preliminary and general picture regarding the presence of a relationship between the mean temperature and the built-up cover and between the mean temperature and the vegetation cover for the overall study area. A more detailed explanation regarding this relationship will be delivered in Section 4.3. Furthermore, these relationships only show a tendency or an indication. The mean temperature of course is also influenced by the increase or decrease in built-up and vegetation cover in a proportional and aggregate way. This means that a large increase in the built-up cover and a small increase in the vegetation cover that happen in the same year will tend to increase the mean temperature, and vice versa.

To show this relationship more clearly, the observation needs to be discussed per year. When the mean temperature shows a downward trend in the period of 1994-2000 (from 24.9 to 23.6°C), the vegetation trend shows an increase (from 60 to 93 km²) while the built-up trend tend to be relatively stable, although there is a slight increase of the built-up cover in the period of 1994-1997 (from 59 to 61 km²). Meanwhile, when the mean temperature trend shows a drastic increase in the period of 2000-2003 (from 23.6 to 30.4°C), the vegetation trend shows a sharp decline (from 93 to 58 km²) and built-up trend remains relatively stable. In the period of 2003-2005, the mean temperature trend shows a slight increase (from 30.4 to 31.4°C). This is similar with the built-up trend (from 61 to 63 km²), whereas the vegetation trend tends to be relatively stable. In the period of 2008-2014, a similar trend is also shown by the mean temperature and the built-up area, both show a drastic increase (from 27.5 to 33.1°C and from 67 to 101 km² respectively). In this period, the vegetation trend tends to be relatively stable or shows only a little fluctuation (from 49 to 51 km²). The mean temperature in 2014 has the highest value when compared to the other years (33.1°C). This reflects that in this most recent year, the extent of vegetated cover has been slightly reduced and the expansion of built-up cover has dramatically grown.
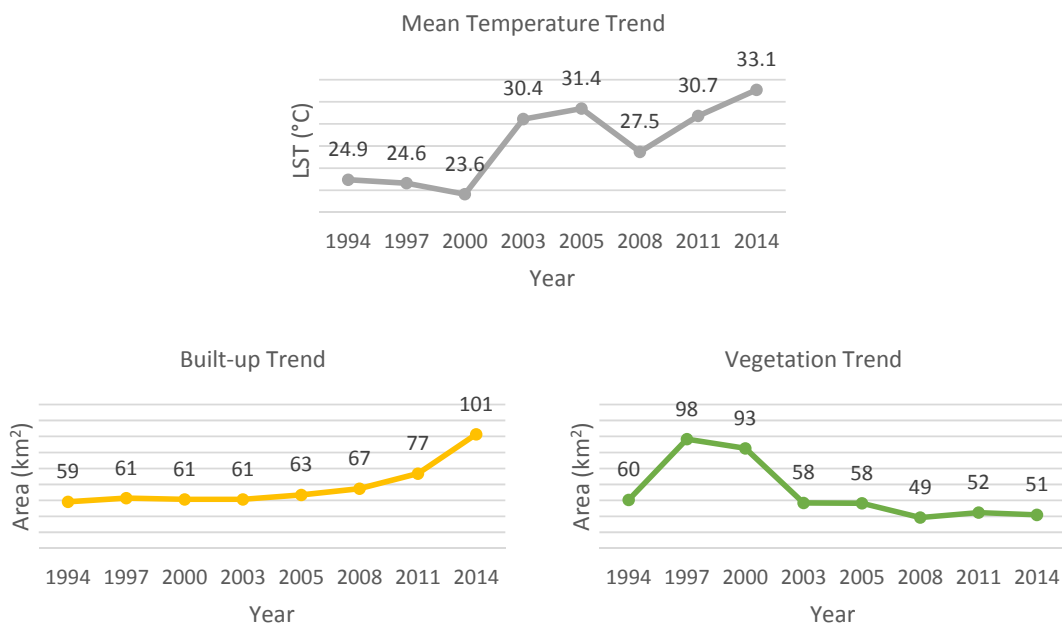
Figure 4.7 - Mean Temperature, Built-up and Vegetation Trend 1994-2014

Once again, the anomaly shown in 2008 in which the mean temperature trend shows a significant decline (from 31.4 to 27.5°C) although built-up cover shows an increasing trend (from 63 to 67 km²) and vegetation cover shows a decreasing trend (from 58 to 49 km²). This anomaly is related to the radiometric conditions of the image of 2008, the image has a thick cloud covers over parts of the study area (Figure 4.8).
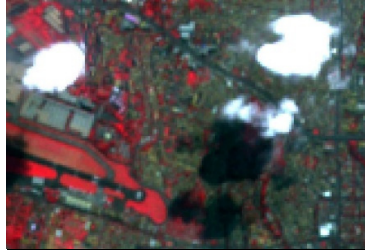
Figure 4.8 - Cloud Cover over the Central Part of the City in Image 2008

The relation of land cover type and mean temperature is shown in Figure 4.9 Built-up cover consistently has the highest mean temperature throughout the 1994-2014 period. Meanwhile, in general, the mean temperatures are lowest for water/shadow and vegetation cover. This result seem fairly consistent for each year. However, there are different and unexpected results for 1997 and 2000 where the mean temperatures are lowest for bare soil.

For the overall period, the mean temperature values had a range of 21-33°C for bare soil, 24-34°C for built-up, 23-31°C for vegetation, and 22-33°C for water/shadow. The lowest mean temperatures for bare soil and water/shadow occurred in 1997, while the lowest mean temperatures for built-up and vegetation occurred in 2000. On the other hand, the highest mean temperatures for all land cover types occurred in 2014. The detail statistics of land surface temperature per land cover class can be seen in Appendix 10.

In addition, the mean temperature differences among different types of land cover consistently show quite low differences. In fact, temperature differences between land covers with the highest and the lowest mean temperature for each year only had a range of 2-5°C. The smallest difference occurred in 2008 (2°C), while the biggest difference occurred in 1997 (5°C). For the overall period, the average difference between the highest and the lowest mean temperature is 3°C.

The absolute temperature difference (Table 4.4) and the mean temperature difference among land cover types are essential in explaining the effect of urban heat island in the study area. A partial use of the absolute temperature difference may lead to an interpretation that the effect of urban heat island is very high. For example, in 2011, the absolute temperature difference was the highest compared to the other years, which reached 28°C. However, for the same year, the mean temperature difference between built-up and vegetation cover was only 3°C.
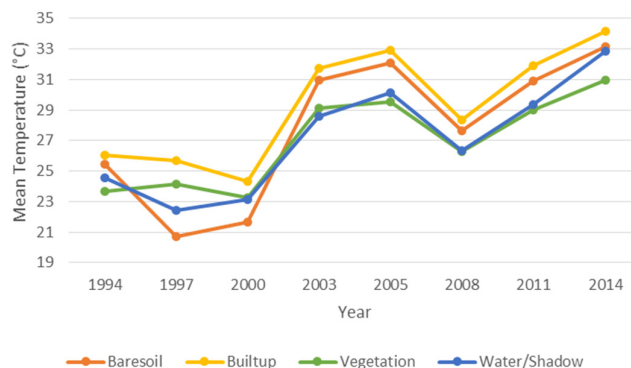
Figure 4.9 - Mean Temperature per Land Cover Class 1994-2014

To identify whether the values of surface temperature can reflect the values of air temperature, the surface temperatures was compared with the measured air temperatures from Bandung Meteorological Station for the same dates of the image acquisition. However, the air temperature data from Bandung Meteorological Station was derived from the measurement over a time span of one day (24 hours). The surface temperature for each year was identified for the corresponding pixel based on the geographical location of the meteorological station (Figure 4.10).

Figure 4.10 - Location of Meteorological Station of Bandung

Table 4.5 and Figure 4.11 show the land surface and air temperature trend of the location of the Meteorological Station of Bandung between 1994-2014. For the overall period, the land surface temperatures are always higher than the daily mean air temperature. The land surface temperature values had a range of 24-33°C. Meanwhile, the mean air temperature values had a range of 22-24°C.

The land surface temperature derived from Landsat TM images (1994-2000) are consistently higher than the mean air temperature and lower than the maximum air temperature. Meanwhile, the land surface temperature derived from Aster images (2003-2014) are even always higher than the maximum air temperature, except in 2008. In fact, the land surface temperature and the maximum air temperature pattern in 2003-2014 is quite similar. For every periods, when the maximum air temperature showed either an increasing or decreasing trend, the land surface temperature also showed the same trend. When the maximum air temperature showed a slight increase in the period of 2003-2005 (from 31.0 to 31.6°C), the land surface temperature also showed a slight increase (from 31.6 to 32.5°C). In the period of 2005-2008, the maximum air temperature trend showed a sharp decline (from 31.6 to 28.8°C). This was similar with the land surface temperature trend (from 32.5 to 27.2°C). In the period of 2008-2014, a similar increasing trend was also shown for the maximum air temperature and the land surface temperature (from 28.8 to 30.2°C and from 27.2 to 32.2°C respectively).

Interpretation of the results discussed above could only give a first indication about the presence of a relationship between surface and air temperature. Hourly air temperature data would be required to establish a clear relation between surface and air temperature to generate a better results. The air temperature from Bandung Meteorological Station was daily data from 24 hours measurement. While, the surface temperature values were obtained at the image acquisition time that varies from 9 to 10 AM.

Since the Meteorological Station is dominated by built-up surfaces that have a strong ability to absorb heat, solar radiation heat up the surfaces to above the air temperature. Moreover, assuming that the maximum surface temperature is formed when the solar radiation reach its peak around 12 AM when the sun is perpendicular above the city, the surface temperatures on the location of Meteorological Station of Bandung can be much higher than the air temperatures. Thus, this finding is consistent with the explanation in literature (U.S. Environmental Protection Agency, 2012).

Date	Land Surface Temperature (°C)	Air Temperature (°C)		
		Min.	Max.	Mean
22/09/1994	27.1*	17.6	30.2	24.1
26/06/1997	25.4*	16.0	29.6	21.9
20/07/2000	24.1*	17.6	29.5	22.7
12/06/2003	31.6**	14.4	31.0	22.6
07/10/2005	32.5**	19.0	31.6	24.4
25/06/2008	27.2**	18.2	28.8	22.7
22/09/2011	30.1**	17.6	29.3	22.8
05/09/2014	32.2**	N/A	30.2	23.5

Table 4.5 - Land Surface Temperature and Air Temperature Trend on the Location of Meteorological Station of Bandung 1994-2014
Note:
* Extracted from Landsat TM image
** Extracted from Aster image
N/A: Data not available
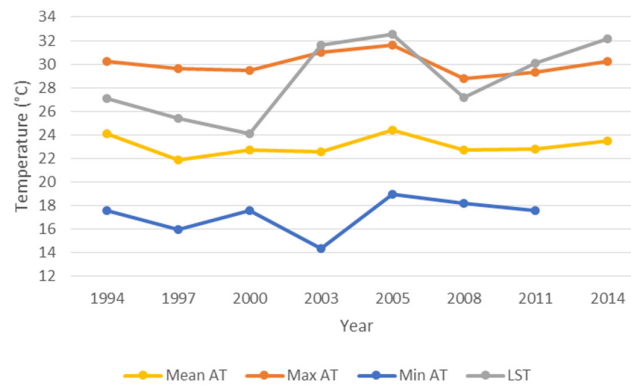
Figure 4.11 - Land Surface and Air Temperature Trend on the Location of Meteorological Station of Bandung 1994-2014
Note:
AT: Air temperature

4.3. The Relationship between Land Surface Temperature and the Composition and Configuration of Land Cover

4.3.1. The Relationship between Land Surface Temperature and NDVI

NDVI of Bandung city 2003-2014 is shown in Figure 4.12. For the overall period, NDVI has a quite stable range, approximately from -0.3 to 0.8. In general, areas with low NDVI values were areas with built-up cover located in the central and western part of the city. Meanwhile, areas with high NDVI values were areas with vegetation cover located on the northwest, northeast, and southeast part of the city. NDVI pattern for each year has relatively not much changed, except for area in the southeast part of the city. This area is an agricultural field so that the differences in NDVI values for each year can be caused by the differences in the planting and harvesting seasons.
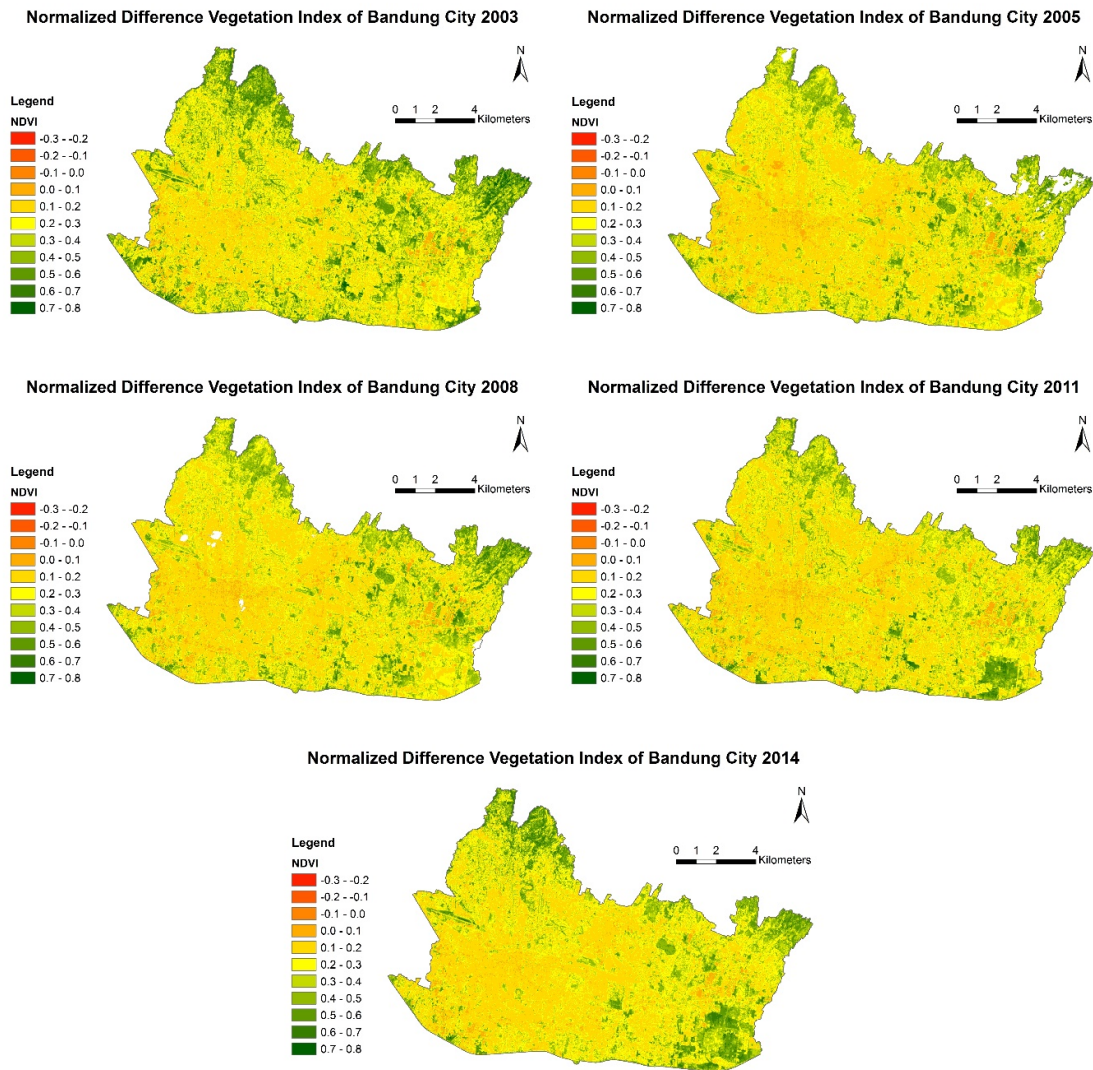
Figure 4.12 - Normalized Difference Vegetation Index of Bandung City 2003-2014
Note: White spots are areas of clouds that have been masked.

Pearson correlation of NDVI and land surface temperature 2003-2014 is shown in Table 4.6. For the overall period, the correlation coefficients have a range from -0.5 to -0.6. Thus, NDVI and land surface temperature has moderate and negative correlation. This means the higher the NDVI value, the land surface temperature tends to be lower. The significant values are always smaller than 0.01, which means the correlations are statistically significant for every years. The lowest correlation coefficient is found in 2003, while the highest correlation coefficient is found in 2014.

	2003	2005	2008	2011	2014
Pearson correlation coefficient	-0.49	-0.53	-0.50	-0.55	-0.59
Significant value (p-value)	0.00	0.00	0.00	0.00	0.00
Number of observation	744,803	735,253	741,585	744,803	744,803

Table 4.6 - Correlation of NDVI and LST 2003-2014

To identify whether the NDVI value of neighbouring pixels could influence the land surface temperature at the central pixel, correlation was calculated between land surface temperature and mean value of NDVI based on the result of focal analysis. Focal analysis was done by calculating the mean value of NDVI in area with a certain radius from the central pixel, and the mean value was then assigned for the central pixel. Sensitivity analysis was then performed to identify the optimal radius that gives the highest correlation coefficient.

Correlation of mean NDVI and land surface temperature 2003-2014 for different radius of focal analysis is shown in Table 4.7 and Figure 4.13. The highest correlation coefficients are found in the radius of 120-150 m or 8-10 pixels. These coefficients have a range from -0.6 to -0.7. For every year, these coefficients are higher than the initial correlation coefficient of NDVI and land surface temperature. Thus, the NDVI value of neighbouring pixels does influence the land surface temperature at the central pixel,. The significant values are always smaller than 0.01, which means the correlations are statistically significant for every years. The lower correlation coefficients are found in 2003 and 2008, while the higher correlation coefficients are found in 2005, 2011, and 2014.

	Radius (m)	Pearson Correlation Coefficient				
		2003	2005	2008	2011	2014
1	15	-0.518	-0.565	-0.525	-0.575	-0.613
2	30	-0.549	-0.602	-0.553	-0.610	-0.642
3	45	-0.579	-0.638	-0.580	-0.643	-0.668
4	60	-0.598	-0.660	-0.597	-0.665	-0.684
5	75	-0.615	-0.679	-0.612	-0.683	-0.696
6	90	-0.624	-0.688	-0.620	-0.694	-0.701
7	105	-0.630	-0.694	-0.624	-0.700	-0.704
8	120	-0.634	-0.698	-0.626	-0.705	-0.704
9	135	-0.635	-0.700	-0.626	-0.707	-0.702
10	150	-0.635	-0.700	-0.624	-0.707	-0.698
11	165	-0.633	-0.698	-0.622	-0.706	-0.694
12	180	-0.631	-0.696	-0.618	-0.704	-0.689
13	195	-0.628	-0.693	-0.613	-0.702	-0.683
14	210	-0.625	-0.690	-0.608	-0.699	-0.678
15	225	-0.621	-0.686	-0.603	-0.696	-0.672

Table 4.7 - Correlation of Mean NDVI and LST 2003-2014 for Different Radius of Focal Analysis
Note:

        The highest correlation coefficient
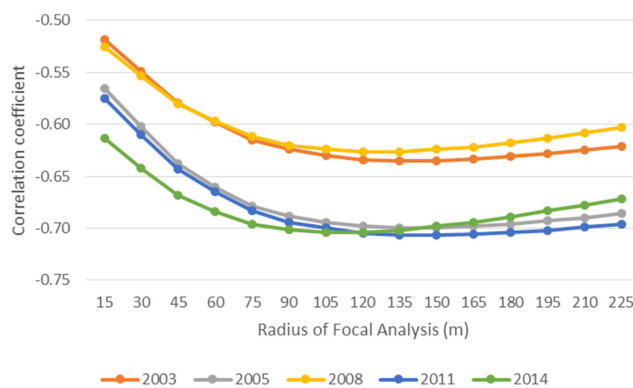
Figure 4.13 - Correlation of Mean NDVI and LST 2003-2014 for Different Radius of Focal Analysis

Since the number of pixel that covers the entire area of the city is considerably large (approximately 750,000 pixels), the observation points on the scatterplot are very dense and the relationship pattern between land surface temperature and mean NDVI is difficult to be observed. Therefore, for each year, the mean value of land surface temperature was calculated for each unique value of mean NDVI in 135 m radius. The radius of 135 m was selected because it is the median of optimal radius from the result of sensitivity analysis. Afterwards, correlation and regression analysis were performed between the mean LST and the unique value of mean NDVI.

Pearson correlation of mean NDVI and mean LST 2003-2014 is shown in Table 4.8. For the overall period, the number of unique value of mean NDVI has a range from 3,000 to 6,000. The correlation coefficients have a range of -0.1 to -0.5. Thus, mean NDVI and mean LST has very weak to moderate and negative correlation. For every year, these coefficients are also lower than the initial correlation coefficient of NDVI and land surface temperature. The significant values are always smaller than 0.01, which means the correlations are statistically significant. The lowest correlation coefficient is found in 2003, while the highest correlation coefficient is found in 2011.

	2003	2005	2008	2011	2014
Pearson correlation coefficient	-0.13	-0.38	-0.22	-0.49	-0.40
Significant value (p-value)	0.00	0.00	0.00	0.00	0.00
Number of observation	3,145	5,815	2,904	4,474	3,956

Table 4.8 - Correlation of Mean NDVI and Mean LST 2003-2014

Scatterplot of mean NDVI and mean LST 2014 is shown in Figure 4.14. Regression line, equation and R^2 value are also shown in the figure. The scatterplot of mean NDVI and mean LST is only shown for the year 2014 as the most recent year. This is because the general pattern is similar for each year. Scatterplot of mean NDVI and mean LST for other years can be seen in Appendix 11. From the scatterplot, mean NDVI and mean LST seem to have linear, strong, and negative correlation for NDVI range of 0.2 - 0.6. In this range, the mean temperature shows a linear decline when the mean NDVI increase. However, irregularities can be seen in many observation points with a low mean NDVI (around 0.1) which have a low mean temperature. These points generally represent water bodies that do have low NDVI but also have a great cooling effect. The irregularity of water body is the cause of the low correlation coefficient and R^2 values, which are -0.4 and 0.2 respectively.
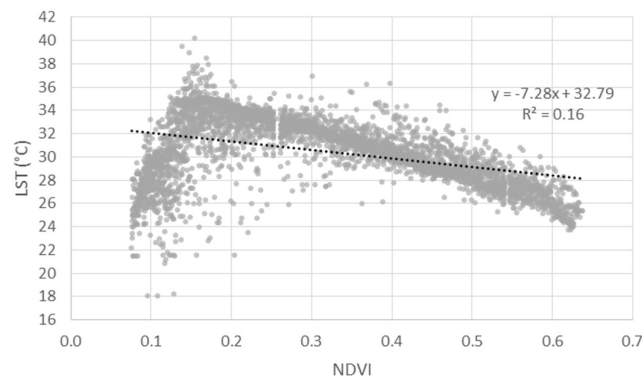
Figure 4.14 - Scatterplot of Mean NDVI and Mean LST 2014

4.3.2.   The Relationship between Land Surface Temperature and Land Cover Density

For identifying the relationship between land surface temperature and land cover density, correlation was calculated between land surface temperature and land cover density for each type of land cover generated using PLAND method. PLAND was performed using moving window method with a circular kernel for a certain radius from central pixel. However, the correlation between land surface temperature and PLAND had different values for different search radius. Therefore, sensitivity analysis was performed to identify the optimal radius that gives the highest correlation coefficient.

Correlation of vegetation density and land surface temperature 2003-2014 for different radius of PLAND is shown in Table 4.9 and Figure 4.15. The highest correlation coefficients are found in the radius of 105-135 m or 7-9 pixels. These coefficients have a range of -0.6 to -0.7. This means land surface temperature and vegetation density have strong and negative correlation. The higher the density of vegetation cover, the land surface temperature tends to be lower. The significant values are always smaller than 0.01, which means the correlations are statistically significant for every year. Similar to the sensitivity analysis of mean NDVI and LST, the lower correlation coefficients are found in 2003 and 2008, while the higher correlation coefficients are found in 2005, 2011, and 2014.

	Radius (m)	Pearson Correlation Coefficient				
		2003	2005	2008	2011	2014
1	15	-0.450	-0.478	-0.432	-0.468	-0.515
2	30	-0.541	-0.575	-0.511	-0.570	-0.613
3	45	-0.595	-0.636	-0.553	-0.638	-0.665
4	60	-0.623	-0.670	-0.572	-0.676	-0.688
5	75	-0.644	-0.696	-0.585	-0.707	-0.703
6	90	-0.654	-0.709	-0.589	-0.723	-0.710
7	105	-0.660	-0.717	-0.591	-0.733	-0.712
8	120	-0.663	-0.722	-0.589	-0.739	-0.712
9	135	-0.664	-0.724	-0.584	-0.741	-0.710
10	150	-0.662	-0.723	-0.578	-0.741	-0.705
11	165	-0.659	-0.721	-0.572	-0.740	-0.701
12	180	-0.656	-0.719	-0.565	-0.737	-0.696
13	195	-0.652	-0.715	-0.556	-0.734	-0.689
14	210	-0.648	-0.711	-0.548	-0.730	-0.683
15	225	-0.644	-0.707	-0.541	-0.726	-0.676

Table 4.9 - Correlation of Vegetation Density and LST 2003-2014 for Different Radius of PLAND
Note:
                The highest correlation coefficient

Figure 4.15 - Correlation of Vegetation Density and LST 2003-2014 for Different Radius of PLAND

Correlation of built-up density and land surface temperature 2003-2014 for different radius of PLAND is shown in Table 4.10 and Figure 4.16. The highest correlation coefficients are found in the radius of 135-180 m or 9-12 pixels. These coefficients have a range of 0.6 to 0.7. This means land surface temperature and built-up density have strong and positive correlation. The higher the density of built-up cover, the land surface temperature tends to be higher. The significant values are always smaller than 0.01, which means the correlations are statistically significant for every year. The lower correlation coefficient is found in 2008, while the higher correlation coefficient is found in 2003.

	Radius (m)	Pearson Correlation Coefficient				
		2003	2005	2008	2011	2014
1	15	0.354	0.302	0.301	0.344	0.343
2	30	0.471	0.421	0.403	0.461	0.457
3	45	0.559	0.514	0.479	0.547	0.541
4	60	0.611	0.569	0.526	0.597	0.590
5	75	0.656	0.615	0.566	0.639	0.628
6	90	0.681	0.641	0.587	0.661	0.647
7	105	0.697	0.658	0.602	0.675	0.659
8	120	0.710	0.670	0.613	0.686	0.666
9	135	0.718	0.678	0.619	0.693	0.669
10	150	0.721	0.683	0.622	0.696	0.668
11	165	0.723	0.685	0.622	0.697	0.665
12	180	0.723	0.685	0.621	0.697	0.662
13	195	0.721	0.684	0.618	0.696	0.657
14	210	0.719	0.683	0.615	0.694	0.652
15	225	0.716	0.681	0.612	0.692	0.646

Table 4.10 - Correlation of Built-up Density and LST 2003-2014 for Different Radius of PLAND
Note:

         The highest correlation coefficient

Figure 4.16 - Correlation of Built-up Density and *LST 2003-2014* for Different Radius of PLAND

Correlation of water/shadow density and land surface temperature 2003-2014 for different radius of PLAND is shown in Table 4.11 and Figure 4.17. The highest correlation coefficients are found in the radius of 15-60 m or 1-4 pixels. These coefficients have a range of -0.1 to -0.4. This means land surface temperature and water/shadow density have weak and negative correlation. The significant values are always smaller than 0.01, which means the correlations are statistically significant for every year. The lower correlation coefficient is found in 2014, while the higher correlation coefficient is found in 2003.

	Radius (m)	Pearson Correlation Coefficient				
		2003	2005	2008	2011	2014
1	15	-0.406	-0.258	-0.341	-0.285	-0.141
2	30	-0.432	-0.289	-0.349	-0.288	-0.133
3	45	-0.440	-0.303	-0.345	-0.283	-0.118
4	60	-0.441	-0.304	-0.337	-0.279	-0.108
5	75	-0.439	-0.300	-0.328	-0.275	-0.101
6	90	-0.436	-0.294	-0.321	-0.273	-0.095
7	105	-0.432	-0.288	-0.315	-0.272	-0.090
8	120	-0.429	-0.280	-0.308	-0.271	-0.084
9	135	-0.426	-0.272	-0.301	-0.270	-0.078
10	150	-0.422	-0.264	-0.296	-0.269	-0.073
11	165	-0.418	-0.257	-0.290	-0.269	-0.068
12	180	-0.415	-0.250	-0.285	-0.268	-0.062
13	195	-0.411	-0.241	-0.279	-0.267	-0.056
14	210	-0.409	-0.234	-0.274	-0.266	-0.051
15	225	-0.406	-0.227	-0.269	-0.266	-0.046

Table 4.11 - Correlation of Water/Shadow Density and LST 2003-2014 for Different Radius of PLAND

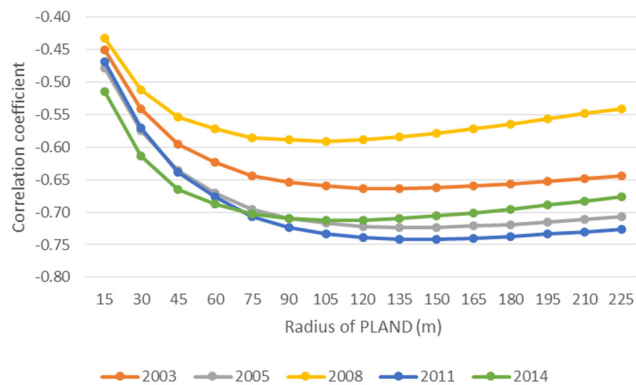Note:

                  The highest correlation coefficient

Figure 4.17 - Correlation of Water/Shadow Density and LST 2003-2014 for Different Radius of PLAND

Correlation of bare soil density and land surface temperature 2003-2014 for different radius of PLAND is shown in Table 4.12 and Figure 4.18. The highest correlation coefficients are found in the radius of 135-180 m or 9-12 pixels. These coefficients have a range of 0.0 to 0.3. This means land surface temperature and bare soil density have very weak or no correlation. Anomaly occurs in 2014 where the highest correlation coefficient is -0.1 and found in the radius of 225 m. However, the significant values are always smaller than 0.01, which means the correlations are statistically significant for every year.

	Radius (m)	Pearson Correlation Coefficient				
		2003	2005	2008	2011	2014
1	15	-0.037	-0.035	-0.091	-0.064	0.031
2	30	-0.004	0.014	-0.078	-0.039	0.016
3	45	0.055	0.083	-0.046	-0.012	-0.008
4	60	0.110	0.139	-0.017	0.005	-0.028
5	75	0.170	0.193	0.013	0.021	-0.048
6	90	0.207	0.226	0.030	0.030	-0.061
7	105	0.233	0.249	0.042	0.036	-0.071
8	120	0.254	0.267	0.050	0.039	-0.080

	Radius (m)	Pearson Correlation Coefficient				
		2003	2005	2008	2011	2014
9	135	0.268	0.279	0.054	0.039	-0.087
10	150	0.276	0.285	0.055	0.039	-0.092
11	165	0.279	0.288	0.053	0.038	-0.095
12	180	0.279	0.289	0.049	0.036	-0.098
13	195	0.276	0.289	0.044	0.033	-0.099
14	210	0.273	0.288	0.038	0.030	-0.100
15	225	0.269	0.286	0.030	0.026	-0.100
16	240	0.265	0.284	0.023	0.023	0.099
17	255	0.259	0.282	0.015	0.018	0.098
18	270	0.253	0.280	0.008	0.014	0.097
19	285	0.247	0.278	0.001	0.009	0.095
20	300	0.241	0.276	0.009	0.004	0.094

Table 4.12 - Correlation of Bare Soil Density and LST 2003-2014 for Different Radius of PLAND
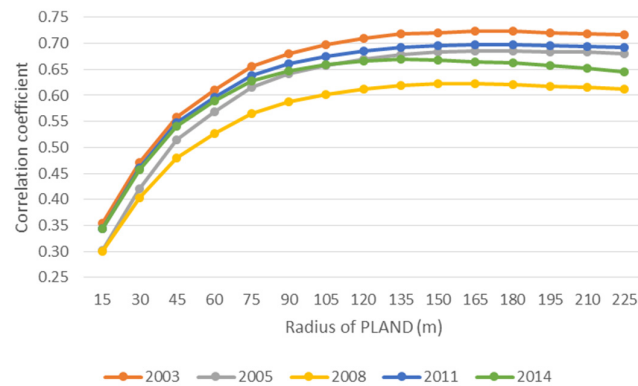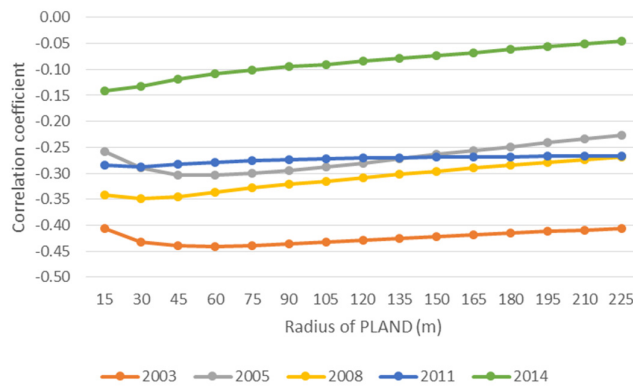Note:
　　　　　　The highest correlation coefficient
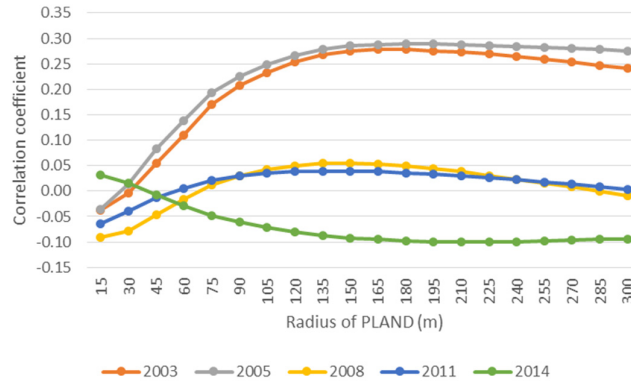
Figure 4.18 - Correlation of Bare Soil Density and LST *2003-2014* for Different Radius of PLAND

In the next step, the correlation calculation was performed only for the identified optimal radius based on the results of the sensitivity analysis. The radius of 135 m was selected based on consideration that this radius gave the highest correlation coefficient in the sensitivity analysis between land surface temperature and land cover density of the dominant land cover types, which are vegetation and built-up.

Samples were selected by limiting observation only for the pixels that have the same land cover type with the observed land cover density. The mean value of land surface temperature was calculated for each unique value of PLAND in 135 m radius. Afterwards, correlation and regression analysis were performed between the mean LST and the unique value of PLAND.

Table 4.13 shows the correlation between mean temperature and land cover density. The mean temperature has very strong and negative correlation with vegetation density (from -0.98 to -0.99) and water/shadow density (from -0.85 to -0.98), while it has very strong and positive correlation with built-up density (from 0.92 to 0.98). However, the correlation between mean temperature and bare soil density do not show a stable values. In 2003 and 2014, the correlation coefficients between mean temperature and bare soil density show positive and moderate correlations (0.67 and 0.59). The correlation coefficients show negative and strong correlation in 2011 (-0.83) and negative and weak correlation in 2005 (-0.36). Meanwhile, in 2008, the correlation coefficient shows no correlation (-0.06).

Year	Bare Soil - LST			Built-up - LST			Vegetation - LST			Water/Shadow - LST		
	PCC	Sig.	N	PCC	Sig.	N	PCC	Sig.	N	PCC	Sig.	N
2003	0.67	0.00	247	0.98	0.00	253	-0.99	0.00	253	-0.91	0.00	253
2005	-0.36	0.00	235	0.92	0.00	253	-0.99	0.00	253	-0.98	0.00	250
2008	-0.06	0.34	252	0.94	0.00	253	-0.99	0.00	253	-0.85	0.00	253
2011	-0.83	0.00	253	0.96	0.00	253	-0.99	0.00	253	-0.91	0.00	252
2014	0.59	0.00	131	0.95	0.00	253	-0.98	0.00	253	-0.95	0.00	250

Table 4.13 - Correlation of Land Cover Density and Mean LST 2003-2014
Note:
PCC : Pearson correlation coefficient
Sig. : Significant value (p-value)
N : Number of observation

Scatterplot of land cover density and mean temperature in the year 2014 is shown in Figure 4.19. Negative relationship is shown between mean temperature and vegetation and water/shadow density. The mean temperature tends to decrease when vegetation and water/shadow density increase. The relationship between mean temperature and vegetation density shows a perfect linear pattern. Meanwhile, for the relationship between mean temperature and water/shadow density, the mean temperature shows stagnation in the range of 0-30% density before declining by a sharp slope in the range of 30-50% density. Then, the mean temperature stable in the range of 50-80% density, and declining with a more gentle slope in the range of 80-100% density. For most density values, the mean temperature shows lower temperature for water/shadow density compared to vegetation density.

Positive and linear relationship is shown between mean temperature and built-up density. However, a slight scattered pattern is shown in the range of 0-10% density. This may indicate that at low density range, the influence of other types of land cover is large. In general, for other years, the mean temperature shows stable values for the different bare soil density (see Appendix 12). However, in 2014, the mean temperature seems scattered, although a small increase pattern can be seen in the range of 10-50% density. The scatterplot shows there are no observation points in the range of 50-100% density. This means areas with bare soil cover in 2014 are always smaller than an area with a radius of 135 m.
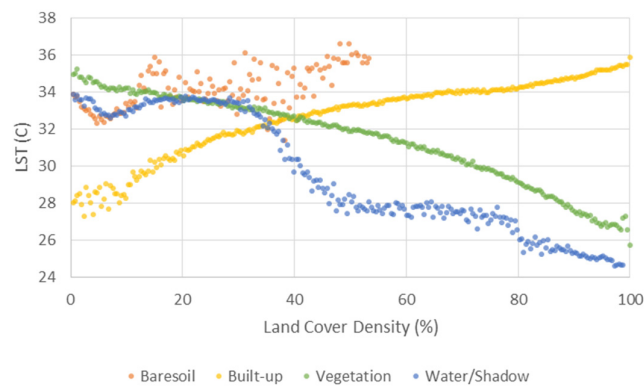
Figure 4.19 - Scatterplot of Land Cover Density and Mean LST 2014

Table 4.14 shows the statistics of simple linear regression analysis for the relationship between land cover density and the mean temperature in the period 2003-2014. From the coefficient in the regression equation, the difference in the mean temperature value can be predicted when the land cover density increased by 1%. Meanwhile, R^2 value indicates the variation of the observation values to the linear regression line based on the regression equation. R^2 has a value range of 0-1, where R^2 value equal to 0 indicates the variation of

observed values to the regression line are very big, whereas R^2 value equal to 1 indicates all the observed values are fit to the regression line perfectly.

For the relationship between mean temperature and bare soil density, R^2 value varies from very low to medium (0.0 - 0.7). The coefficient on the regression equation has a range of -0.03 to 0.04, or an average of 0.00. From the average coefficient value, it can be predicted that the temperature will not change although the bare soil density increased or decreased. On the contrary, stable and very high R^2 values obtained for the relationship between mean temperature and other land cover density. It indicates, in general, the variation of the observation values from the regression line is low. Thus, the mean temperature on various land cover density can be explained by the linear regression line or regression equation. For the relationship between mean temperature and built-up density, R^2 value has a range of 0.84 - 0.96. The regression coefficient has a range of 0.04 – 0.07, with the average of 0.06. Thus, it can be predicted that the mean temperature will show an increase of 0.6°C when built-up density increased by 10%. For the relationship between mean temperature and vegetation density, R^2 value has a range of 0.96 - 0.99. The regression coefficient has a range from -0.08 to -0.05, with the average of -0.07. This means the mean temperature will show a decrease of 0.7°C when vegetation density increased by 10%. For the relationship between mean temperature and water/shadow density, R^2 value has a range of 0.73 - 0.96. The regression coefficient has a range from -0.03 to -0.11, with the average of -0.06. This means the mean temperature will show a decrease of 0.6°C when water/shadow density increased by 10%.

Year	Bare Soil - LST		Built-up - LST		Vegetation - LST		Water/Shadow - LST	
	Equation	R^2	Equation	R^2	Equation	R^2	Equation	R^2
2003	y = 29.75 + 0.03x	0.44	y = 28.13 + 0.07x	0.96	y = 32.67 - 0.07x	0.99	y = 29.96 - 0.05x	0.83
2005	y = 31.76 - 0.02x	0.13	y = 28.62 + 0.07x	0.84	y = 34.21 - 0.08x	0.99	y = 31.75 - 0.07x	0.96
2008	y = 27.48 - 0.00x	0.00	y = 25.88 + 0.04x	0.88	y = 28.77 - 0.05x	0.98	y = 27.10 - 0.03x	0.73
2011	y = 31.58 - 0.03x	0.69	y = 28.13 + 0.06x	0.92	y = 33.00 - 0.08x	0.99	y = 30.06 - 0.04x	0.83
2014	y = 33.05 + 0.04x	0.35	y = 29.21 + 0.07x	0.91	y = 35.48 - 0.08x	0.96	y = 34.75 - 0.11x	0.91

Table 4.14 - Regression Statistics of Land Cover Density and Mean LST 2003-2014
Note:
x : Land cover density
y : Mean LST

To illustrate the relationship between land cover density and surface temperature, 3D illustrations are shown for built-up and vegetation cover as the dominant land cover in the study area and only for 2014 as the most recent year. Illustration of the relationship between built-up density and surface temperature is shown in Figure 4.20, while illustration of the relationship between vegetation density and surface temperature is shown in Figure 4.21. The land cover density represented by the height of circular polygons, while surface temperature is visualized by colours. The method used for surface temperature visualization is quantile method.

As an illustration, built-up and vegetation density is not shown for the entire pixels. The method used to present the illustration was by first making cells (fishnets) with a size of 270 x 270 m that covers the entire area of Bandung. The value of land cover density and surface temperature were then extracted for each of the central pixel in each cell. This is intended to avoid the edge effects. Furthermore, each cell was changed into a circular shape with a radius of 135 m to be able to illustrate the area which gave the highest correlation coefficient between surface temperature and built-up and vegetation density. Overall, there are approximately 2,000 circular polygons in the illustration as samples of approximately 750,000 pixels.

It appears that the highest temperature is generally present in cells that have the highest built-up density, while the lowest temperature generally present in cells that have the lowest built-up density. On the other hand, the highest temperature is generally present in cells that have the lowest vegetation density, while the lowest temperature generally present in cells that have the highest vegetation density. The cells that have the medium built-up density, which means mix areas of built-up and other land cover, tend to have the medium

temperature. The illustration shows the hotspots are located in clusters of high built-up density cells, e.g., an area in the west part of the city. On the contrary, the coldspots are located in clusters of low built-up density cells, e.g., an area in the southeast part of the city. In addition, the cells near the coldspots tend to have low temperature even though they have a high built-up density.
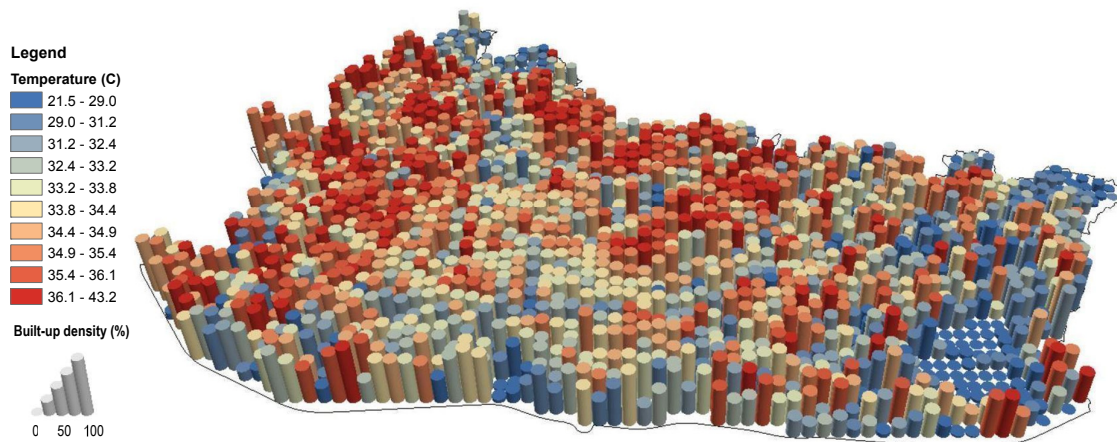
Figure 4.20 - Illustration of Relationship between Built-up Density and LST in Bandung City 2014
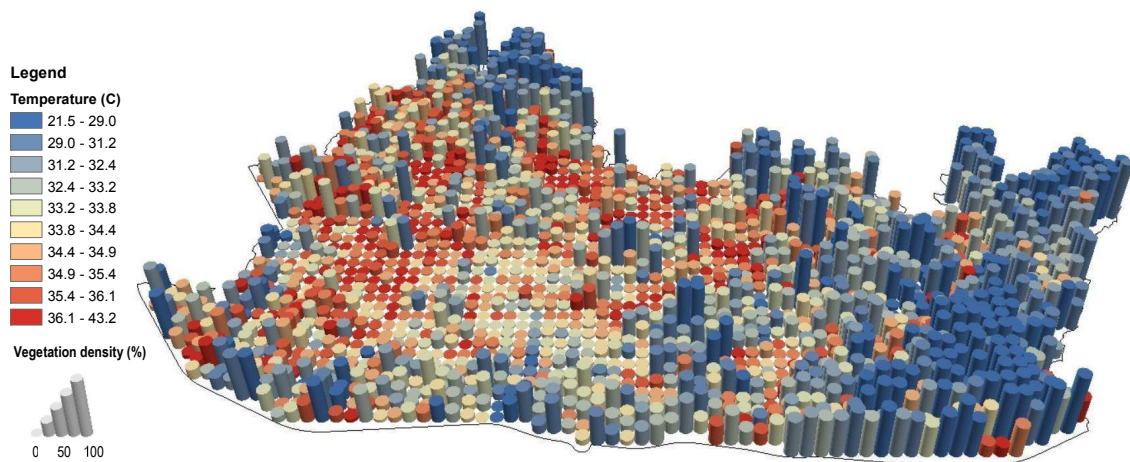
Figure 4.21 - Illustration of Relationship between Vegetation Density and LST in Bandung City 2014

4.3.3. The Relationship between Land Surface Temperature and Land Cover Aggregation Index

For the overall area of the city, the aggregation index was calculated in landscape level using Fragstat software. Figure 4.22 show the aggregation index for each land cover for the overall area of the city in 2003-2014.

In general, bare soil and water/shadow have a lower aggregation index for each year, which has always been under 60%. Meanwhile, vegetation and built-up have a higher aggregation index, which has always been above 68%. An increasing trend is shown by the built-up aggregation index, whereas the aggregation index for other types of land cover show fluctuations. The increasing trend of built-up aggregation index indicates the growth of built up area has been more compact in the city. The highest increase is shown in the period of 2011-2014 where built-up aggregation index increase from 77% to 85%, or increase by 8%. Built-up aggregation index in 2014 has a great difference compared to 2003 (69%), which is higher by 15%. A smaller increasing trend is shown by vegetation aggregation index. However, in 2008- 2011, vegetation aggregation

index shows a decrease (from 74% to 71%), before increasing again in 2011-2014 (from 71% to 76%). This may implies that the expansion of built-up area occurred in some parts of vegetated areas so that the vegetation areas became more fragmented in 2011. Afterwards, in 2014, the development of built-up areas may also occurred in the fragmented vegetated areas so that the vegetation aggregation index increase. In addition, the development of built-up areas in 2014 may also occurred in areas with bare soil cover since there is a sharp decline in bare soil aggregation index from 50% in 2011 to 21% in 2014.
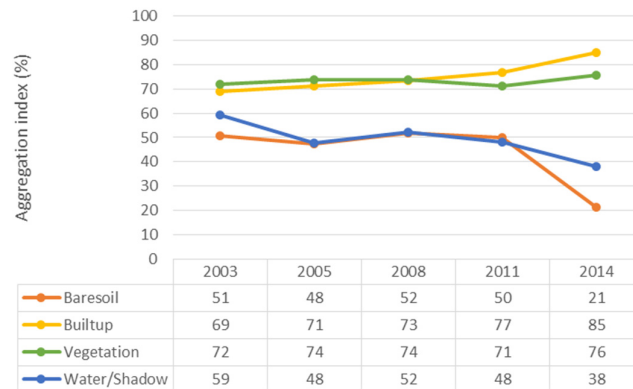
Figure 4.22 - Aggregation Index of Land Cover in Bandung City 2003-2014

Aggregation index was also calculated for the class level using Fragstat software. Aggregation index for all land cover is generated by using moving window method with circular kernel with a radius of 135 m. This is consistent with PLAND with the intention that the correlation between surface temperature and aggregation index of land cover can be compared with the correlation between surface temperature and land cover density. Figure 4.23 shows the spatial pattern of aggregation index of built-up cover 2003-2014, while Figure 4.24 shows the spatial pattern of aggregation index of vegetation cover 2003-2014. The spatial pattern of aggregation index is shown only for built-up and vegetation cover as the dominant land cover in the study area. The spatial pattern of aggregation index of bare soil and water/shadow cover can be seen in Appendix 13 and 14.

The maps show that the built-up areas have been more compact or aggregated in the central part of the city, especially in 2014. In addition, areas with high aggregation index of built-up cover have spread to the eastern part of the city. On the contrary, vegetation areas in the central part of the city have been more fragmented. This means that vegetation patches in the central part of the city have been converted to built-up areas. Areas with high aggregation index of vegetation cover are located in the urban fringe areas in the southeast, the northeast, and the northwest part of the city.

Aggregation Index of Built-up in Bandung City 2003

Aggregation Index of Built-up in Bandung City 2005

Aggregation Index of Built-up in Bandung City 2008

Aggregation Index of Built-up in Bandung City 2011

Aggregation Index of Built-up in Bandung City 2014
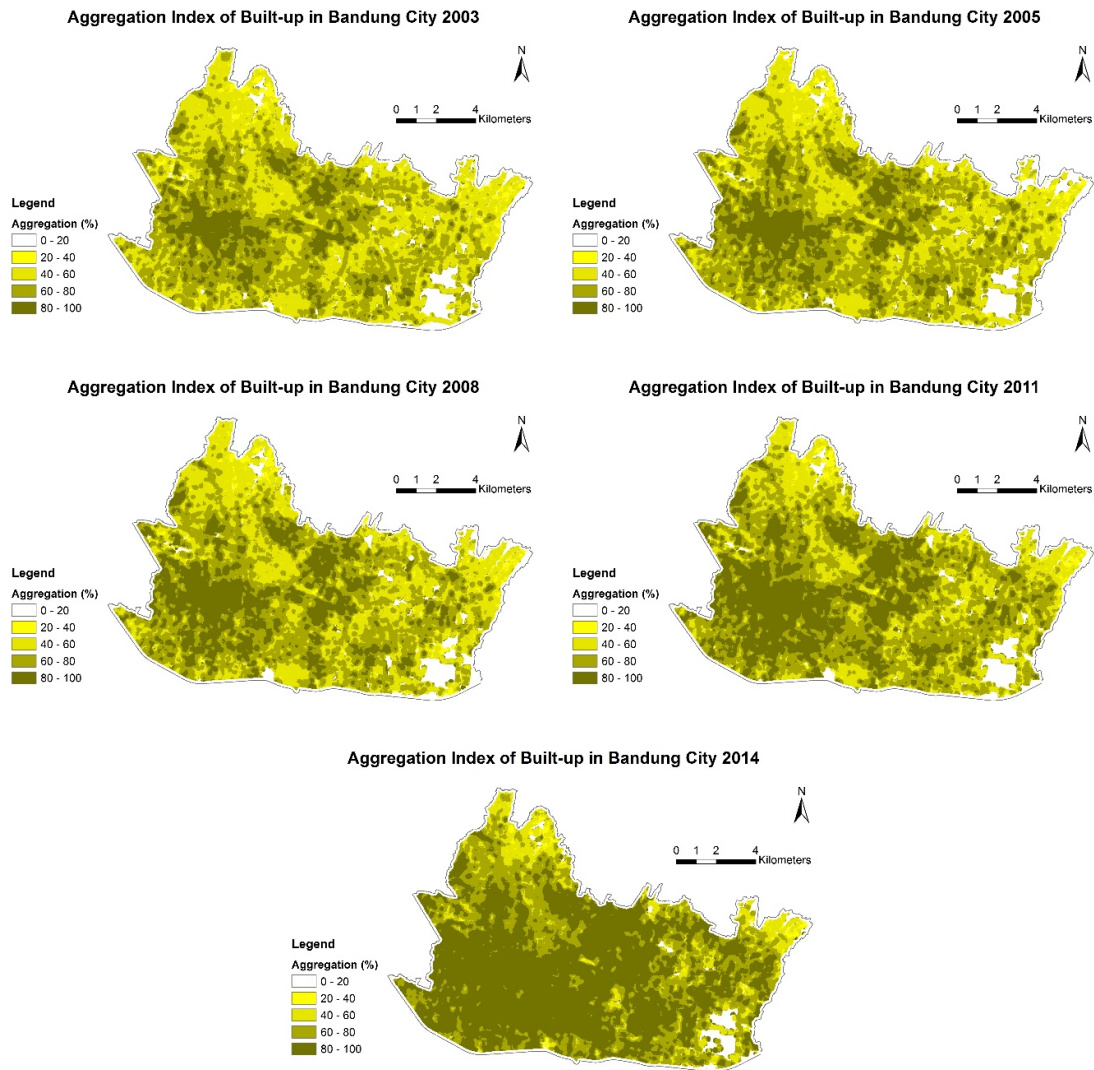
Figure 4.23 - Aggregation Index of Built-up Cover in Bandung City 2003-2014
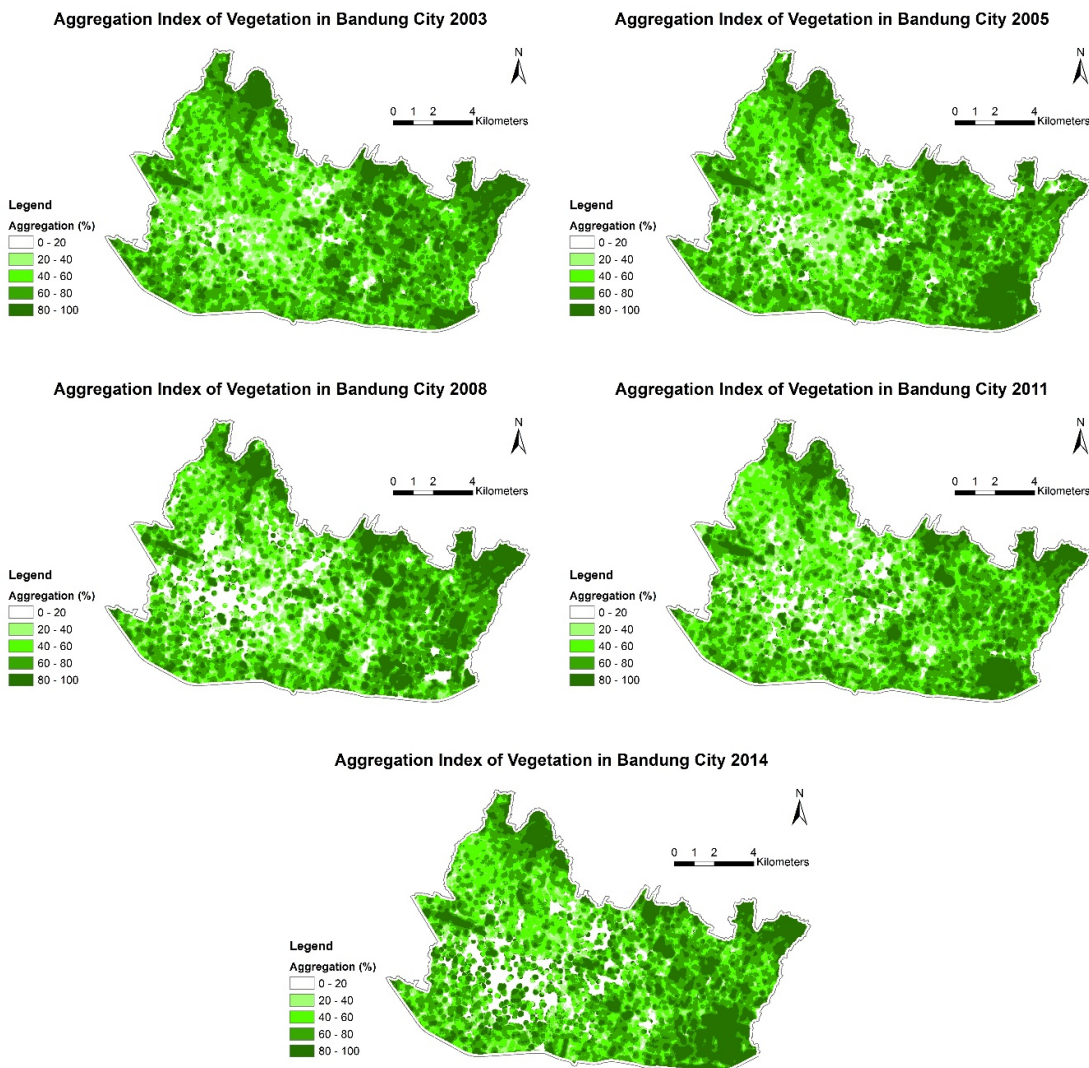
Figure 4.24 - Aggregation Index of Vegetation Cover in Bandung City 2003-2014

Correlation of aggregation index of land cover and surface temperature 2003-2014 is shown in Table 4.15. For all correlation, the significant values are smaller than 0.01, which means the correlation is statistically significant. The surface temperature and vegetation aggregation index has negative and moderate correlation with correlation coefficient ranging from -0.5 to -0.6. On the contrary, the surface temperature and built-up aggregation index has positive and moderate correlation, with correlation coefficient ranging from 0.5 to 0.6. Meanwhile, the surface temperature and water/shadow aggregation index and bare soil aggregation index has negative and very weak correlation, with correlation coefficient ranging from -0.1 to -0.3.

In general, the correlation coefficients between surface temperature and aggregation index of land cover have a lower values compared to correlation between surface temperature and land cover density. This means land cover density has a stronger influence to surface temperature rather than aggregation index of land cover.

Year	Bare Soil - LST			Built-up - LST			Vegetation - LST			Water/Shadow - LST		
	PCC	Sig.	N	PCC	Sig.	N	PCC	Sig.	N	PCC	Sig.	N
2003	-0.18	0.00	684,680	0.54	0.00	672,506	-0.60	0.00	692,448	-0.26	0.00	503,872
2005	-0.21	0.00	672,586	0.48	0.00	662,381	-0.59	0.00	678,565	-0.19	0.00	531,780
2008	-0.26	0.00	686,401	0.50	0.00	670,685	-0.50	0.00	667,003	-0.21	0.00	485,701
2011	-0.17	0.00	685,856	0.55	0.00	674,578	-0.58	0.00	683,176	-0.13	0.00	449,835
2014	-0.06	0.00	387,944	0.55	0.00	684,163	-0.52	0.00	654,739	-0.16	0.00	604,591

Table 4.15 - Correlation of Land Cover Aggregation Index and LST 2003-2014
Note:
PCC : Pearson correlation coefficient
Sig. : Significant value (p-value)
N : Number of observation

In the next step, samples were selected by limiting observation only for the pixels that have the same land cover type with the observed land cover aggregation index. The mean value of land surface temperature was calculated for each unique value of aggregation index. Afterwards, correlation and regression analysis were performed between the mean LST and the unique value of aggregation index.

Table 4.16 shows the correlation between mean temperature and land cover aggregation index. The correlation coefficients increase for all correlation, except for correlation between mean temperature and aggregation index of built-up cover. The significant values are always smaller than 0.01, which means the correlation is statistically significant, except for the correlation between mean temperature and aggregation index of bare soil cover for the year 2014. The mean temperature has strong and negative correlation with vegetation aggregation index (from -0.7 to -0.8), moderate to strong and negative correlation with water/shadow aggregation index (from -0.4 to -0.8), and moderate to strong and positive correlation with built-up aggregation index (from 0.5 to 0.7). However, the correlation between mean temperature and bare soil aggregation index do not show stable values. In 2005, 2008, and 2011, the correlation coefficients between mean temperature and bare soil aggregation index show moderate to strong and negative correlations (from -0.6 to -0.7). The correlation coefficients show weak and negative correlation in 2003 (-0.2). While, in 2014, the correlation coefficient shows no correlation (0.0).

Year	Bare Soil - LST			Built-up - LST			Vegetation - LST			Water/Shadow - LST		
	PCC	Sig.	N	PCC	Sig.	N	PCC	Sig.	N	PCC	Sig.	N
2003	-0.21	0.00	7,735	0.67	0.00	10,297	-0.84	0.00	11,104	-0.56	0.00	7,325
2005	-0.60	0.00	6,495	0.45	0.00	10,384	-0.77	0.00	10,970	-0.42	0.00	5,122
2008	-0.61	0.00	7,872	0.48	0.00	10,646	-0.78	0.00	10,571	-0.40	0.00	6,433
2011	-0.68	0.00	7,346	0.56	0.00	10,491	-0.73	0.00	10,368	-0.57	0.00	4,814
2014	0.01	0.86	808	0.55	0.00	10,554	-0.80	0.00	10,754	-0.83	0.00	4,584

Table 4.16 - Correlation of Land Cover Aggregation Index and Mean LST 2003-2014
Note:
PCC : Pearson correlation coefficient
Sig. : Significant value (p-value)
N : Number of observation

The scatterplot of mean temperature and aggregation index of built-up cover 2014 is shown in Figure 4.25, while the scatterplot of mean temperature and aggregation index of vegetation cover 2014 is shown in Figure 4.26. In addition, the regression line, regression equation and R^2 value are also shown in the figures. Scatterplot of aggregation index of land cover and mean temperature is shown only for the year 2014 as the most recent year and only for vegetation and built-up cover as the dominant land covers in the study area. Scatterplot of mean temperature and aggregation index of bare soil and water/shadow cover can be seen in Appendix 15.

The number of unique values of aggregation index for each land cover types is much larger compared to land cover density. Overall, the unique values of aggregation index for each land cover has a range of 5,000

to 11,000 values. While, the number of unique values of land cover density is approximately 250 values. This causes the observation points on the scatterplot were quite dense, although the relationship pattern can still be observed.

The scatterplot shows a positive relationship between the mean temperature and the built-up aggregation index. In general, the mean temperature increases when the built-up aggregation index increase. The variation around the regression line is quite high so that the R^2 value is low (0.3). Meanwhile, the scatterplot shows a negative relationship between the mean temperature and the vegetation aggregation index. This means the mean temperature tend to decline when vegetation aggregation index increase. The variation around the regression line is moderate so that the R^2 value is also moderate (0.6).
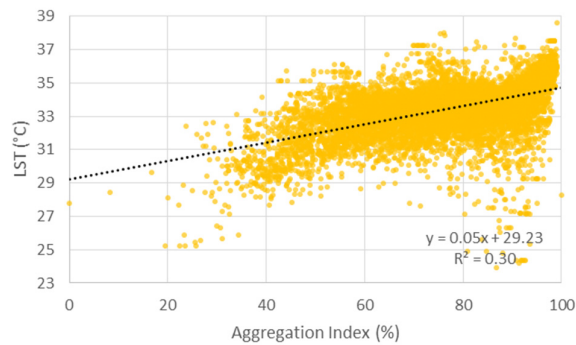
Figure 4.25 - Scatterplot of Aggregation Index of Built-up Cover and Mean LST 2014
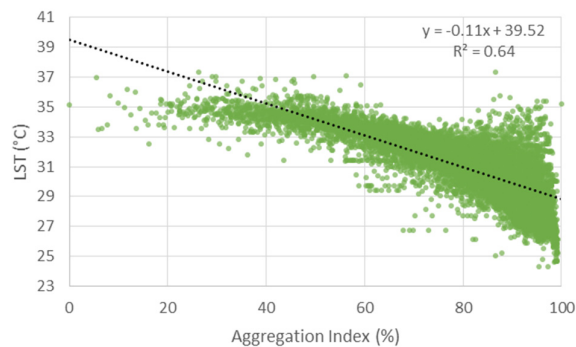
Figure 4.26 - Scatterplot of Aggregation Index of Vegetation Cover and Mean LST 2014

4.4.   The Relation between Green Spaces Planning and Surface Temperature

As described in Section 4.1, for the period 1994-2014, there has been an increasing trend of built-up area in Bandung city (Figure 4.1). The development occurs in the form of densification and vertical development in the central part of the city. Moreover, extensive development of new residential areas occurs in the outskirt areas in the eastern part of the city. This situation has led to reduction of green spaces in the city. In turn, these factors have been considered to be the main causes of the urban warming in Bandung city.

To describe the variation in the temperature between the city centre, the outskirts, and the other areas in the city, mean temperatures were identified for concentric zones with different distances to the city centre of Bandung (Figure 4.27). The zones division was performed with circular buffers for every 1 km distance from the centre point in the city centre. The assigned location for the centre point is an open space surrounded by large buildings which are the centre of government, business, commercial, and religious activities. The zones were named based on their distance to the city centre. For example, zone that has a

distance of 0-1 km was named Zone 1, zone that has a distance of 1-2 km was named Zone 2, and so on. The farthest zone from the city centre has a distance of 14-15 km (Zone 15).

Moreover, to illustrate temperature variation over different land cover types, the surface temperature 2003-2014 was identified along horizontal and vertical transect lines that pass through the centre point. The transect lines pass around 1,200 pixels for the west-east direction and around 800 pixels for the south-north direction.

Figure 4.27 - Transect Lines and Buffer Zones by Distance to Bandung City Centre

Figure 4.28 shows the mean temperature for different buffer zones in line graph, while the exact temperature value is shown in Appendix 16. In general, lower temperatures were found in 1994-2000 (Landsat TM), while higher tempera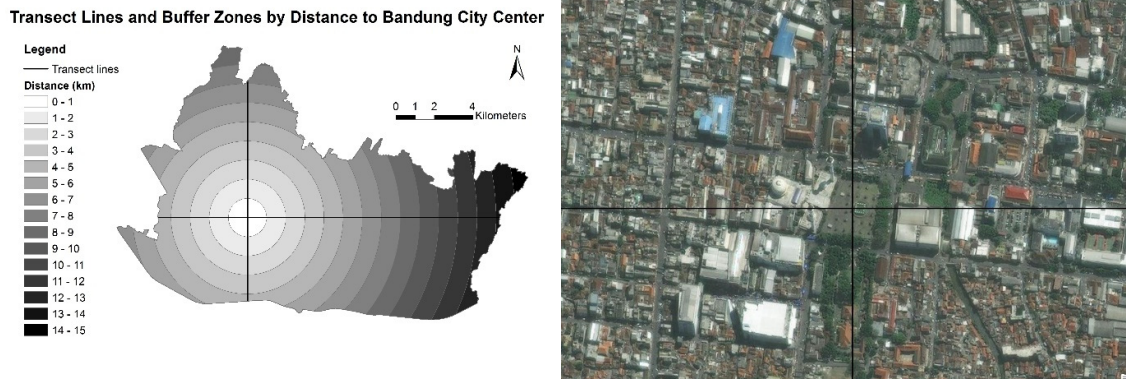tures were found in 2003-2014 (Aster). For the entire zones, the year 2000 consistently showed the lowest mean temperatures with a range of 21-24°C. On the contrary, the year 2014 consistently showed the highest mean temperatures with a range of 28-35°C, except for Zone 15 where the highest mean temperatures occurred in 2011. For both years (2000 and 2014), the lowest mean temperature occurred on Zone 15, while the highest mean temperature occurred on Zone 1.

For every year, the lowest mean temperature occurred for the zone that is farthest from the city centre, which was Zone 15. The exception was in the year 2011 where the lowest mean temperatures occurred in the Zone 11. On the contrary, the highest mean temperatures occurred for the zones that are close to the city centre, which were Zone 1, 2, and 3. Furthermore, the highest mean temperature occurred mostly in Zone 1 (0-1 km from the city centre).

The mean temperature differences between zones with the highest and the lowest mean temperature for each year showed significant differences, with a range of 3-7°C. The smallest difference occurred in 2000 (3°C), while the biggest difference occurred in 2005 (7°C). For the overall period, the average difference between the highest and the lowest mean temperature was 5°C. Thus, the further away from the city centre, the lower the mean temperature. However, exceptions were shown for Zone 12 and 13 where the decreasing temperature pattern from previous zones (Zone 1-11) turns into a slight increase on these zones, before decreasing again on the next zones (Zone 14 and 15). This fits with the fact that Zone 12 and 13 cover a dominated built-up area that has been designated as a sub centre of the city. The zones that are located in the eastern part of the city represent the outskirt of Bandung city where built-up density increases every year with a lot of development of new residential areas and other infrastructures. In addition, the mean temperatures in Zone 13 were consistently higher than in Zone 12, except in 1994. This could means that the built-up density in Zone 13 was higher than in Zone 12.

Although the mean temperatures in Zone 12 and 13 were higher than in the surrounding zones, but the mean temperatures in these zones were still lower compared to the city centre (Zone 1). More specifically, the mean temperature differences between Zone 1 and Zone 13 for each year had a range of 1-5°C. The

smallest difference occurred in 2000 (1°C), while the biggest difference occurred in 2005 (5°C). For the overall period, the average difference was 3°C.

In conclusion, the results show a significant difference in the mean temperature between the city centre and the outskirt area of Bandung city. Thus, although the expansion of built-up area is increasing in the outskirt area, the city centre still has a lower green spaces and a higher built-up density and therefore, higher mean temperature than the outskirt area.
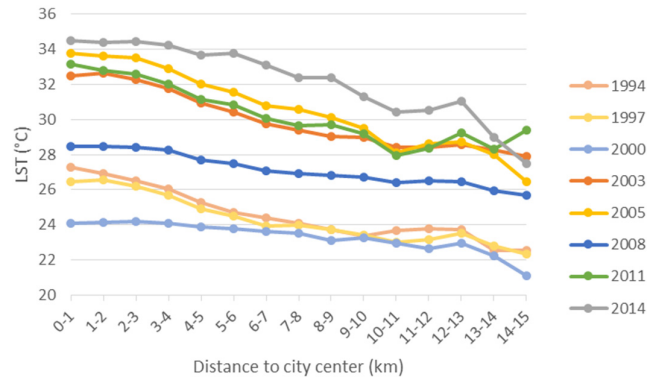
Figure 4.28 - Mean Temperature on the Buffer Zones

The temperature variations along the transect lines are shown only for 2014 (the most recent year). The temperature variations along the transect lines for other years can be seen in Appendix 17.

Figure 4.29 shows the land surface temperature along the west-east transect line. Built-up was the dominant land cover along the transect line. The temperature values had a range of 25-37°C. The temperature in the city centre was 33°C. The high temperatures with a relatively low variation appeared at a distance of 0-3 km to the west of the city centre where the transect line passed through a homogeneous built-up area, a high density commercial area. Pixels with the highest temperature were also found at this range. Different land cover types, particularly vegetation, were found mainly in the east of the city centre, here the temperature had greater variations and lower temperatures were found more common. The lowest temperature appeared at a distance of 9-10 km to the east of city centre where the transect line passed through a large vegetated area (rice field). However, small patches of green areas and water bodies were often found along the transect line but they did not have a great impact to decrease the temperature.
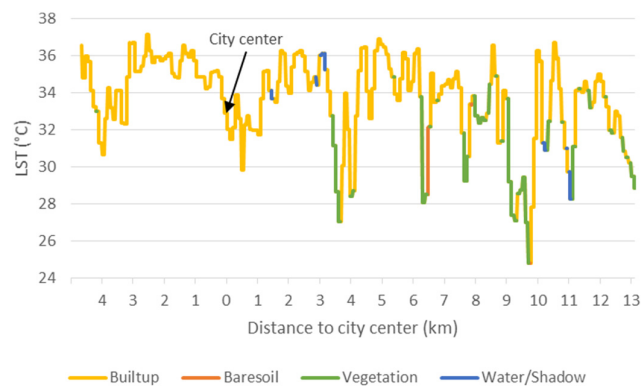
Figure 4.29 - Land Surface Temperature Along the West-East Transect Line 2014

Figure 4.30 shows the land surface temperature 2014 along the south-north transect line. The dominant land cover along this transect line was also the built-up cover. The temperature values had a range of 27-38°C. The high temperatures with a relatively low variation appeared at a distance of 0-3 km to the north of city centre where the transect line passed through a large high density built-up area, being a non formal residential area (slum). Pixels with the highest temperature were also found at this range. The lowest temperature appeared where the transect line passed through vegetation covers in the form of urban forest (3-4 km to the north of city centre) and farm field (7 km to the north of city centre). When the transect line passed through the urban forest, the temperature pattern even decrease quite dramatically, implying a great cooling effect from area with a high density of trees. The cooling effect in urban forest was much greater compared to the cooling effect in grass land at a distance of 1-2 km to the south of city centre. In addition, significant lower temperatures are found at a distance of 4 km to the south of city centre where the transect line passed through a low density residential area.

In conclusion, the surface temperature has a very high variation along the transect lines. Temperature variation is considerably large even for the same land cover type. However, the variation is still greater for the different land cover types. The built-up cover tends to have higher temperatures than the other land covers. While, temperatures tend to be lower when the transect lines pass through an area with a vegetation cover. However, the heating and the cooling effects are very much depend on the size and the type of built-up and green area, e.g. large high density built-up areas will have high temperatures while large areas of tree cover will have low temperatures.

The heating effect of built-up cover and the cooling effect of vegetation and water/shadow cover also influence each other. For example, when the transect lines pass through a homogenous built-up area which has a high temperatures and then pass through a homogenous vegetated area which has a low temperatures, the adjacent pixels tend to have an intermediate temperatures. In addition, the surface temperature is also influenced by the dominant land cover types. For example, a built-up pixel surrounded by more dominant vegetation pixels tends to show low temperatures. On the contrary, a water/shadow pixel surrounded by more dominant built-up pixels tends to show a high temperatures.
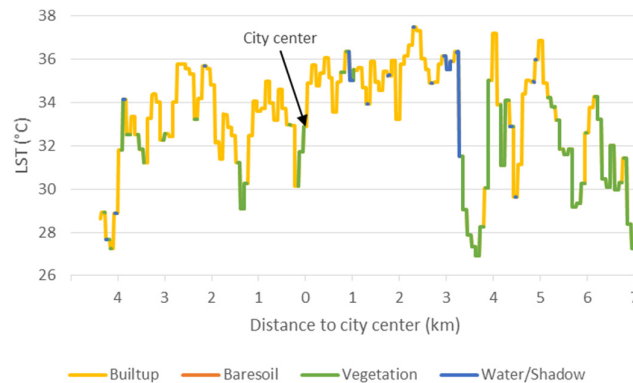
Figure 4.30 - Land Surface Temperature Along the South-North Transect Line 2014

The above findings indicate that the different types of urban land use/typology have different influence to the surface temperature. For example, a high density built-up areas in the form of slums have a stronger heating effect compared to a low density formal residential area. While, urban forest with a high density of trees provides stronger cooling effect compared to grass lands. Therefore, this section discusses the surface temperature in different urban land use/typology. The observed urban typology consist of 20 areas to represent the different typology which are common in the study area. The typology also represents the different types of vegetation, water bodies and built-up cover. The images for each topology are shown in Figure 4.31, while location of each typology is shown in Figure 4.32.

Urban forest

Parks

Golf course and sport field

Grass

Rice field

Farm field

Plantation

Wet rice field

River

Industrial with more green spaces

Industrial with less green spaces

Commercial

Offices

Low density formal residential

Medium density formal residential

High density formal residential

High density non formal residential

Road with street trees

Road without street trees

Road surrounded by high buildings
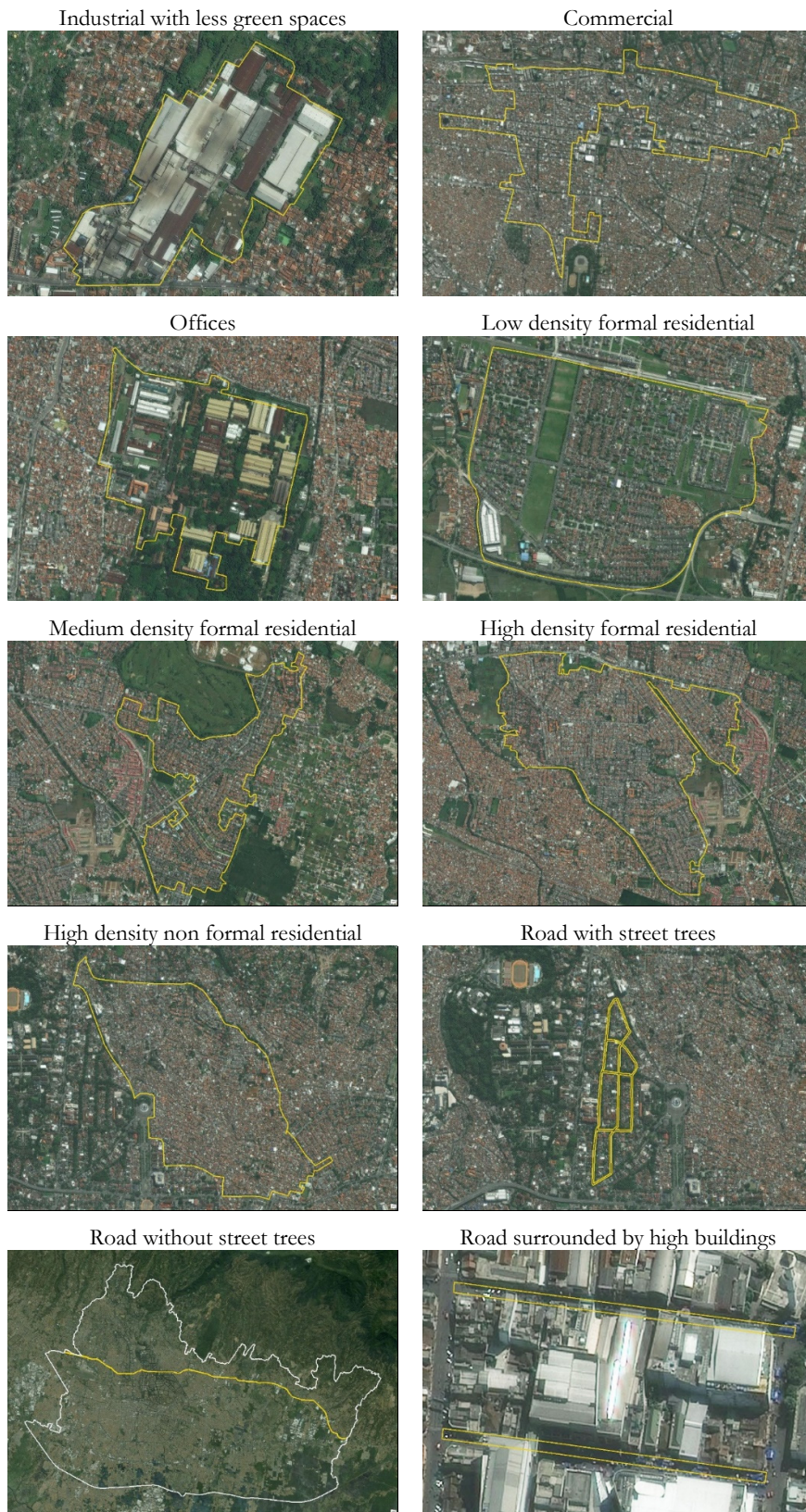
Figure 4.31 - Observed Urban Land Use/Typology
Source: ArcGIS Online Imagery, 2015
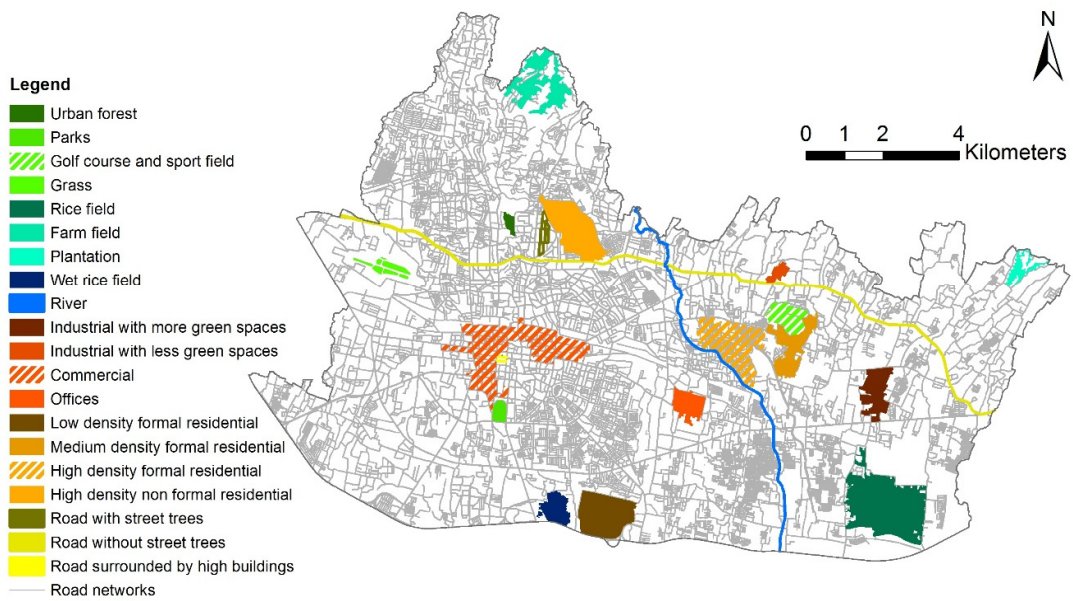
Figure 4.32 - Location of the Observed Urban Land Use/Typology
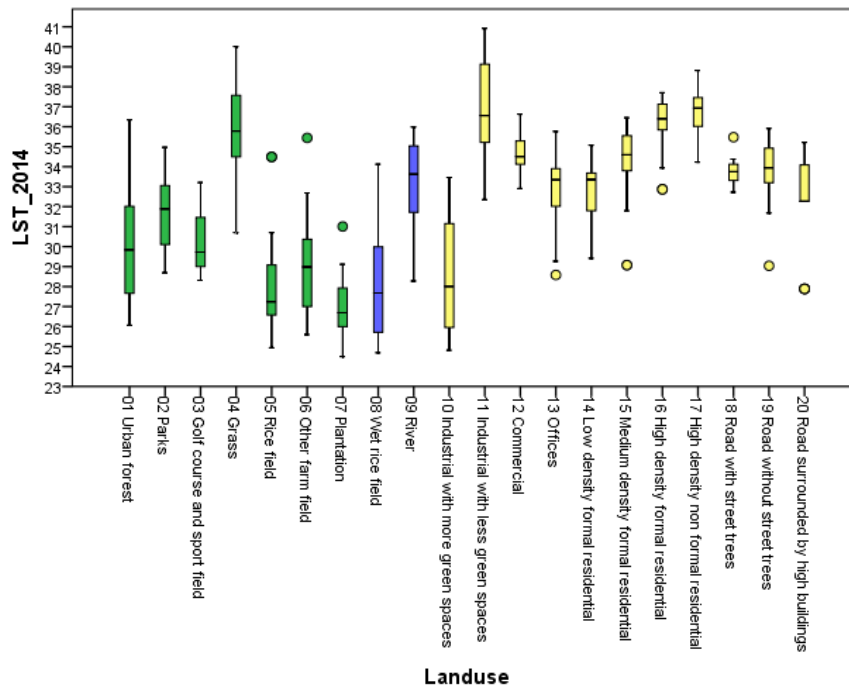
Figure 4.33 - Land Surface Temperature of the Observed Urban Land Use/Typology 2014

The general pattern that can be observed is that the typologies which represent built-up cover have higher temperature than the typologies which represent vegetation cover and water bodies. For the typologies which represent vegetation cover, the lowest temperature is found in the agricultural fields (rice fields, farm fields, and plantation). These three agricultural fields are located in the southeast, northwest and northeast part of the city. One contributing factor is the size of these three agricultural lands is much larger compared to other representations of vegetation cover.

The typology which has a slightly higher temperature range than agricultural fields is urban forest. This typology has a very large temperature range of 10°C. The urban forest has a high density of trees that has a great cooling effect. However, the size of the urban forest area is quite small. Moreover, it is located adjacent to a high density slum area which has very high temperature. These are factors that could explain the large range of maximum and minimum temperature owned by the urban forest.

Another typology which dominated by trees is a park. The park is also surrounded by a dense commercial area. The size of the selected park is only slightly larger than the urban forest. However, the characteristics that distinguish the park with the urban forest is the presence of other land covers within the park area, namely bare soil (open space), built-up (monument), and water (swimming pool). The trees in the park are segregated, thus lowering its cooling effect. This causes the minimum and the median temperature of park is higher than the urban forest.

The golf course/sports field and the grass land are relevant to be compared. Both typologies are dominated by grass. The grass land is located on the airport area which has a very high surface temperature. In addition, the grass land has a smaller and segregated area, while the golf course has a large and homogenous area of grass. Therefore, both typologies have a large temperature difference with the grass land has a higher temperature. Moreover, similar to urban forest, the influence of the surrounding pixels which have a high temperature causes the temperature range of grass land to be very large (9°C).

For the typologies that represent water bodies, the wet rice field has a lower temperature range than the river. The temperature range of the wet rice field is almost similar to the agricultural fields although the wet rice field area is much smaller than the agricultural fields. The temperature range of wet rice field is slightly larger than agricultural fields due to the influence of the surrounding areas which are built-up areas that have higher temperature. On the contrary, the temperature range of the river is quite high. The river passes through various built-up areas that have heating effect on the river. In addition, the observed river also have a small width. The observed river has a maximum width of approximately 20 m, much smaller than the spatial resolution of Aster thermal band (90 m).

For the typologies which represent built-up cover, a large difference in the temperature range is shown between the two different industrial areas, with industrial area with more green spaces have lower temperatures than industrial area with less green spaces. The similarity is both industrial areas have a large range of maximum and minimum temperature, such as those encountered in other mixed areas. In addition to differences in the size of green spaces around the industrial area, the industrial area with less green spaces has large buildings adjacent to each other so it is highly aggregated. While, the industrial area with more green spaces has smaller buildings and there is a fair distance between the buildings so it is more fragmented. The industrial area with less green spaces is located in the middle of a high density residential area. While, the industrial area with more green spaces is located near rice fields and a low density residential area.

Both commercial and offices areas have a close maximum temperature, but have a minimum temperature difference that is quite far. The offices area has a much lower minimum temperature than commercial area. Despite the observed commercial area has a very large area, but the range of maximum and minimum temperature is quite small compared to the offices area. This means the commercial area has a relatively high temperature with low temperature variation, while the office area has a high temperature variation. The commercial area is located in the city centre with a very dense and aggregated built-up area. By contrast, the buildings at offices area are not too crowded and the area has many trees or green spaces.

Residential typology includes a low, medium and high density formal residential area and high density non-formal residential area (slum). Respectively, higher temperature range is found in more dense residential area. This implies that fewer green spaces found in a more dense residential area. The density of residential area is inversely related to socio-economic status of its inhabitants. Low density residential areas have large-sized houses and inhabited by higher income people, medium density residential areas have medium-sized houses and mostly inhabited by middle income people, while high density residential areas have small-sized houses and generally inhabited by low income people. Thus, the impact of high temperature is greater for

low income (poor) people. For example, high income people can easily afford to buy an air conditioner although their housing area have low temperature. Conversely, low income people generally cannot afford to buy an air conditioner but in their housing area high temperature occur. Thus, the planning effort, including green space planning, needs to be directed to support the low income people by improving their living environment.

The next typology which represents built-up cover is a road with street trees and a road without street trees. For the road with street trees, the maximum and minimum temperature range appears to be lower than the street without trees. This indicates the influence of the cooling effect of street trees so that the temperature variation of road with street trees is lower. However, the mean and median temperature between the two topologies has the same value. This means the cooling effect is not very significant because the spatial extent of the trees is too small. Moreover, the observed road has a maximum width of approximately 30 m, much smaller than the spatial resolution of Aster thermal band (90 m). Thus, it is difficult to observe the cooling effect of street trees to the surrounding areas at the available spatial resolution of TIR bands.

The last typology is a narrow road surrounded by high buildings (urban canyon). Based on the discussion in the Literature Review (Chapter 2), there are positive and negative impacts that occur at the urban canyon during daytime. The positive impact is the cooling effect through shading from buildings, while, the negative impact is the heating effect to the building walls due to the reflection of solar radiation. At the time of image acquisition (9 to 10 AM), some parts of the road were exposed to the sun, while the other parts covered by the shadow of the buildings. The possibility of a cooling effect on the road can be indicated by the presence of outlier which has a very low value. However, the width of the road which is much smaller than the spatial resolution of the images causes the urban canyon effect is difficult to be observed.

For future green space planning, provision of green spaces should be done to better support cooling effect for the neighbouring areas. the provision of green space to decrease surface temperature need to consider the allocation of larger patches of tree covers adjacent to densely built-up areas. The significant role of the trees is indicated by the lower temperature profile of road with street trees compared to road without street trees, and the lower temperature profile of industrial area with more green spaces compared to industrial area with less green spaces. Green space planning should maintain the existing green space for not be converted into built-up areas. This is necessary especially for green areas located in the city centre and other areas in the central part of the city. On the other hand, for the areas in the outskirt of Bandung city (sub centre), green space planning should be integrated with infrastructure development planning. Planners should consider to layout new built-up areas to have a less strong impact on the inhabitant by high temperatures. Furthermore, green space planning should be prioritized for the slum areas. This is not only because the areas has the highest temperature, but also because of the low capacity of its inhabitants, which are generally low income (poor) people. The implementation of green roof or green wall should be an alternative measure. This arrangement should mainly be implemented for large buildings, such as in industrial, commercial, and offices areas that were found in the observed typology. Another alternative measure is to provide green space network, e.g. street trees. Although it have a lower cooling effect compared to large areas of trees cover, green space in the form of street trees will be effective to segregate the built-up areas, thus decreasing its heating effect.

5.   CONCLUSION AND RECOMMENDATIONS

5.1.   Conclusion

This study analysed land surface temperature extracted from thermal satellite imagery as a consideration for green spaces planning in Bandung city, Indonesia. Satellite images from Landsat TM and Aster in 1994-2014 period is used for analysis. The main objective is approached by identifying the trend of land cover, the trend of land surface temperature, the relationship between land surface temperature and the composition and configuration of land cover, and the relation between green spaces planning and land surface temperature.

The findings of this study indicate that the city has been growing to a relatively compact urban agglomeration. The concentration of built-up area in the central part of the city has been getting bigger and more aggregated. However, urban expansion has also happened extensively in urban fringes, converting agricultural to built-up areas. The growth of built-up areas has mainly occurred in the eastern part of the city with a lot of development of new residential areas and infrastructures.

The land cover trend in Bandung city for the period 1994-2014 shows dramatic changes for the dominant land cover types, which are built-up and vegetation cover. Built-up cover has increased by 25% (from 35% in 1994 to 60% in 2014), or with an average of 4% per year. The city has experienced rapid growth particularly in the last few years, with built-up cover increased by 15% in 2011-2014. On the contrary, vegetation cover has decreased by 6%, from 36% in 1994 to 30% in 2014. Green spaces in the urban fringe areas in the southeast, the northeast, and the northwest part of the city have been getting smaller, indicating the conversion of agricultural fields into built-up areas. While, vegetation patches in the central part of the city have been diminishing and more fragmented.

The land cover changes have an impact on the land surface temperature in the city. The increasing trend of built-up area and the decreasing trend of vegetated area over the years has led to an increase of the surface temperature. The mean surface temperature has increased by 8°C, from 25°C in 1994 to 33°C in 2014. The mean surface temperature has a significant differences for the different land cover. The mean temperatures are highest for built-up cover. While, the mean temperatures are generally lowest for water/shadow and vegetation cover. The average difference between land cover with the highest and the lowest mean temperature is 3°C. This relatively low value represents temperature difference at the time of image acquisition, which is in the morning (9 to 10 AM). Thus, in the afternoon (around 12 AM), the differences will be higher.

The spatial pattern of surface temperature varies over the years. However, there are much larger areas affected by the high surface temperature. High density built-up areas in particular are most affected by high surface temperature. Areas with high surface temperature (hotspots) are mainly located in the central and the west parts of the city. On the other hand, large vegetated areas (agricultural fields) in the urban fringe areas in the northwest, the northeast, and the southeast parts of the city consistently have low temperature.

The composition or the density of land cover influences the surface temperature. Vegetation density has a strong negative influence to the surface temperature. For the period of 2003-2014, Pearson correlation coefficients between land surface temperature and vegetation density generated using PLAND have a range from -0.6 to -0.7. The coefficients are only slightly lower for correlation between land surface temperature and NDVI (from -0.5 to -0.6). On the other hand, built-up density has a strong positive influence to the surface temperature. The correlation coefficients between land surface temperature and built-up density have a range of 0.6-0.7. Meanwhile, the surface temperature has weak negative correlation with water/shadow density (from -0.1 to -0.4) and very weak or no correlation with bare soil density (from 0.0 to 0.3).

The configuration of land cover has a slightly lower influence to the surface temperature compared to the composition of land cover. For each land cover type, the correlation between surface temperature and

aggregation index of land cover has a slightly lower coefficient compared to the correlation between surface temperature and land cover density. The surface temperature has moderate negative correlation with aggregation index of vegetation cover (from -0.5 to -0.6), moderate positive correlation with aggregation index of built-up cover (0.5-0.6), and very weak negative correlation with aggregation index of water/shadow and bare soil cover (from -0.1 to -0.3).

Thus, increasing green area is the more effective measure to mitigate UHI. However, mitigation measure can also be carried out more efficiently by optimizing the configuration of green areas. This finding is beneficial for green space planning particularly in urban areas where land prices are high.

In general, the further away from the city centre of Bandung, the lower the temperature. The mean temperature differences between city centre and area that are farthest from the city centre has a range of 3-7°C. However, the temperature has been rising in the sub centre of the city with a lot of planned infrastructure development. Apparently, the infrastructure development planning was not integrated with green space planning.

Surface temperature profile along the transect line shows a very high temperature variation, even for the same land cover type. Small patches of green areas and water bodies were often found along the transect line but they did not have a great impact to decrease the temperature. On the other hand, large patch of green area has a great cooling effect. Thus, the size of green area has an impact on the cooling effect. Moreover, the cooling effect of green area and the heating effect of built-up area is also very much depend on the type of the green area and the built-up area. The cooling effect of a smaller green area with a high density of trees is greater compared to a larger area of grass land. While, a high density residential area (slum) or commercial area has a significantly higher temperature than a low density residential area.

The results show the role of green spaces for the urban climate. The provision of green space to decrease surface temperature need to consider the allocation of larger patches of tree covers adjacent to densely built-up areas. The significant role of the trees is indicated by the lower temperature profile of road with street trees compared to road without street trees, and the lower temperature profile of industrial area with more green spaces compared to industrial area with less green spaces.

5.2. Recommendations

In this study, there are limitations that mainly related with data and methods used for analysis. The absence of reference image caused the accuracy assessment could not be performed for land cover classification 1994-2000. The wider bandwidth of Landsat TM causes the temperature values extracted from Landsat TM images tends to be lower than Aster. Meanwhile, the existence of thick cloud cover in the image of 2000, 2005 and 2008 caused changes in the spatial pattern of temperature. The daily air temperature data also led to difficulties in explaining the relation between surface temperature and air temperature. Finally, the the coarse spatial resolution of Landsat TM and Aster thermal band caused temperature profile for several urban typology that has small areas (e.g. road and river) are difficult to observe.

In addition, for the land cover classification, there are difficulties to obtain good training sets for bare soil cover. This led to anomalies in the classification results for 1997 and 2000 in which many bare soil pixels were classified into vegetation cover. Another limitation related to methods used for analysis is the manual selection of urban typology which was done only based on knowledge of the study area.

Future research on land surface temperature using both Landsat TM and Aster images can improve surface temperature extraction using different extraction methods. Cloud/haze removal techniques and more advanced atmospheric correction can also be applied to generate better results. To identify a clear relation between surface and air temperature, future research should use hourly air temperature data. The use of bare soil index to acquire better training sets of bare soil in land cover classification process may also be beneficial. Finally, for the classification of urban typology, future studies on urban heat island should use local climate zone classification method with the use of high spatial resolution image that would allow a more detailed urban typology extracted from image analysis.
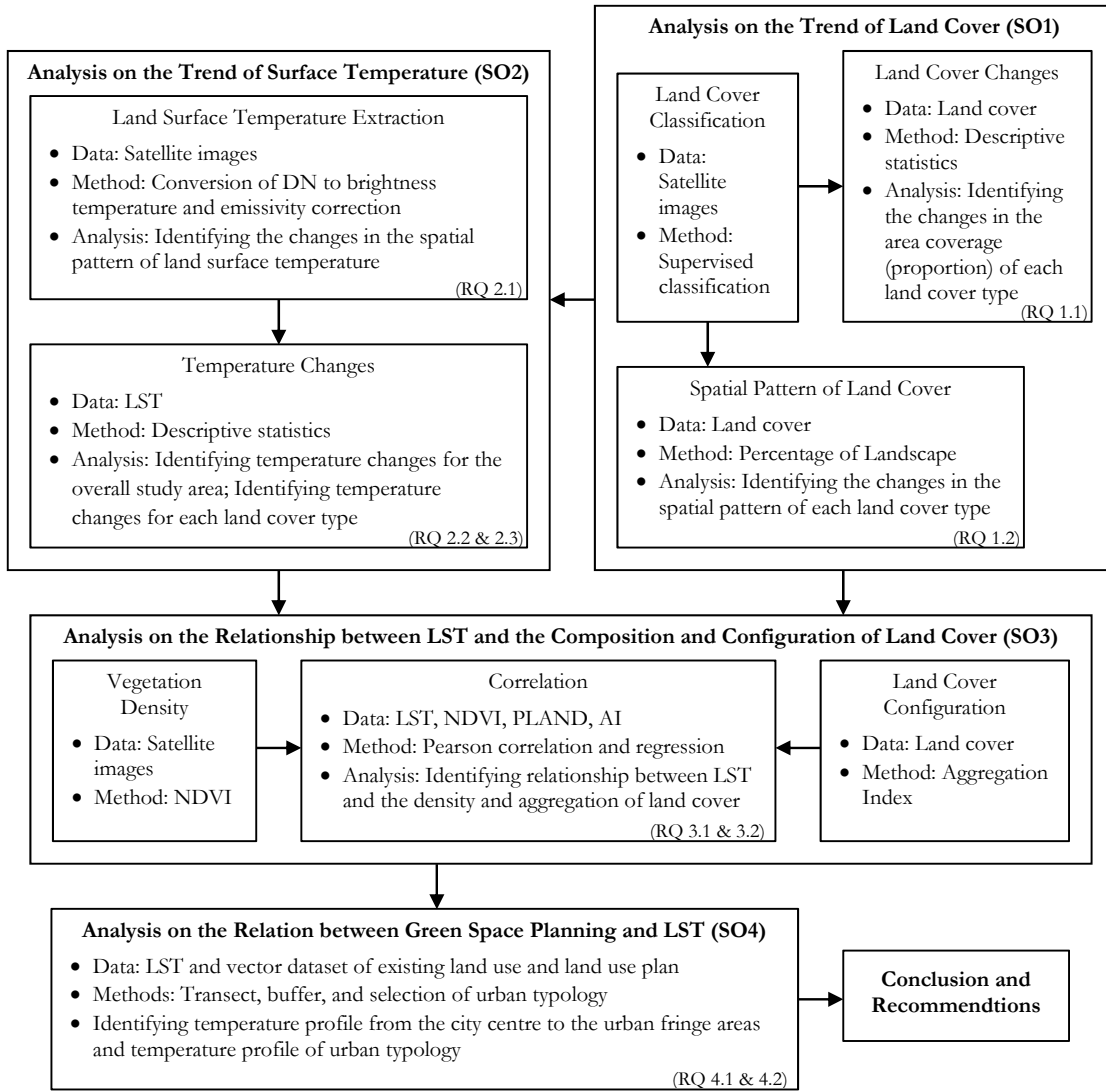
LIST OF REFERENCES

Anniballe, R., Bonafoni, S., & Pichierri, M. (2014). Spatial and temporal trends of the surface and air heat island over Milan using MODIS data. *Remote Sensing of Environment*, *150*, 163–171. doi:10.1016/j.rse.2014.05.005

Arrau, C. P., & Peña, M. A. (2011). The urban heat island (UHI) effect. Retrieved January 31, 2015, from http://www.urbanheatislands.com/

Artis, D. A., & Carnahan, W. H. (1982). Survey of emissivity variability in thermography of urban areas. *Remote Sensing of Environment*, *12*(4), 313–329. doi:10.1016/0034-4257(82)90043-8

Bechtel, B., Alexander, P., Böhner, J., Ching, J., Conrad, O., Feddema, J., … Stewart, I. (2015). Mapping Local Climate Zones for a Worldwide Database of the Form and Function of Cities. *ISPRS International Journal of Geo-Information*, *4*(1), 199–219. doi:10.3390/ijgi4010199

Chander, G., Markham, B. L., & Helder, D. L. (2009). Summary of current radiometric calibration coefficients for Landsat MSS, TM, ETM+, and EO-1 ALI sensors. *Remote Sensing of Environment*, *113*(5), 893–903. doi:10.1016/j.rse.2009.01.007

Chen, X. L., Zhao, H. M., Li, P. X., & Yin, Z. Y. (2006). Remote sensing image-based analysis of the relationship between urban heat island and land use/cover changes. *Remote Sensing of Environment*, *104*, 133–146. doi:10.1016/j.rse.2005.11.016

Ghulam, A. (2009). How to calculate reflectance and temperature using ASTER data. Retrieved January 31, 2015, from http://www.pancroma.com/downloads/ASTER Temperature and Reflectance.pdf

Gill, S. E., Handley, J. F., Ennos, A. R., & Pauleit, S. (2007). Adapting cities for climate change: The role of the green infrastructure. *Built Environment*, *33*, 115–133. doi:10.2148/benv.33.1.115

Government of Bandung Municipality. (2011). *Rencana Tata Ruang Wilayah Kota Bandung 2011-2031*. Bandung, Indonesia. Retrieved from http://bandung.go.id/rwd/index.php?fa=pemerintah.detail&id=1897

Government of Indonesia. (2007). *Undang-Undang Republik Indonesia Nomor 26 Tahun 2007 tentang Penataan Ruang*. Jakarta, Indonesia. Retrieved from http://birohukum.pu.go.id/uploads/PRI/2007/UU26-2007.pdf

Kardinal Jusuf, S., Wong, N. H., Hagen, E., Anggoro, R., & Hong, Y. (2007). The influence of land use on the urban heat island in Singapore. *Habitat International*, *31*, 232–242. doi:10.1016/j.habitatint.2007.02.006

Li, J., Wang, X., Wang, X., Ma, W., & Zhang, H. (2009). Remote sensing evaluation of urban heat island and its spatial pattern of the Shanghai metropolitan area, China. *Ecological Complexity*, *6*, 413–420. doi:10.1016/j.ecocom.2009.02.002

Liu, L., & Zhang, Y. (2011). Urban heat island analysis using the Landsat TM data and ASTER data: A case study in Hong Kong. *Remote Sensing, 3*, 1535–1552. doi:10.3390/rs3071535

Maimaitiyiming, M., Ghulam, A., Tiyip, T., Pla, F., Latorre-Carmona, P., Halik, Ü., & Caetano, M. (2014). Effects of green space spatial pattern on land surface temperature: Implications for sustainable urban planning and climate change adaptation. *ISPRS Journal of Photogrammetry and Remote Sensing*, *89*, 59–66. doi:10.1016/j.isprsjprs.2013.12.010

Mallick, J., Rahman, A., & Singh, C. K. (2013). Modeling urban heat islands in heterogeneous land surface and its correlation with impervious surface area by using night-time ASTER satellite data in highly urbanizing city, Delhi-India. *Advances in Space Research*, *52*(4), 639–655. doi:10.1016/j.asr.2013.04.025

Meteorology Climatology and Geophysics Agency of Indonesia. (2012). *Buku Informasi Perubahan Iklim dan Kualitas Udara di Indonesia*. Jakarta, Indonesia. Retrieved from http://id.scribd.com/doc/195997870/Dokumen-Buku-Informasi-Perubahan-Iklim-Dan-Kualitas-Udara#scribd

Nichol, J. E. (1994). A GIS-based approach to microclimate monitoring in Singapore's high-rise housing estates. *Photogrammetric Engineering and Remote Sensing*, *60*(10), 1225–1232. doi:35400004273117.0020

Nichol, J. E., Fung, W. Y., Lam, K. S., & Wong, M. S. (2009). Urban heat island diagnosis using ASTER satellite images and "in situ" air temperature. *Atmospheric Research*, *94*(2), 276–284. doi:10.1016/j.atmosres.2009.06.011

Oke, T. R. (1976). The distinction between canopy and boundary layer urban heat islands. *Atmosphere*, *14*(April 2014), 268–277. doi:10.1080/00046973.1976.9648422

Quan, J., Chen, Y., Zhan, W., Wang, J., Voogt, J., & Wang, M. (2014). Multi-temporal trajectory of the urban heat island centroid in Beijing, China based on a Gaussian volume model. *Remote Sensing of Environment*, *149*, 33–46. doi:10.1016/j.rse.2014.03.037

Roth, M., Oke, T. R., & Emery, W. J. (1989). Satellite-derived urban heat islands from three coastal cities and the utilization of such data in urban climatology. *International Journal of Remote Sensing*, *10*(November 2014), 1699–1720. doi:10.1080/01431168908904002

Santana, L. M. (2007). Landsat ETM+ image applications to extract information for environmental planning in a Colombian city. *International Journal of Remote Sensing*, *28*(October 2014), 4225–4242. doi:10.1080/01431160701244856

Schwarz, N., Schlink, U., Franck, U., & Großmann, K. (2012). Relationship of land surface and air temperatures and its implications for quantifying urban heat island indicators - An application for the city of Leipzig (Germany). *Ecological Indicators*, *18*, 693–704. doi:10.1016/j.ecolind.2012.01.001

Sobrino, J. a., Jiménez-Muñoz, J. C., & Paolini, L. (2004). Land surface temperature retrieval from LANDSAT TM 5. *Remote Sensing of Environment*, *90*(4), 434–440. doi:10.1016/j.rse.2004.02.003

Streutker, D. R. (2003). Satellite-measured growth of the urban heat island of Houston, Texas. *Remote Sensing of Environment*, *85*, 282–289. doi:10.1016/S0034-4257(03)00007-5

Tran, H., Uchihama, D., Ochi, S., & Yasuoka, Y. (2006). Assessment with satellite data of the urban heat island effects in Asian mega cities. *International Journal of Applied Earth Observation and Geoinformation*, *8*, 34–48. doi:10.1016/j.jag.2005.05.003

U.S. Environmental Protection Agency. (2012). *Reducing Urban Heat Islands: Compendium of Strategies - Urban Heat Island Basics*.

United Nations. (2014). *World Urbanization Prospects: The 2014 Revision*. doi:10.4054/DemRes.2005.12.9

Voogt, J. A., & Oke, T. R. (2003). Thermal remote sensing of urban climates. *Remote Sensing of Environment*, *86*, 370–384. doi:10.1016/S0034-4257(03)00079-8

Weng, Q., Lu, D., & Schubring, J. (2004). Estimation of land surface temperature-vegetation abundance relationship for urban heat island studies. *Remote Sensing of Environment*, *89*, 467–483. doi:10.1016/j.rse.2003.11.005

Xian, G., & Crane, M. (2006). An analysis of urban thermal characteristics and associated land cover in Tampa Bay and Las Vegas using Landsat satellite data. *Remote Sensing of Environment*, *104*, 147–156. doi:10.1016/j.rse.2005.09.023

APPENDIX

Appendix 1 – Research Framework

Analysis on the Trend of Land Cover (SO1)

Land Cover Classification
- Data: Satellite images
- Method: Supervised classification

Land Cover Changes
- Data: Land cover
- Method: Descriptive statistics
- Analysis: Identifying the changes in the area coverage (proportion) of each land cover type

(RQ 1.1)

Spatial Pattern of Land Cover
- Data: Land cover
- Method: Percentage of Landscape
- Analysis: Identifying the changes in the spatial pattern of each land cover type

(RQ 1.2)

Analysis on the Trend of Surface Temperature (SO2)

Land Surface Temperature Extraction
- Data: Satellite images
- Method: Conversion of DN to brightness temperature and emissivity correction
- Analysis: Identifying the changes in the spatial pattern of land surface temperature

(RQ 2.1)

Temperature Changes
- Data: LST
- Method: Descriptive statistics
- Analysis: Identifying temperature changes for the overall study area; Identifying temperature changes for each land cover type

(RQ 2.2 & 2.3)

Analysis on the Relationship between LST and the Composition and Configuration of Land Cover (SO3)

Vegetation Density
- Data: Satellite images
- Method: NDVI

Correlation
- Data: LST, NDVI, PLAND, AI
- Method: Pearson correlation and regression
- Analysis: Identifying relationship between LST and the density and aggregation of land cover

(RQ 3.1 & 3.2)

Land Cover Configuration
- Data: Land cover
- Method: Aggregation Index

Analysis on the Relation between Green Space Planning and LST (SO4)
- Data: LST and vector dataset of existing land use and land use plan
- Methods: Transect, buffer, and selection of urban typology
- Identifying temperature profile from the city centre to the urban fringe areas and temperature profile of urban typology

(RQ 4.1 & 4.2)

Conclusion and Recommendtions

Note:
SO : Sub-objective
RQ : Research Question

Appendix 2 - Spectral Characteristics of Landsat 5 TM and Terra Aster

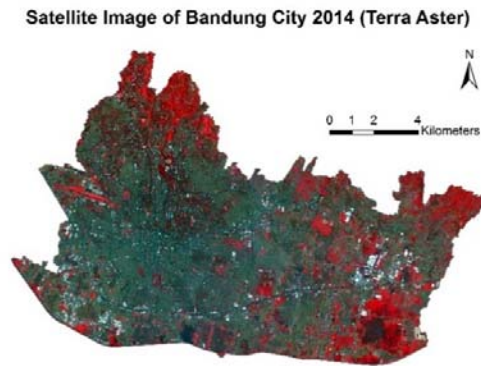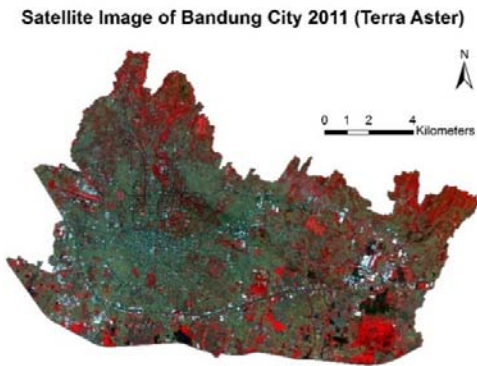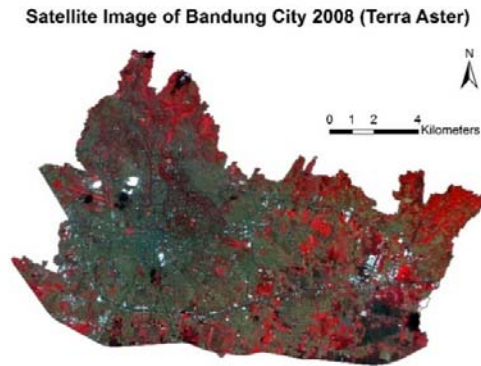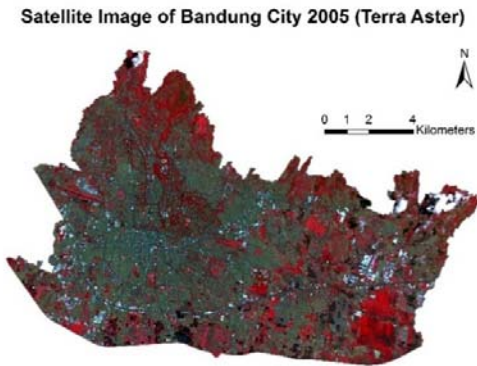| No.	Satellite and Sensor	Band	Wavelength (µm)	Resolution (m)
1	Landsat 5 TM (launched 1 Mar 1984, decommissioned 5 Jun 2013)	Band 1 (VIS)	0.45 - 0.52	30
		Band 2 (VIS)	0.52 - 0.60	30
		Band 3 (VIS)	0.63 - 0.69	30
		Band 4 (NIR)	0.76 - 0.90	30
		Band 5 (SWIR)	1.55 - 1.75	30
		Band 6 (TIR)	10.4 - 12.5	120*
		Band 7 (MWIR)	2.08 - 2.35	30
2	Terra Aster (launched 18 Dec 1999)	Band 1 (VIS)	0.52 - 0.60	15
		Band 2 (VIS)	0.63 - 0.69	15
		Band 3n (NIR)	0.76 - 0.86	15
		Band 3b (NIR)	0.76 - 0.86	15
		Band 4 (SWIR)	1.6 - 1.7	30
		Band 5 (SWIR)	2.145 - 2.185	30
		Band 6 (SWIR)	2.185 - 2.225	30
		Band 7 (SWIR)	2.235 - 2.285	30
		Band 8 (SWIR)	2.295 - 2.365	30
		Band 9 (SWIR)	2.36 - 2.43	30
		Band 10 (TIR)	8.125 - 8.475	90
		Band 11 (TIR)	8.475 - 8.825	90
		Band 12 (TIR)	8.925 - 9.275	90
		Band 13 (TIR)	10.25 - 10.95	90
		Band 14 (TIR)	10.95 - 11.65	90

Source: USGS, 2015; ITC, 2015

Note:

* The original TM thermal image was acquired at 120 meters resolution, but the image had been resampled to 30 meters by the USGS.

Appendix 3 – Satellite Image of Bandung City 1994-2014

Satellite Image of Bandung City 1994 (Landsat TM)

Satellite Image of Bandung City 1997 (Landsat TM)

Satellite Image of Bandung City 2000 (Landsat TM)

Satellite Image of Bandung City 2003 (Terra Aster)

Satellite Image of Bandung City 2005 (Terra Aster)

Satellite Image of Bandung City 2008 (Terra Aster)

Satellite Image of Bandung City 2011 (Terra Aster)

Satellite Image of Bandung City 2014 (Terra Aster)

Appendix 4 – The Workflow of and the Parameters Used for the Conversion of Digital Number to Reflectance and Brightness Temperature
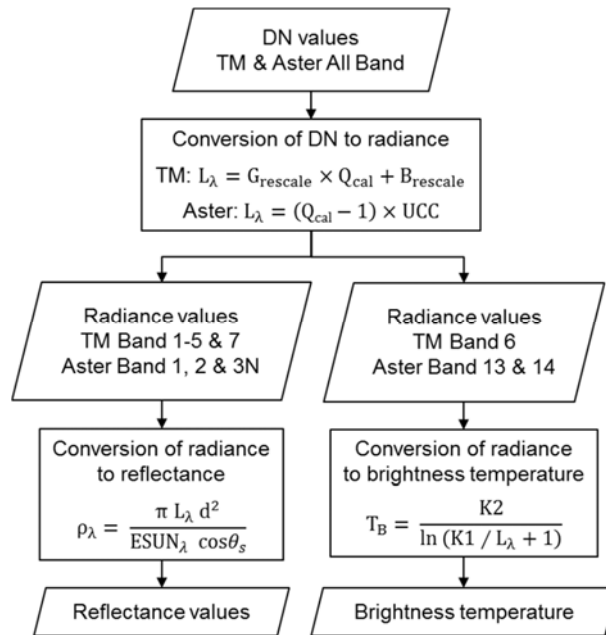
Parameters for Landsat TM Images

Band	Gr	Br	ESUNλ	K1	K2
1	0.8	-2.3	1983		
2	1.5	-4.3	1796		
3	1.0	-2.2	1536		
4	0.9	-2.4	1031		
5	0.1	-0.5	220		
6	0.1	1.2		608	1261
7	0.1	-0.2	83		

Parameters for Aster Images

Band	Gain	UCC	ESUNλ	K1	K2
1	High	0.7	1846		
2	High	0.7	1556		
3n	Normal	0.9	1119		
13	Normal	0.1		867	1350
14	Normal	0.1		641	1271

Earth-Sun Distance & Zenith Angle

Satellite and Sensor	Date	Day of Year	d	θs
Landsat TM	22 Sep 1994	265	1.00	37.8
Landsat TM	26 Jun 1997	177	1.02	46.8
Landsat TM	20 Jul 2000	202	1.02	44.5
Terra Aster	12 Jun 2003	163	1.02	38.3
Terra Aster	07 Oct 2005	280	1.00	21.5
Terra Aster	25 Jun 2008	177	1.02	39.0
Terra Aster	22 Sep 2011	265	1.00	23.8
Terra Aster	05 Sep 2014	248	1.01	26.4

Appendix 5 – The Workflow of the Extraction of Land Surface Temperature
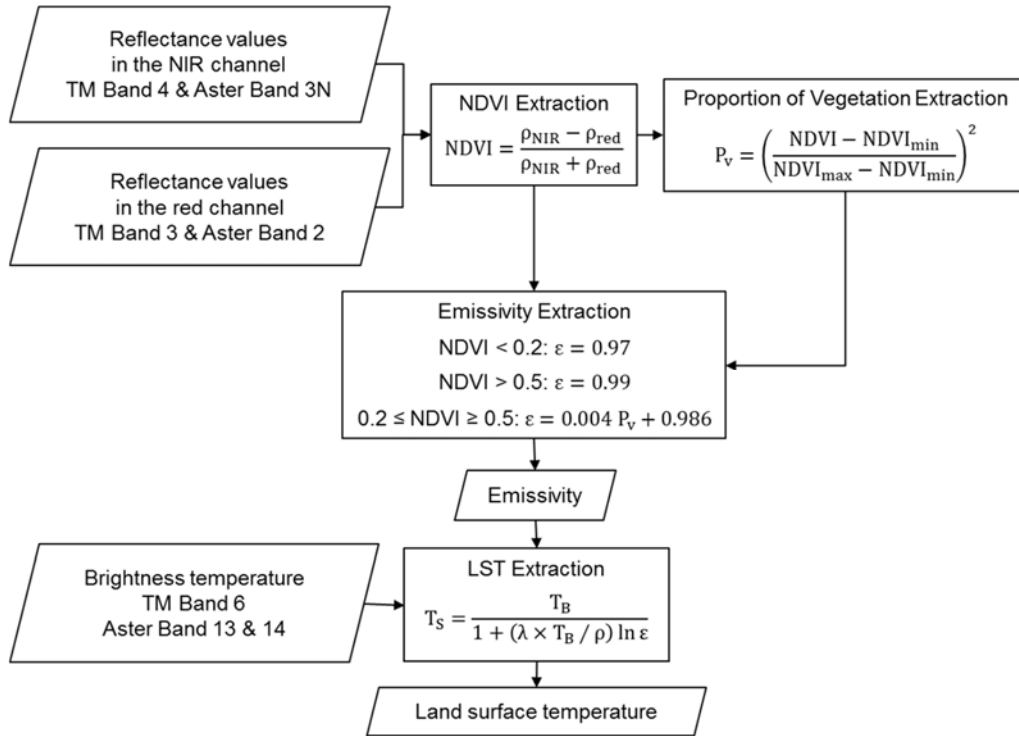
Central Wavelength

Satellite and Sensor	Sensor/Band	λ
Landsat TM	Band 6	11.4
Terra Aster	Band 13	10.6
	Band 14	11.3

Appendix 6 - Land Cover Classification Accuracy Assessment Report

1. Land Cover 2003

Error Matrix

Classified Data	Reference Data				
	Bare Soil	**Built-up**	**Vegetation**	**Water/Shadow**	**Total**
Bare soil	34	24	2	0	60
Built-up	0	78	1	0	79
Vegetation	2	9	66	0	77
Water/Shadow	0	2	2	36	40
Total	36	113	71	36	256

Accuracy Totals

Class Name	Reference Totals	Classified Totals	Number Correct	Producers Accuracy	Users Accuracy
Bare soil	36	60	34	94%	57%
Built-up	113	79	78	69%	99%
Vegetation	71	77	66	93%	86%
Water/Shadow	36	40	36	100%	90%
Totals	256	256	214		

Overall Classification Accuracy = 84%

Kappa Statistics

	Bare Soil	Built-up	Vegetation	Water/Shadow
Kappa	0.50	0.98	0.80	0.88

Overall Kappa Statistics = 0.77

2. Land Cover 2008

Error Matrix

Classified Data	Reference Data				
	Bare Soil	**Built-up**	**Vegetation**	**Water/Shadow**	**Total**
Bare soil	32	28	4	0	64
Built-up	1	81	1	0	83
Vegetation	0	5	64	0	69
Water/Shadow	1	7	0	32	40
Total	34	121	69	32	256

Accuracy Totals

Class Name	Reference Totals	Classified Totals	Number Correct	Producers Accuracy	Users Accuracy
Bare soil	34	64	32	94%	50%
Built-up	121	83	81	67%	98%
Vegetation	69	69	64	93%	93%
Water/Shadow	32	40	32	100%	80%
Totals	256	256	209		

Overall Classification Accuracy = 82%

Kappa Statistics

	Bare Soil	Built-up	Vegetation	Water/Shadow
Kappa	0.42	0.95	0.90	0.77

Overall Kappa Statistics = 0.75

3. Land Cover 2011

Error Matrix

Classified Data	Reference Data				
	Bare Soil	Built-up	Vegetation	Water/Shadow	Total
Bare soil	35	16	6	0	57
Built-up	1	79	8	0	88
Vegetation	0	22	49	0	71
Water/Shadow	0	3	1	36	40
Total	36	120	64	36	256

Accuracy Totals

Class Name	Reference Totals	Classified Totals	Number Correct	Producers Accuracy	Users Accuracy
Bare soil	36	57	35	97%	61%
Built-up	120	88	79	66%	90%
Vegetation	64	71	49	77%	69%
Water/Shadow	36	40	36	100%	90%
Totals	256	256	199		

Overall Classification Accuracy = 78%

Kappa Statistics

	Bare Soil	Built-up	Vegetation	Water/Shadow
Kappa	0.55	0.81	0.59	0.88

Overall Kappa Statistics = 0.69

4. Land Cover 2014

Error Matrix

Classified Data	Reference Data				
	Bare Soil	Built-up	Vegetation	Water/Shadow	Total
Bare soil	32	8	0	0	40
Built-up	6	93	1	0	100
Vegetation	2	3	64	0	69
Water/Shadow	2	16	3	26	47
Total	42	120	68	26	256

Accuracy Totals

Class Name	Reference Totals	Classified Totals	Number Correct	Producers Accuracy	Users Accuracy
Bare soil	42	40	32	76%	80%
Built-up	120	100	93	78%	93%
Vegetation	68	69	64	94.%	93%
Water/Shadow	26	47	26	100%	55%
Totals	256	256	215		

Overall Classification Accuracy = 84%

Kappa Statistics

	Bare Soil	Built-up	Vegetation	Water/Shadow
Kappa	0.76	0.87	0.90	0.50

Overall Kappa Statistics = 0.77

Appendix 7 - Bare Soil Density of Bandung City 1994-2014

Baresoil Density of Bandung City 1994

Baresoil Density of Bandung City 1997

Baresoil Density of Bandung City 2000

Baresoil Density of Bandung City 2003

Baresoil Density of Bandung City 2005

Baresoil Density of Bandung City 2008

Baresoil Density of Bandung City 2011

Baresoil Density of Bandung City 2014

Legend
Density (%)
0 - 20
20 - 40
40 - 60
60 - 80
80 - 100
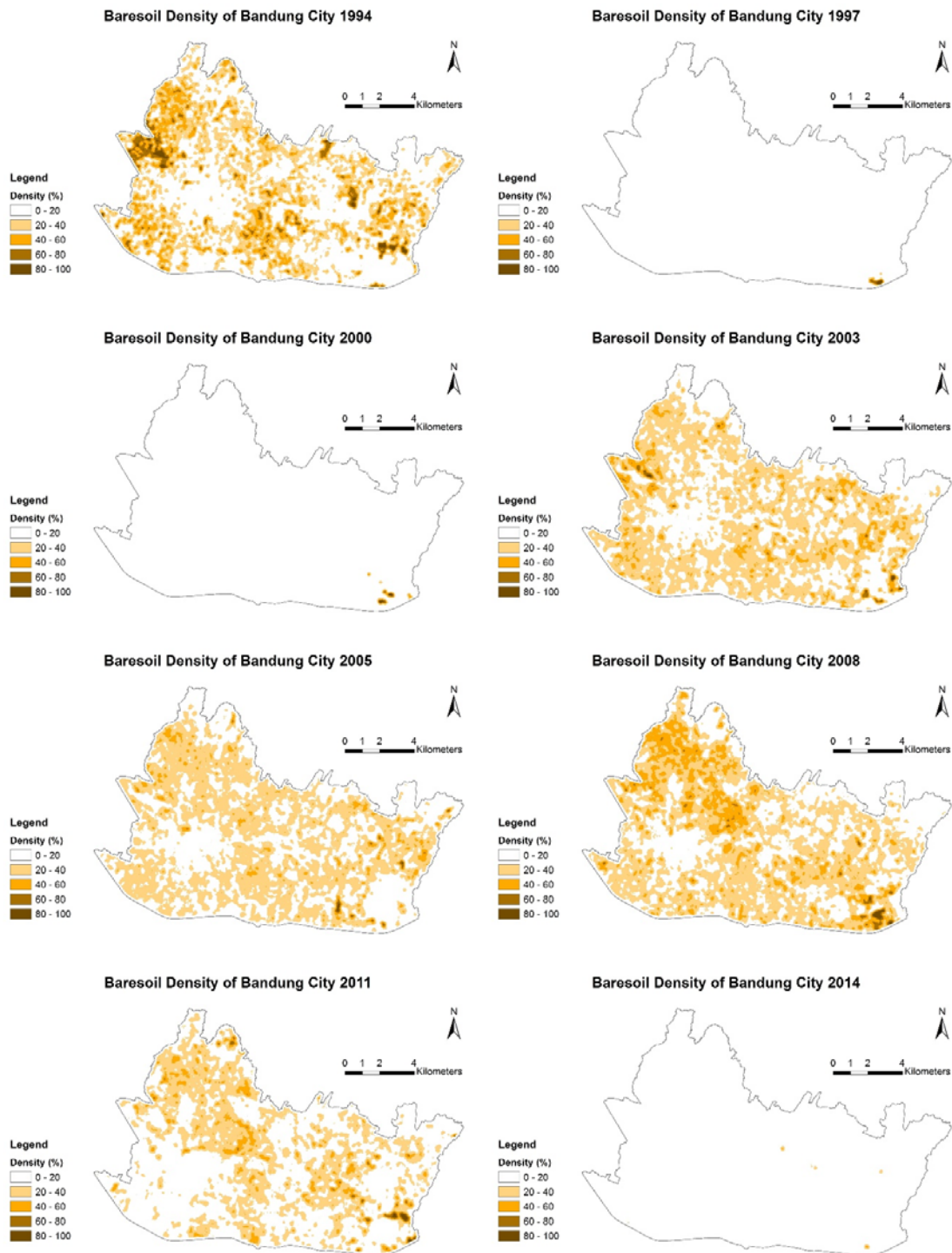
Appendix 8 - Water/Shadow Density of Bandung City 1994-2014

Water/Shadow Density of Bandung City 1994

Water/Shadow Density of Bandung City 1997

Water/Shadow Density of Bandung City 2000

Water/Shadow Density of Bandung City 2003

Water/Shadow Density of Bandung City 2005

Water/Shadow Density of Bandung City 2008

Water/Shadow Density of Bandung City 2011

Water/Shadow Density of Bandung City 2014

Legend
Density (%)
0 - 20
20 - 40
40 - 60
60 - 80
80 - 100

Appendix 9 - Spatial Pattern of Land Surface Temperature of Bandung City 1994-2014 Visualized in Equal Temperature Classes

Land Surface Temperature of Bandung City 1994

Land Surface Temperature of Bandung City 1997

Land Surface Temperature of Bandung City 2000

Land Surface Temperature of Bandung City 2003

Land Surface Temperature of Bandung City 2005

Land Surface Temperature of Bandung City 2008

Land Surface Temperature of Bandung City 2011

Land Surface Temperature of Bandung City 2014
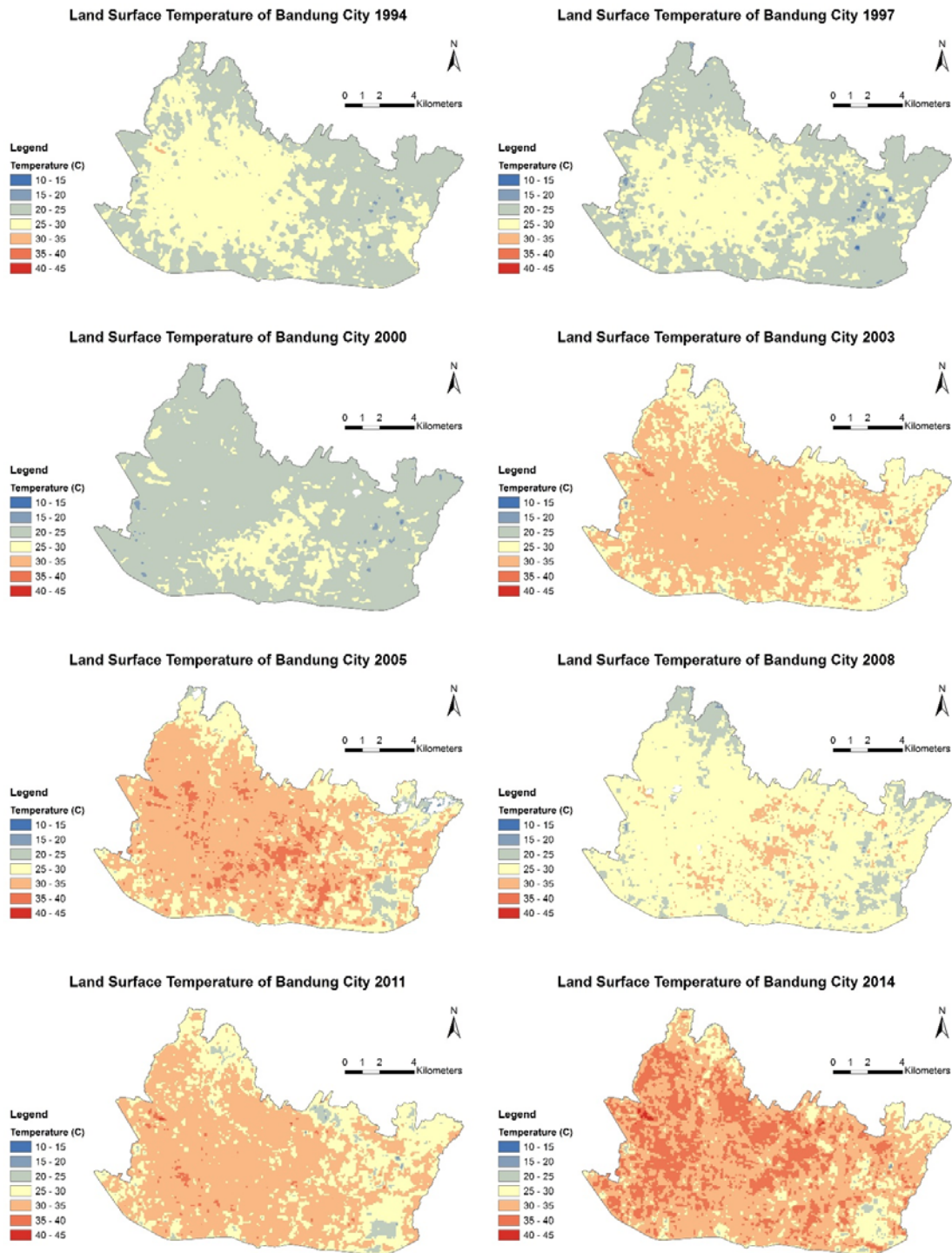
Appendix 10 - Land Surface Temperature per Land Cover Class 1994-2014

Year	Land Cover	Land Surface Temperature (°C)			
		Min.	Max.	Range	Mean
1994	Bare soil	16.2	33.2	17.0	25.4
	Built-up	15.7	31.2	15.5	26.0
	Vegetation	16.2	30.4	14.2	23.6
	Water/Shadow	20.2	30.4	10.2	24.5
1997	Bare soil	19.3	23.3	3.9	20.7
	Built-up	10.1	30.4	20.3	25.7
	Vegetation	12.9	30.0	17.1	24.2
	Water/Shadow	13.9	28.3	14.5	22.4
2000	Bare soil	20.2	25.0	4.8	21.7
	Built-up	14.3	28.8	14.4	24.3
	Vegetation	15.3	30.4	15.1	23.3
	Water/Shadow	18.0	28.8	10.8	23.1
2003	Bare soil	18.0	24.6	6.6	21.7
	Built-up	13.8	39.4	25.6	31.0
	Vegetation	13.8	39.4	25.6	31.7
	Water/Shadow	13.8	38.6	24.8	29.1
2005	Bare soil	18.3	37.3	19.0	28.6
	Built-up	13.6	39.5	25.9	32.1
	Vegetation	11.4	39.5	28.1	32.9
	Water/Shadow	14.3	39.3	25.0	29.5
2008	Bare soil	14.8	39.3	24.5	30.2
	Built-up	9.5	32.5	23.0	18.9
	Vegetation	16.6	33.9	17.2	27.6
	Water/Shadow	16.6	36.2	19.6	28.4
2011	Bare soil	17.0	33.9	16.8	26.3
	Built-up	18.7	33.9	15.2	26.3
	Vegetation	14.7	31.0	16.3	21.6
	Water/Shadow	18.3	43.0	24.8	30.9
2014	Bare soil	14.8	43.0	28.2	31.9
	Built-up	14.8	41.6	26.8	29.0
	Vegetation	18.5	43.0	24.5	29.4
	Water/Shadow	17.7	43.3	25.7	33.1

Year	Mean Temperature (°C)				Δ
	Bare Soil	Built-up	Vegetation	Water/Shadow	
1994	25.4	26.0**	23.6*	24.5	2.4
1997	20.7*	25.7**	24.2	22.4	5.0
2000	21.7*	24.3**	23.3	23.1	2.6
2003	31.0	31.7**	29.1	28.6*	3.1
2005	32.1	32.9**	29.5*	30.2	3.4
2008	27.6	28.4**	26.3*	26.3*	2.1
2011	30.9	31.9**	29.0*	29.4	2.9
2014	33.1	34.2**	31.0*	32.8	3.2

Note:
* The lowest mean temperature
** The highest mean temperature
Δ : The difference between the highest and the lowest mean temperature

Appendix 11 - Scatterplot of Mean NDVI and Mean LST 2003-2011

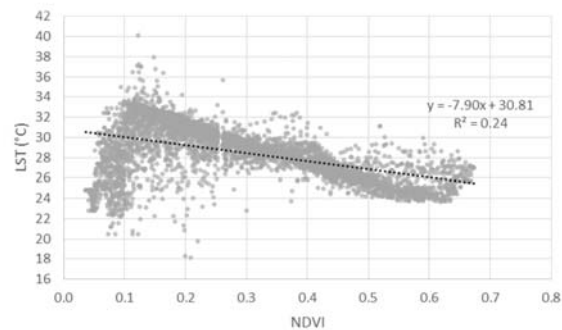Scatterplot of Mean NDVI and Mean LST 2003
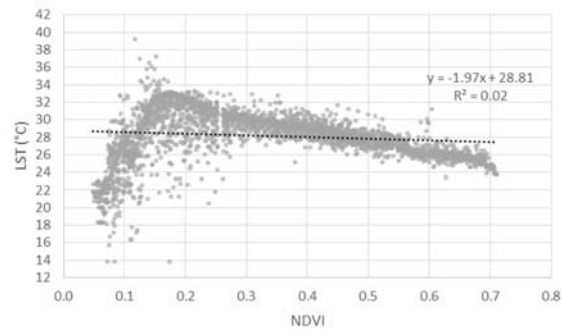
Scatterplot of Mean NDVI and Mean LST 2005
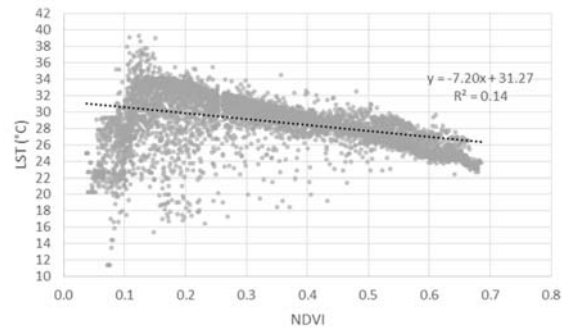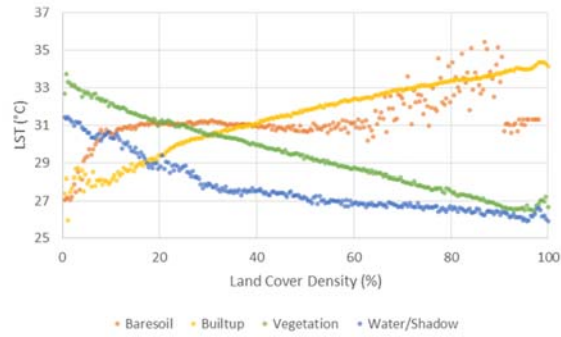

Scatterplot of Mean NDVI and Mean LST 2008
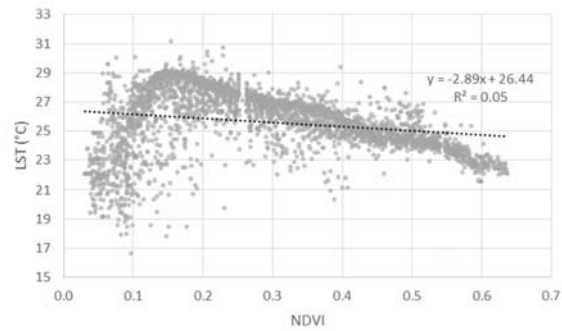
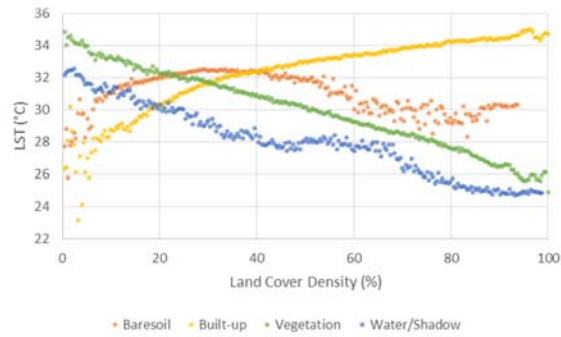Scatterplot of Mean NDVI and Mean LST 2011

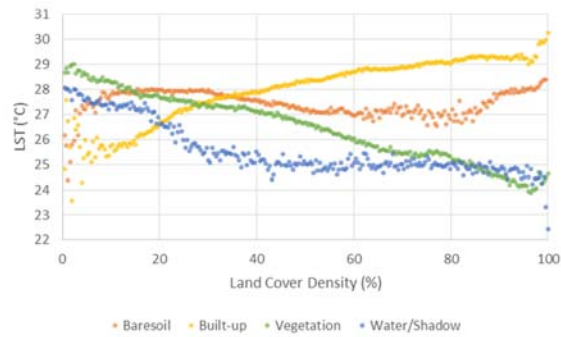**Appendix 12 - Scatterplot of Land Cover Density and Mean LST 2003-2011**

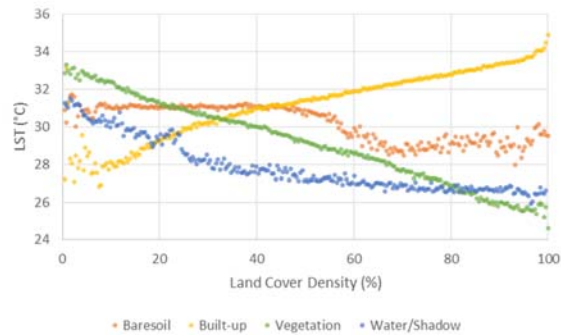Scatterplot of Land Cover Density and Mean LST 2003

Scatterplot of Land Cover Density and Mean LST 2005
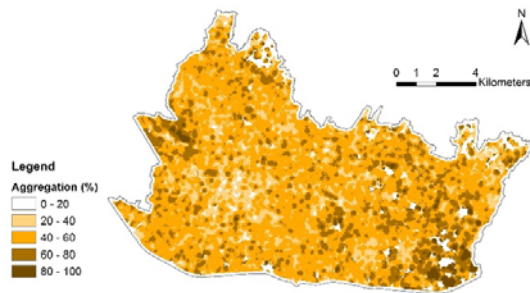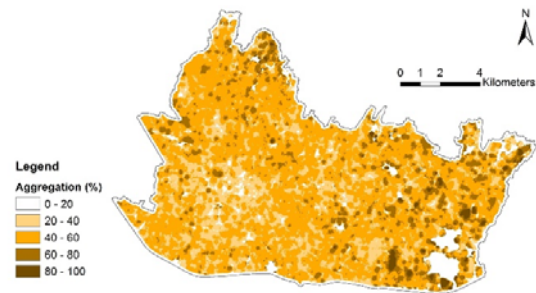

Scatterplot of Land Cover Density and Mean LST 2008

Scatterplot of Land Cover Density and Mean LST 2011

Appendix 13 - Aggregation Index of Bare Soil in Bandung City 2003-2014

Aggregation Index of Baresoil in Bandung City 2003

Aggregation Index of Baresoil in Bandung City 2005

Aggregation Index of Baresoil in Bandung City 2008
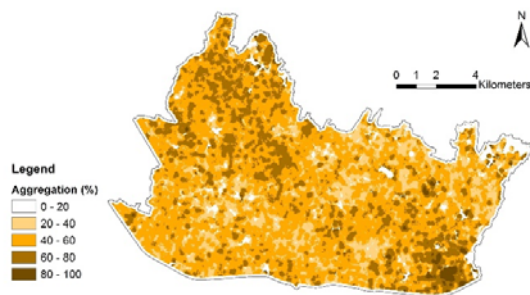
Aggregation Index of Baresoil in Bandung City 2011

Aggregation Index of Baresoil in Bandung City 2014
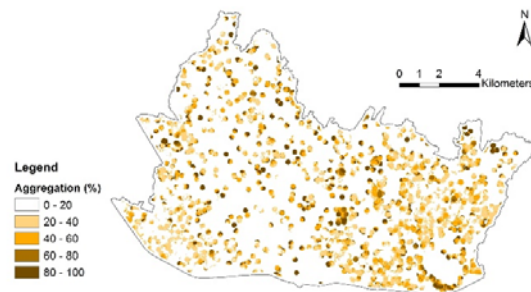
**Appendix 14 - Aggregation Index of Water/Shadow in Bandung City 2003-2014**

Aggregation Index of Water/Shadow in Bandung City 2003

Aggregation Index of Water/Shadow in Bandung City 2005

Aggregation Index of Water/Shadow in Bandung City 2008

Aggregation Index of Water/Shadow in Bandung City 2011

Aggregation Index of Water/Shadow in Bandung City 2014
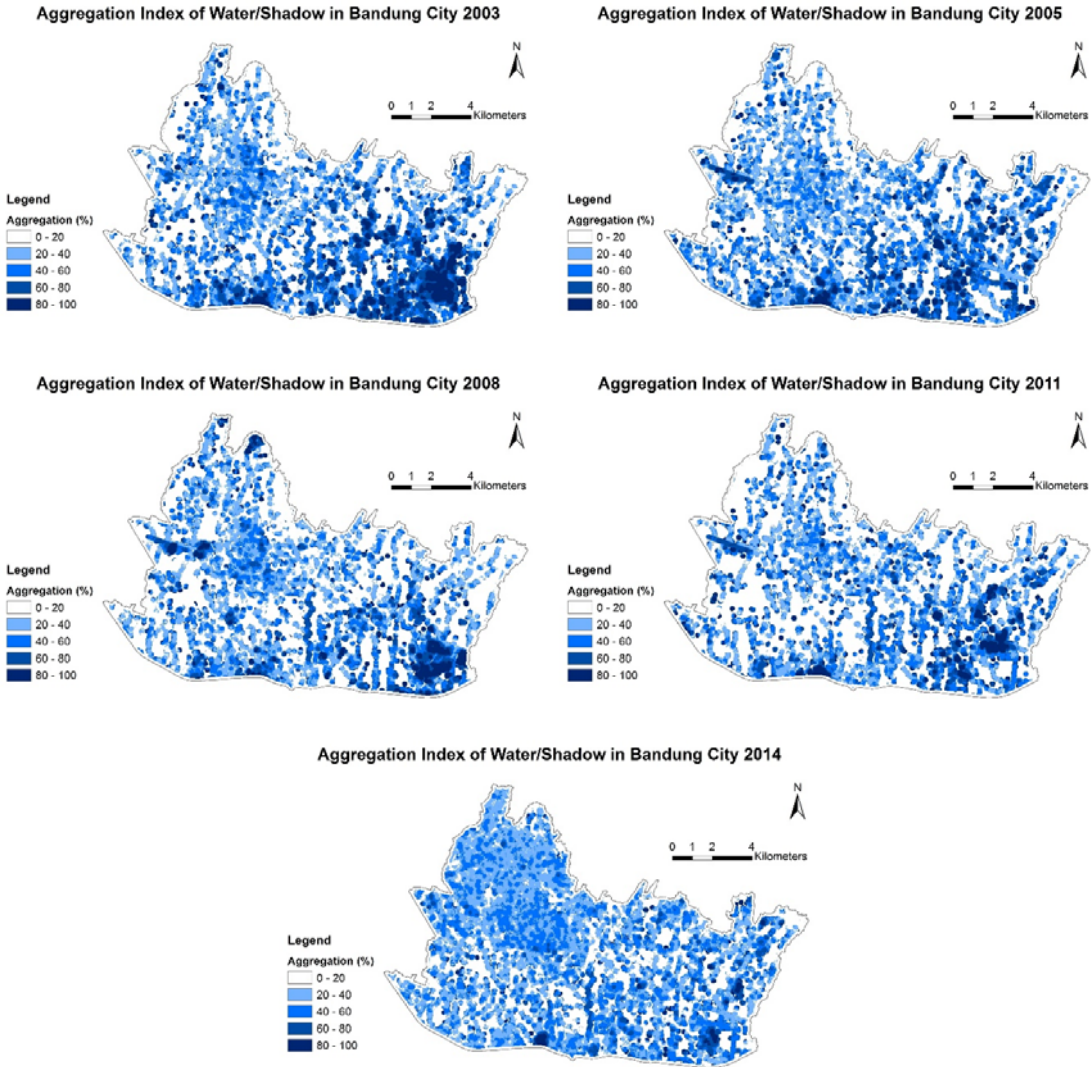
Appendix 15 - Scatterplot of Mean LST and Aggregation Index of Bare Soil and Water/Shadow Cover 2014

Scatterplot of Aggregation Index of Bare Soil Cover and Mean LST 2014
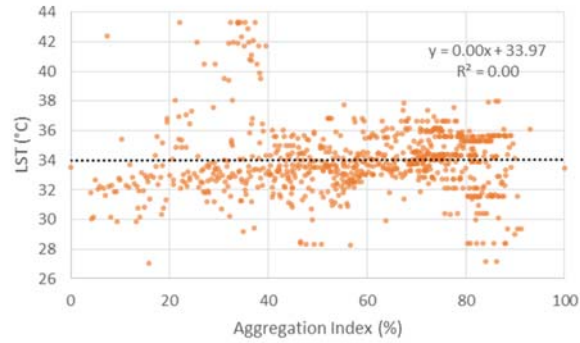
Scatterplot of Aggregation Index of Water/Shadow Cover and Mean LST 2014
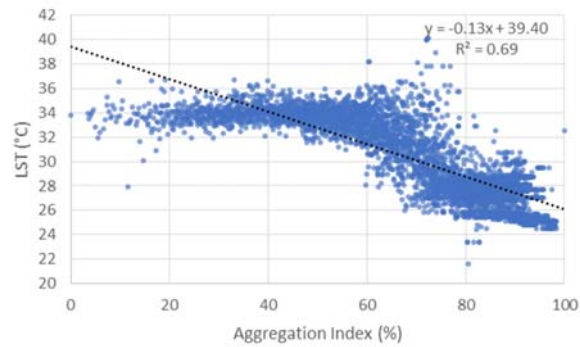
Appendix 16 - Mean Temperature on the Buffer Zones

| Zone	Distance to City Centre (km)	Mean Temperature (°C)							
		1994	1997	2000	2003	2005	2008	2011	2014
1	0-1	27.3**	26.5**	24.1	32.5	33.8**	28.5**	33.1**	34.5**
2	1-2	26.9	26.5**	24.1	32.6**	33.6	28.5**	32.8	34.4
3	2-3	26.5	26.2	24.2**	32.3	33.5	28.4	32.6	34.4
4	3-4	26.1	25.7	24.1	31.8	32.9	28.3	32.0	34.3
5	4-5	25.3	24.9	23.9	30.9	32.0	27.7	31.2	33.7
6	5-6	24.7	24.5	23.8	30.4	31.5	27.5	30.9	33.8
7	6-7	24.4	23.9	23.6	29.7	30.8	27.1	30.1	33.1
8	7-8	24.1	24.0	23.5	29.4	30.6	26.9	29.7	32.4
9	8-9	23.7	23.7	23.1	29.0	30.1	26.8	29.7	32.4
10	9-10	23.4	23.4	23.3	29.0	29.5	26.7	29.2	31.3
11	10-11	23.7	23.0	23.0	28.4	28.1	26.4	28.0*	30.4
12	11-12	23.8	23.1	22.6	28.4	28.6	26.5	28.4	30.5
13	12-13	23.7	23.5	23.0	28.6	28.7	26.5	29.2	31.0
14	13-14	22.5*	22.8	22.2	28.3	28.0	26.0	28.3	29.0
15	14-15	22.5*	22.3*	21.1*	27.9*	26.4*	25.7*	29.4	27.5*
Δ		4.8	4.2	3.1	4.7	7.4	2.8	5.1	7.0
Δ₁₋₁₃		3.6	3.0	1.1	3.9	5.1	2.0	3.9	3.5

Note:
* The lowest mean temperature
** The highest mean temperature
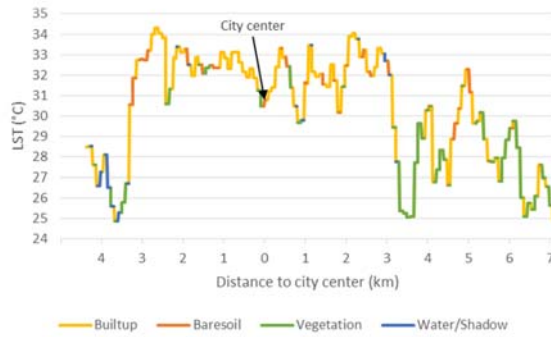Δ : The difference between the highest and the lowest mean temperature
Δ_{1-13} : The difference between the mean temperature on Zone 1 and Zone 13

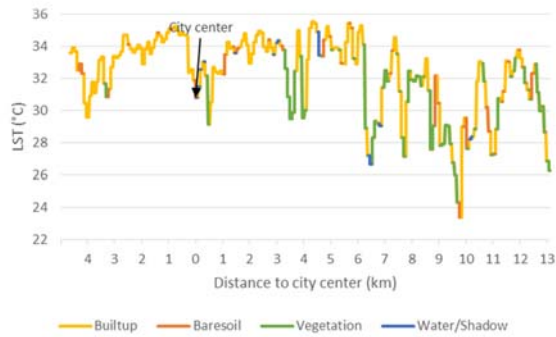**Appendix 17 - Land Surface Temperature Along the Transect Lines 2003-2011**

Land Surface Temperature Along the West-East Transect Lines 2003
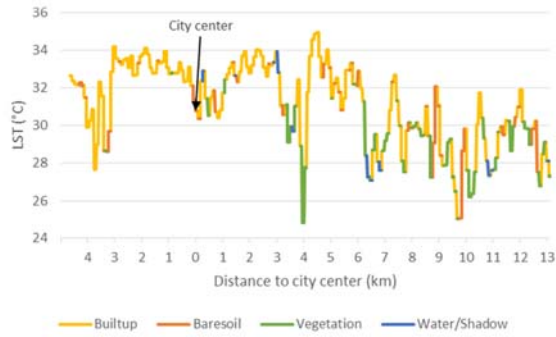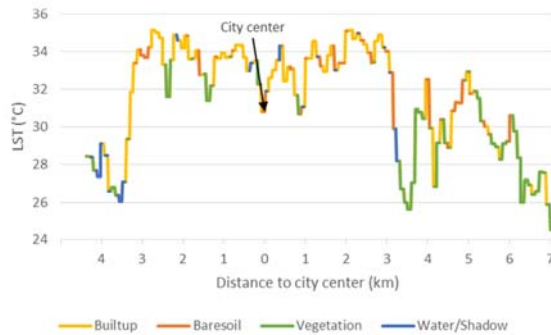

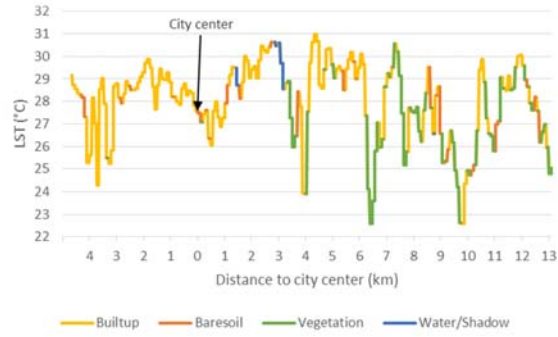Land Surface Temperature Along the South-North Transect Lines 2003

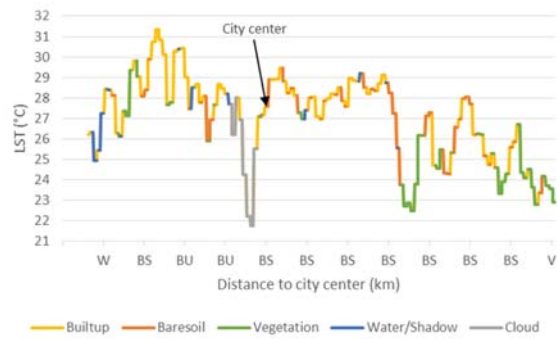Land Surface Temperature Along the West-East Transect Lines 2005

Land Surface Temperature Along the South-North Transect Lines 2005
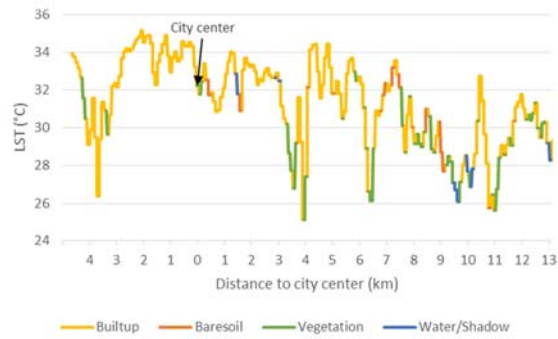
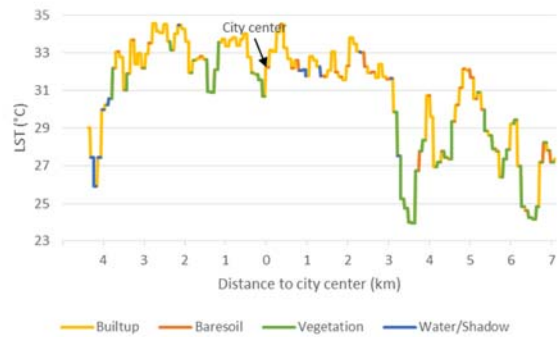Land Surface Temperature Along the West-East Transect Lines 2008

Land Surface Temperature Along the South-North Transect Lines 2008

Land Surface Temperature Along the West-East Transect Lines 2011

Land Surface Temperature Along the South-North Transect Lines 2011

Appendix 18 - Statistics of Land Surface Temperature of the Observed Urban Land Use/Typology 2014

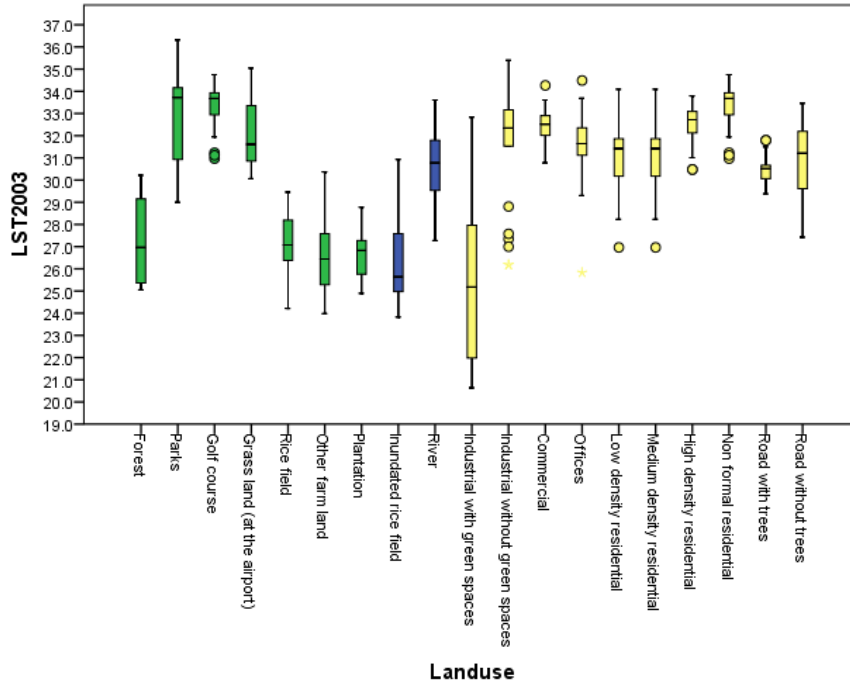| Urban Land Use/Topology	Land Surface Temperature (°C)							
	Mean	Min.	Max.	Range	1st Q	Median	3rd Q	IQR
Urban forest	30	26	36	10	28	30	32	4
Parks	32	29	35	6	30	32	33	3
Golf course and sport field	30	28	33	5	29	30	31	2
Grass	36	31	40	9	34	36	38	3
Rice field	28	25	31	6	27	27	29	2
Farm field	29	26	33	7	27	29	30	3
Plantation	27	24	29	5	26	27	28	2
Wet rice field	28	25	34	9	26	28	30	4
River	33	28	36	8	32	34	35	3
Industrial with more green spaces	29	25	33	8	26	28	31	5
Industrial with less green spaces	37	32	41	9	35	37	39	4
Commercial	35	33	37	4	34	35	35	1
Offices	33	30	36	6	32	33	34	2
Low density formal residential	33	30	35	5	32	33	34	2
Medium density formal residential	34	32	36	4	34	35	36	2
High density formal residential	36	35	38	3	36	36	37	1
High density non formal residential	37	34	39	5	36	37	37	1
Road with street trees	34	33	34	1	33	34	34	1
Road without street trees	34	32	36	4	33	34	35	2
Road surrounded by high buildings	33	32	35	3	32	32	34	2

Note:
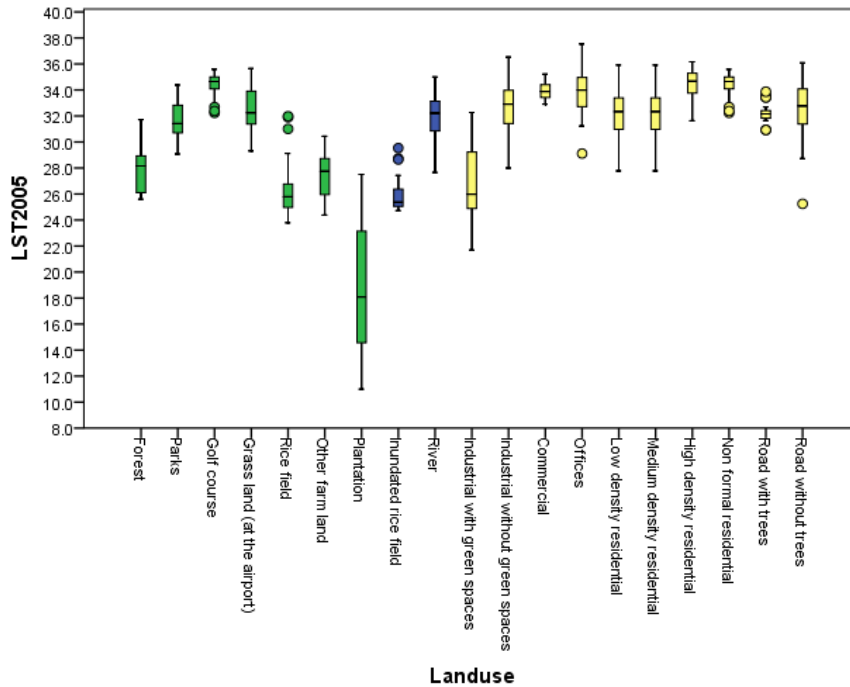1st Q : First (lower) quartile
3rd Q : Third (upper) quartile
IQR : Inter quartile range

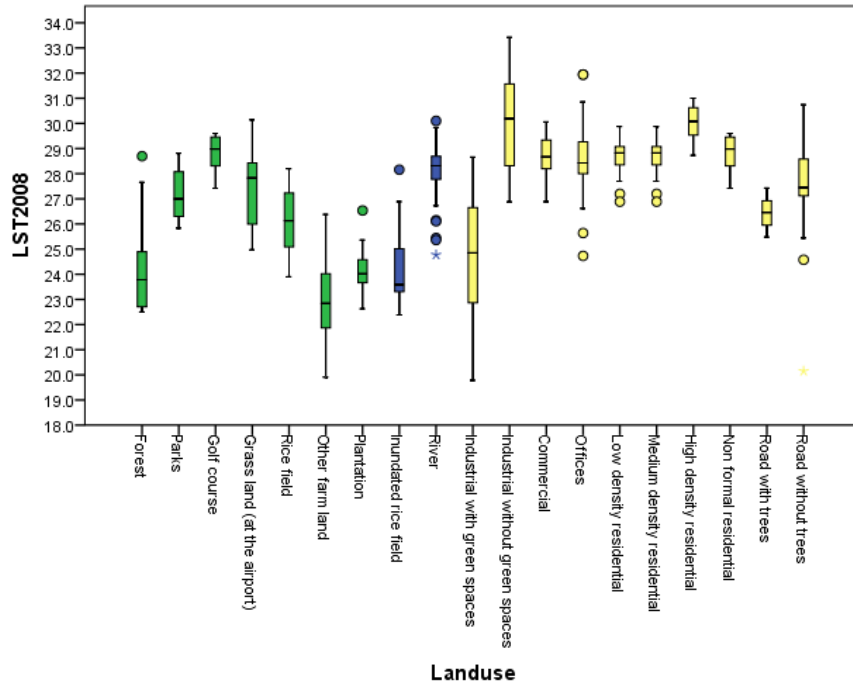**Appendix 19 - Land Surface Temperature of the Observed Urban Land Use/Typology 2003-2011**

Land Surface Temperature of the Observed Urban Land Use/Typology 2003

Land Surface Temperature of the Observed Urban Land Use/Typology 2005

Land Surface Temperature of the Observed Urban Land Use/Typology 2008

Land Surface Temperature of the Observed Urban Land Use/Typology 2011